Implementation of Primary Cells for Mechanistic Investigations of Inflammatory and Metabolic Diseases

Inauguraldissertation

zur

Erlangung der Würde eines Doktors der Philosophie

vorgelegt der

Philosophisch-Naturwissenschaftlichen Fakultät

der Universität Basel

von

Philippe Marbet

aus Luzern, Schweiz

Basel, 2018

Genehmigt von der Philosophisch-Naturwissenschaftlichen Fakultät

auf Antrag von Prof. Dr. Alex Odermatt und Prof. Dr. Jörg Huwyler

Basel, den 27.03.2018

Dekan

Prof. Dr. Martin Spiess

Table of Content

1. Summary

Cell-based *in vitro* experiments consist an essential tool in many research fields as they offer a far less complex and easier to manipulate system compared to *in vivo* models. In most cases, investigators can either use established continuous cell lines or opt for primary cells directly isolated from the tissue of interest. While cell lines are cost-effective and easy to obtain in high numbers, continuous growth is facilitated by their cancer background or by genetic manipulation, both of which often limit their ability to simulate the physiology of the tissue of origin. Primary cells on the other hand require labor-intensive isolation procedures but therefore much closer resemble the *in vivo* situation in terms of sensitivity, transporter expression and physiological behavior. To choose the appropriate tool for each experiment a detailed knowledge of the abilities and limitations of both systems is essential, whereas it is always recommendable to repeat at least some key experiments in a primary cell system. The present thesis aims to assess the implementation of bone marrow-derived macrophages (BMDMs), a 3D model of rat brain as well as primary proximal tubular cells (PTCs) for mechanistic investigations of inflammatory and metabolic diseases in different research projects.

The first project implements BMDMs in the assessment of hexose-6-phosphate dehydrogenase (H6PD) function in macrophage differentiation and metabolism. Macrophages are phagocytic cells present in essentially all tissues fulfilling various functions vital for tissue repair, homeostasis and immunity. During pathological and homeostatic inflammatory reactions they arise from the bone marrow under the influence of macrophage-colony stimulating factor, patrol the body and eventually enter compromised tissue. Presence of lipopolysaccharide and interferon gamma will differentiate them into a pro-inflammatory M1 phenotype producing toxic effector molecules and inflammatory cytokines whereas interleukin-4 induces an anti-inflammatory M2 phenotype involved in resolution of inflammation and promotion of tissue remodeling. For the first study, BMDMs were derived from bone marrow progenitor cells flushed from the femurs of wild-type (WT) and *H6pd* knockout (KO) mice. The H6PD produces the cofactor NADPH for the activation of glucocorticoids by oxo-reduction activity of 11β-hydroxysteroid dehydrogenase type 1 (11β-HSD1) in the endoplasmic reticulum (ER). In macrophages this could influence the phenotypic and functional differentiation and therefore also their metabolism. Absence of *H6pd* was reported to cause a switch in the bidirectional 11β-HSD1 towards an inactivation of glucocorticoids. Comparing BMDMs of WT and *H6pd* KO mice we found no such switch but only a decrease in 11β-HSD1 oxo-reduction activity by 40-50 %, indicating an alternative source of NADPH. Furthermore, *H6pd* KO did not cause a major disturbance in macrophage phenotypic differentiation although it caused a slightly exaggerated M1 phenotype as well as an overall reduced glucose consumption. This study showed the suitability of BMDMs to study macrophage differentiation

and to perform a variety of assays to assess characteristic macrophage parameters like phagocytosis, nitric oxide production or metabolism. Most importantly, by using animal derived cells, we could use a *H6pd* KO mouse which circumvents an incomplete gene knockdown by siRNA.

In the second project, BMDMs were implemented to investigate the contribution of secondary calciprotein particles (CPPs) to the process of vascular calcification frequently observed in chronic kidney disease (CKD) patients. The formation of primary CPPs is a physiological process in which serum proteins prevent the precipitation of calcium and phosphate as hydroxyapatite by forming spherical complexes instead. In CKD patients, primary transform into secondary CPPs, which were shown to activate macrophages. Nuclear factor erythroid 2-related factor 2 (NRF2), a master regulator of oxidative cell defense, was reported to play an important role in CPP-induced inflammation in CKD. Using BMDMs derived from WT and *Nrf2* KO mice we showed the induction of macrophages by secondary CPPs at concentrations measured in CKD patients. Mechanistic studies suggested a TLR4-mediated CPP response, which could be reduced or exacerbated by induction or knockdown of *Nrf2*. Whereas the use of *Nrf2* KO mice facilitated complete absence of the target gene, the relevance of the study would benefit from the use of a human model like human PBMCs.

A primary cell system that includes a specific type of macrophage, the microglia found in brain, can be obtained as part of an *in vitro* 3D brain model derived from rat embryonic brain tissue. These 3D cultures contain all cell types of the brain, including neurons, oligodendrocytes, astrocytes and microglia cells. The latter two are involved in neuroinflammation, which can be caused by heavy metals such as trimethyltin. The project investigates the combination of three risk factors of neurodegenerative diseases, namely the metabolic syndrome characterized by low brain insulin and high glucocorticoid levels as well as trimethyltin exposure. Therefore, an approach consisting of the described 3D rat brain model, the murine microglia cell line BV-2 as well as a mouse model of diabetes was used to report the absence of an additive effect of the risk factors to neurodegeneration but an increased neuroinflammatory response. The implementation of models with various levels of complexity allowed to address mechanistic questions using the BV-2 cell line but also to draw more *in vivo* relevant conclusions by using a primary 3D model and *in vivo* mouse experiments.

In a fourth project, the implementation of primary PTCs in the investigation of metabolic acidosis was assessed. Within the functional unit of a kidney, the nephron, the proximal tubule is responsible for 65 % of the total sodium reabsorption as well as most solutes, amino acids and low molecular weight proteins. In addition, the proximal tubule plays an important role in counteracting metabolic acidosis via a process that involves the uptake of glutamine by the glutamine transporter SNAT3 which is mainly expressed in the second and third proximal

tubule segment. To test the involvement of *Nrf2* in the upregulation of SNAT3 in response to metabolic acidosis, we exposed primary PTCs isolated from mouse kidneys to acidified medium. We could observe an upregulation of *Snat3* mRNA, which was prevented by siRNA knockdown of *Nrf2*. Studies in *Nrf2* KO mice fed with high acid diet confirmed the *in vitro* findings but also revealed a compensatory adaption of other transporters not detected in the primary cell model.

Overall, the four projects revealed many abilities but also some disabilities of the implemented primary cell systems. As the availability of human material is very limited, inducible pluripotent stem cell technology will grow more and more important as it increases translational relevance of *in vitro* experiments. However, the described primary cell models will probably remain of great use, especially in basic research.

2. Preface

The four papers contained in this thesis describe research projects I contributed to in fields that are not directly connected to each other. Whereas field-relevant findings are discussed in the respective papers, the thesis focusses on critically evaluating the implementation of the different primary cell models in these projects.

3. Introduction

3.1 Immortalized vs Primary Cells

When Ross Granville Harrison in 1907 placed small pieces of spinal cord on clotted tissue fluid to examine neuronal outgrowth, he laid the groundwork for modern cell culture [1, 2]. Nowadays, the availability of more than 3600 cell lines from over 150 different species on the American Type Culture Collection (ATCC) alone indicates the growing importance of cell-based *in vitro* experiments ever since [3]. Cell lines most likely owe their frequent use to the fact that they are a cost-effective and easy-to-use tool allowing for high throughput experiments free from the ethical concerns that animal testing would bring along. Despite offering all these advantages, one should be aware that cell lines are genetically manipulated to facilitate continuous growth which may influence their native functions, phenotype or ability to response to stimuli. Furthermore, constant passaging required to prevent overgrowth as well as the lack of tissue architecture could cause a genetic drift leading to changes in proliferation rate, metabolic activities and marker expression [4-8]. Another major problem is the cross-contamination with other cells [3]. In 1970 it was discovered that many cell lines used at that time were contaminated with HeLa cells [9], which is still a problem today [10, 11]. Finally, according to a study performed in 1994 a contamination with mycoplasma was suspected in 15-35 % of all cell lines which can alter gene expression and cell behavior [12].

At the cost of throughput and labor time, the use of primary cells can solve most of the above-mentioned problems often observed in cell lines such as uncertain identity or genetic drift, as they are isolated directly from the original tissue. Many isolation protocols include a dissection of the target tissue and/or a treatment of the tissue with proteolytic enzymes like collagenase or trypsin to digest the extracellular matrix connecting the cells [13, 14]. As these cells are not modified to facilitate continuous growth, they can only be used for a few passages at best. In exchange, they mimic the original cell type much closer in terms of transporter functionality, sensitivity and behavior allowing to draw conclusions that are more relevant for the *in vivo* situation [15-17]. Indifferent of immortalized or primary cells, many publications fail to mention essential cell culture parameters like passage number, detailed culture conditions or activities of used enzymes like trypsin. Furthermore, FBS which is used as a supplement for the culture of immortalized and some primary cells shows great batch to batch differences in its composition, owed to its natural origin [18]. Finally yet importantly, the person carrying out the experiments introduces an additional source of reproducibility issues as slight differences in the isolation procedure or cell handling can influence the experimental outcome.

It is obvious that there is no universal answer whether to use immortalized or primary cells. The statistician George Box once said, “All models are wrong but some are useful” which can be condensed into “know your model”. The choice of the suitable model should always depend

on the question at hand, which requires detailed knowledge about abilities and disabilities of all available systems. In terms of cell models this means, which characteristics of the original tissue are still preserved and which were lost by immortalization or during continuous culture. There is no point in using a cell line to investigate a transporter that is no longer expressed. Isolating primary cells to investigate basic cell physiology preserved in every immortalized cell line is equally impractical. To unite the best of both worlds, basic experiments should be performed in a suitable cell line while at least some key experiments should be repeated in the appropriate primary cell model.

3.2 Bone Marrow-Derived Macrophages

Macrophages are a type of myeloid cells historically characterized by Ilya Metchnikoff via their ability to perform phagocytosis, the uptake of solid particles [19]. Today we distinguish many different types of macrophages throughout the body displaying a wide range of functional diversity depending on their anatomical location [20]. Examples of those specialized resident macrophages are the Kupffer cells in the liver, the osteoclasts in the bone or the microglia in the brain [21-23]. Together with dendritic cells and monocytes, macrophages form the mononuclear phagocyte system (MPS) vital for tissue repair, homeostasis and immunity [24-28]. According to the MPS model, in adult mammals, bone marrow progenitor cells give rise to circulating blood monocytes, which enter the tissue where they undergo differentiation to replenish the tissue-resident macrophages population [24, 25]. This system has been challenged recently as adult tissue macrophage populations were attributed long-term persistence relying on self-renewal and many embryonic macrophage populations are being established before the appearance of circulating monocytes [29-32]. Nevertheless, it was shown in transplantation experiments that bone marrow-derived macrophages (BMDMs) can reconstitute most tissue-resident macrophages expect Langerhans cells of skin and mucosa and microglia cells located in brain and spinal cord [30]. Additionally, bone marrow-derived monocytes infiltrating tissue remain an important source of macrophages throughout adulthood in pathological and homeostatic inflammatory reactions [33, 34].

In the adult hematopoiesis, monocytes arise from the bone marrow and enter the blood circulation under the influence of macrophage-colony stimulating factor (M-CSF) which regulates their survival, proliferation and differentiation [35-37]. Subsequently, these patrolling monocytes can be recruited to sites of inflammation by tissue-resident macrophages and sentinel monocytes releasing chemokines like monocyte chemoattractant protein 1 (MCP-1) [38]. Upon binding of MCP-1 to the C-C chemokine receptor type 2 on the monocyte surface, they leave the blood vessel and differentiate into tissue macrophages [39, 40]. These newly recruited tissue macrophages also upregulate the major histocompatibility complex class II and the co-stimulatory molecules CD80 and CD86 allowing them to present

antigens and thereby activate local adaptive immune responses [41, 42]. Depending on the type of stimuli, macrophages can develop a broad range of different phenotypes, whereas the M1/M2 polarization scheme describes the two extreme forms of that spectrum [43]. Thereby the M1 phenotype occurs upon combined stimulation with interferon gamma (IFNγ) and the recognition of a pathogen associated molecular pattern like bacterial lipopolysaccharide (LPS) via toll-like receptors (TLRs) at the macrophage surface [44]. M1 macrophages show a strong microbicidal and tumoricidal activity and are characterized by the production of toxic effector molecules like reactive oxygen species and nitric oxide as well as inflammatory cytokines such as interleukin 1 beta (IL-1β), tumor necrosis factor alpha (TNFα) and interleukin 6 (IL-6) [45]. M2 macrophages are involved in parasite containment, resolution of inflammation and promotion of tissue remodeling and occur in response to the cytokines interleukin 4 (IL-4) or interleukin 13, immune complexes, simultaneous triggering of Fc gamma receptor and TLRs or anti-inflammatory molecules such as interleukin 10, transforming growth factor beta or glucocorticoids (GCs) [46-51].

Displaying great functional diversity and plasticity, macrophages are critically involved in numerous physiological processes, but therefore also a potent source of many pathologies. Prominent examples thereof are their involvement in heart/vasculature maintenance and atherosclerosis, bone remodeling and osteoporosis, hematopoiesis and leukemia, metabolism and diabetes as well as immunity and arthritis as reviewed in detail elsewhere [28, 52-57]. This selection demonstrates the importance of a detailed understanding of macrophages in order to treat those and many other disorders. Consequently, a wide range of macrophage cell models with different characteristics as the mouse RAW 264.7, J774A1, IC-21 or BV-2 as well as the human THP-1 or U937 has been established [58-63]. Despite the advantage of practically endless propagation, all of these cell lines are either cancer-derived, transfected with an oncogene or virally transformed which bares obvious and well-documented disadvantages compared to primary macrophages. RAW 264.7 cells for example showed significantly reduced phagosome functions and impaired inflammasome activation compared to BMDMs, which is essential to know when planning to investigate phagocytosis and inflammation [64, 65]. J774A1 were found to respond delayed and much less extensive to infection with *Mycobacterium tuberculosis* [66]. THP-1 cells on the other hand completely lack production of the cytokines IL-6 and IL-10 upon stimulation with *Pseudomonas aeruginosa* and are far less responsive to LPS than their *in vivo* counterparts, the peripheral blood monocytes [67, 68]. As this list goes on it becomes obvious, that confirmation of *in vitro* results by a primary cell model should be considered, at least for key experiments.

Whereas human primary cells often raise ethical concerns, mouse primary macrophages are accessible much more easily. There are multiple ways to isolate murine macrophages from

different sources: residential or elicited peritoneal macrophages, alveolar macrophages and BMDMs [69]. Whereas the number of residential macrophages in the peritoneal cavity is insufficient for most experiments, increasing their yield by elicitation with thioglycollate bears the risk of changed physiology and a hyperresponsive phenotype [69, 70]. Alveolar macrophages, influenced by their normal tissue environment show multiple macrophage untypical characteristics like an aerobic metabolism, production of hepatocyte growth factor or differences in cell surface antigens [71-73]. BMDMs on the other hand can be isolated in large numbers and in a relatively quiescent state, preserving the responsiveness to *in vitro* activation stimuli [74, 75]. For this purpose, the bone marrow which contains macrophage progenitor cells is flushed from the shaft of the femurs and incubated with M-CSF for 7 days, usually resulting in a 90 % homogenous population of mature macrophages (Fig. 1) [69]. Since the isolation procedure gives rise to resting macrophages, they can be further differentiated into functional M1 or M2 phenotypes by exposing them to LPS and IFNγ or IL-4 respectively, allowing the study of different macrophage phenotypes and their differentiation processes. Therefore, BMDMs are a versatile and close to *in vitro* tool to investigate a broad range of macrophage functions and phenotypes in health and disease.

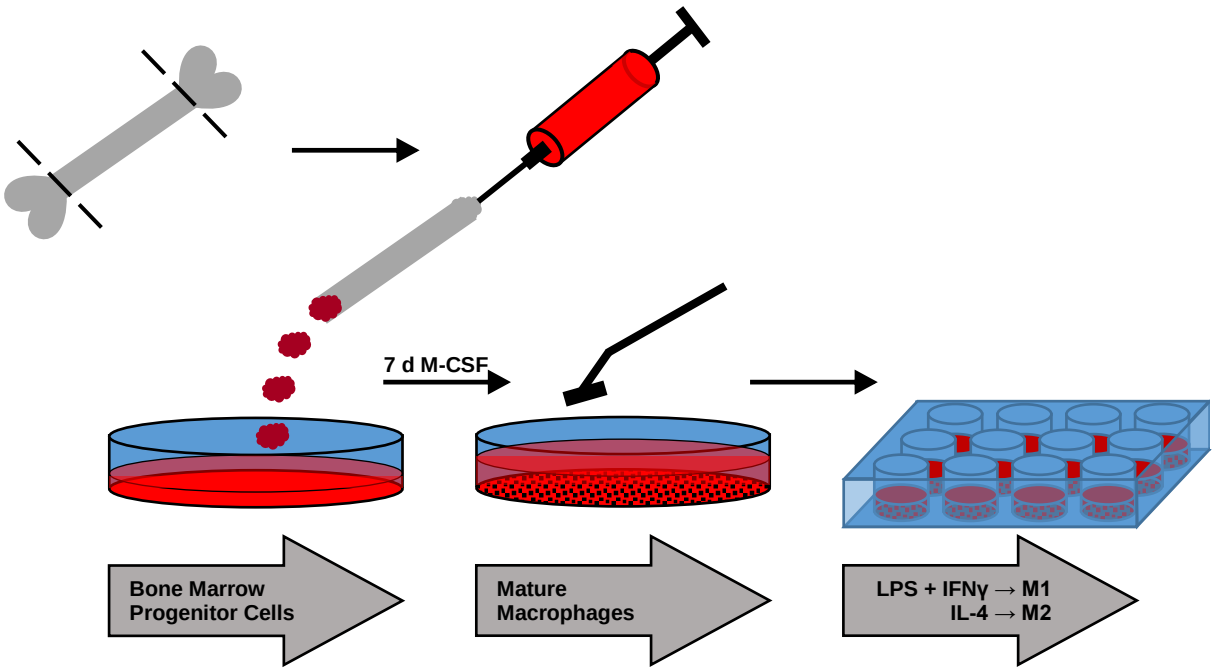

Fig. 1. Isolation and differentiation of bone marrow-derived macrophages. *Both femurs of a mouse are dissected and the epiphyses are cut. The bone marrow is flushed from the bone using a syringe, re-suspended and incubated for seven days in presence of M-CSF, whereas additional medium is added at day 3. Mature macrophages are then scraped, seeded into the final well format and differentiated into M1 or M2 phenotype. M-CSF (macrophage colony-stimulating factor); LPS (Lipopolysaccharide); IFNγ (Interferon gamma); IL-4 (Interleukin 4).*

3.3 3D Cultures of Rat Brain

Irrespectively of its anatomical complexity and functional importance, on a cellular level the brain mainly consists of two broad categories of cells: neurons and glia cells [76]. Whereas the function of the neurons is reviewed elsewhere, the glia cells, which largely outnumber the neurons, serve as a support for the neural network [77, 78]. Mainly based on their morphology, the glia cells are further separated into astrocytes, oligodendrocytes and microglia [78]. Partly isolated from the rest of the body through the blood brain barrier, each of them fulfill specific functions within the brain [79]. Astrocytes maintain water and ion homeostasis, participate in synaptic function and contribute to the maintenance of the blood brain barrier whereas oligodendrocytes produce the myelin that insulates the axons of the neurons facilitating rapid signal conduction [80-82]. Finally, the microglia are phagocytic and immunocompetent cells, able to polarize into a pro-inflammatory M1- or an anti-inflammatory M2 like phenotype depending on the stimulus [83-86]. Together with astrocytes, microglia cells contribute to neuroinflammation, which is a major contributor to neurodegeneration [87, 88]. Therefore, it is important to study these cell types as well as their interplay during homeostasis and under pathological conditions.

To study the brain and its unique cell types a variety of models with various complexity are available ranging from immortalized cell lines to primary 3D and organotypic brain slice cultures [89-91]. Whereas the latter are suitable to perform complex experiments like electrophysiological recordings and stimulations, retrograde tracing of fluorescent dyes or long term live imaging they require labor intensive dissection steps [89, 92-94]. When focusing on a single cell type like microglia, cell lines such as the well-established mouse BV-2 constitute a suitable and easy to use model mimicking primary microglia in terms of LPS and IFNγ response as well as astrocyte stimulation [91]. Further, there are established protocols for the isolation of primary microglial cells obtained from neonatal rats [95]. Obviously, a culture of homogenous cells lacks the possibility to study interactions between different cell types, as they would occur *in vivo*, where amplification of astrocyte response by microglial cytokines consists a mechanism of neurotoxicity [96]. 3D rat brain cell cultures on the other hand contain all types of brain cells and offer a suitable model to study such processes circumventing the ethical concerns of using aborted human fetal brain tissue [97, 98]. These cultures can be established by mechanical dissociation of rat embryonic brain tissue and culturing of the resulting cell mixture in serum-free, chemically defined medium under continuous agitation which results in aggregate formation, subsequent rearrangement and maturation [90, 99]. The high yield, robustness and serum-free growth and development of this 3D culture system makes it a valuable tool to investigate neurotoxicity [90].

3.4 Proximal Tubular Cells

Enabled by its proximal and distal tubular segments the kidney fulfills a fundamental role in maintaining the body salt and fluid balance as well as blood pressure homeostasis [100]. Failure to do so could causes major disturbances in the circulation and cellular functions like blood pressure, cell volume or cellular pH levels [100, 101]. Whereas the adult human kidney is estimated to filter 180 liters of blood per day, only 1 % of the therein-contained electrolytes, solutes and fluid is excreted, indicating its remarkable reabsorption capabilities [102]. This task is performed by the major structural and functional kidney unit, the nephron, which spans the regions of the cortex as well as the medulla [103]. Each nephron consists of a glomerular tuft containing a capillary network and the Bowman's capsule as well as a tubule unit with the proximal tubule, loop of Henle, distal tubule, connecting tubule and the collecting duct [103]. Functionally, a nephron filters blood, reabsorbs electrolytes and fluid and excretes waste products, overly abundant electrolytes and water [104]. Thereby, the proximal tubule is responsible for approximately 65 % of the total sodium reabsorption as well as most solutes, amino acids and low molecular weight proteins [105]. Further, it is involved in the body's acid-base balance and glucose metabolism by reabsorbing bicarbonate and glucose [106-108]. Structurally, the proximal tubule is separated into three different segments (S1-S3) whereas the S1 marks the first part of the proximal convoluted tubule, the S2 contains its late portion and the beginning of the proximal straight tubule and the S3 consists of the remaining part of the proximal straight tubule [103]. Characteristic for the S1 segment are wide brush border membranes and a high number of microvilli as well as a well-developed vacuolar-lysosomal system and endocytic compartments, indicating its high transport activity and endocytic function [103]. Therefore, the S1 shows the highest rate of solute, amino acid, sodium and fluid transport of all renal tubular segments [105]. Along the segments, this capacity decreases together with the width of the brush border membrane and the luminal surface area available for transport processes [103].

In addition to many homeostatic functions, the kidney is also responsible for excretion and detoxification of toxic metabolites and drugs [109]. Especially the cells of the proximal convoluted tubule with their high transport activity are exposed to high concentrations of drugs and their metabolites and therefore the site most frequently damaged [110]. Therefore, many models exist to mimic the proximal convoluted tubule *in vitro*, ranging from immortalized cell lines like the HK-2 to primary cells and a complete reconstruction of single perfusable tubules using 3D bio printing [111, 112]. Choosing the most suitable model is a trade-off between ease of use and closeness to the *in vivo* situation. Easiest to use are established cell lines like the mentioned HK-2, OK, MDCK or LLC-PK1, which despite their usefulness in certain studies show limitations in mimicking important proximal tubular cell features [113-115]. For example, HK-2 and LLC-PK1 cells failed to express organic anion transporters which limits their use for

uptake experiments [116, 117]. LLC-PK1 in addition are unable to perform gluconeogenesis and show only a moderate response to medium that simulates metabolic acidosis [117, 118]. MDCK cells on the other hand showed low activities of apical membrane enzymes whereas OK cells lack alkaline phosphatase activity [119, 120]. At the other end of the spectrum are highly sophisticated, three dimensional convoluted renal proximal tubules on a chip created by using a bio printed extracellular matrix and population by perfusion with renal proximal tubule epithelial cells (RPTECs) [111]. Laying in between, primary cells show a good resemblance to the *in vivo* situation while allowing for reasonable throughput due to optimized isolation procedures.

As the kidney contains various functionally and morphologically different compartments, a manual dissection step is inevitable in all isolation protocols for primary proximal tubular cells (PTCs). Primary PTCs can be isolated from animal kidneys by subjecting dissected cortex pieces to collagenase digestion followed by a sieving step separating the longer proximal tubule fragments from other segments or glomeruli (Fig. 2) [121]. Afterwards, primary PTCs will then grow out of the seeded fragments during a seven-day incubation. Other methods relying on microdissection of individual nephron segments have been reported but produce lower amounts of starting material and subject cells to mechanical stress [13]. Although frozen aliquots of human RPTECs are commercially available and the above described isolation procedure could also be applied to rabbit or rat, the lower costs, the relative closeness to human and the variety of genetically altered mice makes them the favorable source [122]. Mouse primary PTCs grown on a cell culture plate were reported to show proximal tubule specific characteristics like the development of a monolayer of polarized cells expressing microvilli on the apical side as well as dome formation, which is indicative of tight junctions and an intact transcellular transport process [123]. A study using a similar isolation protocol but growing the cells on collagen coated membranes reports functional expression of an endocytic apparatus, brush border enzymes and a functional sodium-dependent glucose transport allowing to perform trans-well transport assays [121]. Despite the dedifferentiation issue, which is always a limitation in primary cells cultured outside the tissue of origin, mouse primary PTCs retain many functions of the original tissue and therefore offer a great model to study processes in health and disease.

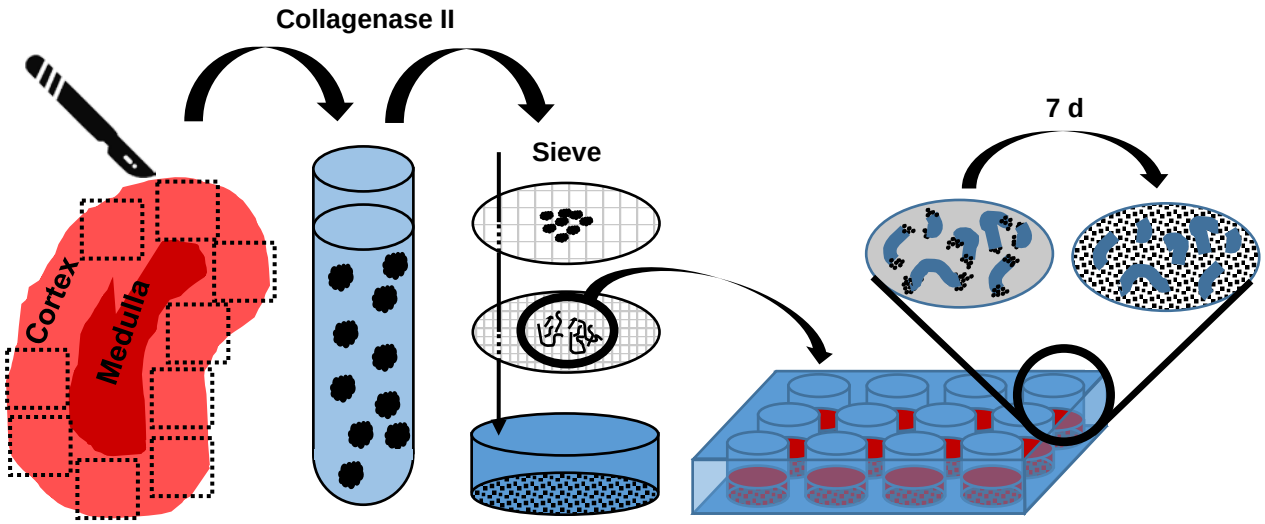

Fig. 2. Dissection and growth of primary proximal tubular cells. *Both kidneys of a mouse are removed, de-capsuled and cortex pieces are isolated. The product of a collagenase II digestion is then added onto a sieve tower accumulating proximal tubular fragments on the lower sieve. Fragments are then plated and incubated for seven days to allow for outgrowth of proximal tubular cells.*

4. Results and Discussion

4.1 Implementation of Bone Marrow-Derived Macrophages

4.1.1 Comparison of Bone Marrow-Derived Macrophage Differentiation and Function between Wild-Type and Hexose-6-Phosphate Dehydrogenase Knockout Mice

The hexose-6-phosphate dehydrogenase (H6PD) is an enzyme located in the lumen of the endoplasmic reticulum (ER) [124]. Using glucose-6-phosphate, it locally regenerates the co-factor nicotinamide adenine dinucleotide phosphate (NADPH), which can only be replenished from the ER-luminal NADP+ pool, as the ER-membrane is impermeable for pyridine nucleotides [125]. Currently, the H6PD is the only well documented ER-enzyme thought to be responsible for keeping a high luminal NADPH/NADP+ ratio. Consequently, the H6PD is interesting for two reasons: firstly, by maintaining a high NADPH/NADP+ ratio, the H6PD exerts oxoreduction activity upon the bi-directional enzyme 11β-hydroxysteroid dehydrogenase type 1 (11β-HSD1) which faces to the ER lumen and uses NADPH as a co-factor for local glucocorticoid (GC) activation [126-128]. Activated GCs like cortisol in human or corticosterone in mice are vital for the regulation of many physiological functions and have a great influence on cells of the immune system such as macrophages [129-131]. Secondly, by converting glucose-6-phosphate to 6-phosphogluconate, the H6PD is able to catalyze the first two steps of the ER pentose phosphate pathway, thereby affecting overall metabolic functions which could regulate macrophage phenotypic differentiation [132-134]. Therefore, we hypothesized that 11β-HSD1 in macrophages of *H6pd* KO mice would no longer function as an oxoreductase activating GCs and that this would influence the phenotypic and functional differentiation.

Trying to answer these questions, we compared BMDMs isolated from wild-type (WT) and *H6pd* knockout (KO) mice. This approach is well suited to study the function of a specific gene and the effects of its loss since it circumvents incomplete *in vitro* gene knockdown which would require a 48 h time window to allow degradation of residual H6PD protein and always bares the risk of influencing normal cell behavior. Additionally, deriving macrophages from bone marrow instead of gaining them from other sources results in high numbers of relatively quiescent macrophages which is a necessity when aiming to study macrophage phenotypic differentiation [69]. BMDMs have been implemented in identical or at least similar experiments as the ones performed in the following paper. Already shown for example was the use of BMDMs to study the activity of 11β-HSD1 by measuring corticosterone formation upon addition of 11-dehydrocorticosterone as well as the resulting reduction in the mRNA expression of inflammatory markers [135, 136]. As BMDMs resemble the patrolling monocytes they are often activated *in vitro* using different stimuli and used for the investigation of macrophage differentiation, including phenotype-specific markers and M1-specific cytokine release [137-

139]. Furthermore, many general macrophage functions like phagocytosis, M1-specific nitric oxide release and cholesterol efflux are preserved as shown by frequent use of BMDMs as a model to study those processes [135, 140, 141]. Finally, BMDMs have already been successfully applied in metabolism experiments using an extracellular flux analyzer, as the metabolic switch from oxidative phosphorylation in M0 macrophages to aerobic glycolysis in LPS-induced M1 macrophages is well preserved in this model [142]. Overall, the following paper implements BMDMs to compare a variety of typical macrophage functions between WT and *H6pd* KO to assess the role of H6PD in macrophage.

4.1.2 Submitted Manuscript: Absence of Hexose-6-Phosphate Dehydrogenase Results in Reduced Overall Glucose Consumption but Does not Prevent 11β-Hydroxysteroid Dehydrogenase 1 Dependent Glucocorticoid Activation in Macrophages

Philippe Marbet[a], Petra Klusonova[a], Julia Birk[a], Denise V. Kratschmar[a], Alex Odermatt[a]

[a] Division of Molecular and Systems Toxicology, Department of Pharmaceutical Sciences, University of Basel, Klingelbergstrasse 50, 4056 Basel, Switzerland

Contribution:

- Planned and carried out the experiments
- Analyzed and interpreted data
- Wrote the paper

W

W

W

W

W

W

W

W

W

W

W

W

W

W

W

W

W

W

W

W

W

W

W

W

W

W

W

W

W

W

W

W

W

W

W

W

W

W

W

W

W

W

W

W

W

W

W

W

W

W

W

W

W

W

W

W

W

W

W

W

W

W

W

W

W

W

W

W

W

W

W

W

W

W

W

W

W

W

W

W

W

W

W

W

W

W

W

W

W

W

W

W

W

W

W

W

W

W

W

W

W

W

W

W

W

W

W

W

W

W

W

W

W

W

W

W

W

W

W

W

W

W

W

W

W

W

W

W

W

W

W

W

W

W

W

W

W

W

W

W

W

W

W

W

W

W

W

W

W

W

W

W

W

W

W

W

W

W

W

W

W

W

W

W

W

W

W

W

W

W

W

W

W

W

W

W

W

W

W

W

W

W

W

W

W

W

W

W

W

W

W

W

W

W

W

W

W

W

W

W

W

W

W

W

W

W

W

W

W

W

W

W

W

W

W

W

W

W

W

W

W

W

W

W

W

W

W

W

W

W

W

W

W

W

W

W

W

W

W

W

W

W

W

W

W

W

W

W

W

W

W

W

W

W

W

W

W

W

W

W

W

W

W

W

W

W

W

W

W

W

W

W

W

W

W

W

W

W

W

W

W

W

W

W

W

W

W

W

W

W

W

W

W

W

W

W

W

W

W

W

W

W

W

W

W

W

W

W

W

W

W

W

W

W

W

W

W

W

W

W

W

W

W

W

W

W

W

W

W

W

W

W

W

W

W

W

W

W

W

W

W

W

W

W

W

W

W

W

W

W

W

W

W

W

W

W

W

W

W

W

W

W

W

W

W

W

W

W

W

W

W

W

W

W

W

W

W

W

W

W

W

W

W

W

W

W

W

W

W

W

W

W

W

W

W

W

W

W

W

W

W

W

W

W

W

W

W

W

W

W

W

W

W

W

W

W

W

W

W

W

W

W

W

W

W

W

W

W

W

W

W

W

W

W

W

W

W

W

W

W

W

W

W

W

W

W

W

W

W

W

W

W

W

W

W

W

W

W

W

W

W

W

W

W

W

W

W

W

W

W

W

W

W

W

W

W

W

W

W

W

W

W

W

W

W

W

W

W

W

W

W

W

W

W

W

W

W

W

W

W

W

W

W

W

W

W

W

W

W

W

W

W

W

W

W

W

W

W

W

W

W

W

W

W

W

W

W

W

W

W

W

W

W

W

W

W

W

W

W

W

W

W

W

W

W

W

W

W

W

W

W

W

W

W

W

W

W

W

W

W

W

W

W

W

W

W

W

W

W

W

W

W

W

W

W

W

W W

W

W

W

W

W

W

W

W

W

W

W

W

W

W

W

W

W

W

W

W

W

W

W

W

W

W

W

W

W

W

W

W

W

W

W

W

4.1.3 Discussion

The M1/M2 classification scheme simplifies a continuous spectrum of intermediate phenotypes, which a macrophage can adopt *in vivo* to facilitate an adequate response to a certain insult [143]. In literature, a broad range of LPS and IFNγ concentrations is used to induce M1 differentiation. As we opted for distinct phenotypes, the concentrations chosen for this study were located at the higher end, causing the subsequent characterization to clearly show the expected M1/M2 differences in phenotypic marker expression and NO release. This indicates a normal differentiation of BMDMs *in vitro* despite the fact that applied standard culture conditions differ from *in vivo* situation in terms of oxygen exposure, glucose concentrations or the presence of fetal bovine serum. Therefore, they seem to be a valid model in our hands to assess macrophage differentiation in WT and *H6pd* KO.

A whole body knockdown of a gene can cause adaptive changes in the animal, which could interfere with the process desired to study. In case of the H6PD, KO animals showed increased adrenal size and adrenocorticotropic hormone-stimulated circulating corticosterone concentrations, most likely caused by resistance to feedback inhibition of the hypothalamic-pituitary-adrenal axis normally induced by corticosterone [144, 145]. A similar phenotype was observed in 11β-HSD1 KO animals, which caused hyper responsiveness to LPS injection as indicated by elevated pro-inflammatory cytokine levels [146, 147]. This hyper responsiveness was induced or prevented in BMDMs of both WT and 11β-HSD1 KO mice simply by *in vitro* differentiation in presence or absence of GCs [147]. In our study, this influence of GCs is eliminated by *ex vivo* differentiation of BMDMs of WT and *H6pd* KO animals, as both are cultured in the same medium. This allows the study of a *H6pd* KO avoiding the compensatory effects present during *in vivo* studies of a full body KO. Therefore, the observed increases in mRNA expression and release of cytokines in KO M1 macrophages are most likely GC independent.

The assessment of the reductase activity of 11β-HSD1 in our BMDM model is essential to test the occurrence of the switch from reductase to dehydrogenase activity in absence of *H6pd*. Interestingly, in the *H6pd* KO a reduction in reductase activity by 40-50 % rather than a switch did occur. When using non-human cells, it is always important to beware of any species-specific differences relevant to the hypothesis. In our case, the expression of 11β-HSD1 is induced in human M2 macrophages by IL-4, which does not occur in mouse BMDMs [148]. This however should not be relevant to our results, as they are obtained from macrophages of the M1 phenotype. Additionally, the approximately 50 % reduction of 11β-HSD1 reductase activity in *H6pd* KO was confirmed in our lab using perfused liver of the same *H6pd* KO mice, indicating that the absence of a switch from reductase to dehydrogenase activity is an overall phenotype and not a special feature of macrophages (unpublished data). To draw conclusions

from this finding it is vital to use a KO animal instead of just knocking down H6PD as otherwise the observed GC conversion would be suggested to be enabled by remaining H6PD protein activity. Finally, 11β-HSD1 is most likely the source of the remaining corticosterone formation, as no more corticosterone was detectable upon treatment with an 11β-HSD1 specific inhibitor. All this indicates that there is an alternative source of NADPH within the ER.

Various enzymes have been suggested to contribute to NADPH regeneration in the lumen of the ER, two of them are the malic enzyme and the isocitrate dehydrogenase [149]. Even though both were shown to increase NADPH in liver microsomes by a factor of ten, they did not influence 11β-HSD1 reductase activity, most likely because they do not interact with the 11β-HSD1 kinetically in contrast to the H6PD [150]. Another candidate would be the 6-phosphogluconate dehydrogenase, which occurs in the cytosol but was suggested to be shuttled into the ER where it could contribute to the NADPH pool [151]. An approach called BioID suited to identify possible sources was recently reported [152]. Briefly, a protein of interest is fused to a promiscuous biotin ligase, which will then biotinylated proteins in close proximity. Upon cell lysis and protein denaturation the biotinylated proteins can be purified and identified by mass spectrometry [152]. By fusing the biotin ligase to 11β-HSD1, interacting proteins could be identified, whereas the already established co-localized H6PD could serve as a positive control.

Metabolism is an important contributor to macrophage phenotypic polarization and an essential prerequisite for their M1 or M2 specific functions. Whereas M1 macrophages undergo a switch towards greatly enhanced aerobic glycolysis, M2 macrophages show an increased fatty acid oxidation and mitochondrial oxidative phosphorylation [153-157]. In turn, assessment of macrophage metabolism can serve as a measure of their polarization status and inflammatory potential to detect the influence of a gene KO on macrophage differentiation [142]. Using BMDMs from WT and *H6pd* KO animals an extracellular flux analyzer is an ideal approach to further investigate the differences in M1 phenotypic differentiation observed on mRNA and protein levels. In addition to the already performed glycolysis stress test, recently developed assay kits for the extracellular flux analyzer focus purely on assessing the glycolytic rate, allowing for a more precise measurement and optimized detection of metabolic switching. Results gained by gene expression studies of both macrophage phenotypes led us to target the M1 phenotype for further metabolic investigations. However, additional hints about H6PD function could be gathered by comparing mitochondrial oxidation in macrophages of the M2 phenotype using the same platform.

In conclusion, BMDMs isolated and differentiated under the described conditions are a suitable tool to assess the role of H6PD in GC activation and metabolism in macrophages by comparing cells from WT and *H6pd* KO mice. Due to the controlled conditions of an *in vitro* culture,

activation of GC as well as GC independent effects can be studied. Further investigations of an alternative source of NADPH in the ER could involve BioID whereas more insight into the contribution of H6PD to cell metabolism could be gained by extending the metabolic flux analyzer experiments.

4.1.4 Application of Bone Marrow-Derived Macrophages in Mechanistic Investigations of Calcification and Inflammation

Vascular calcification (VC) is associated with an increased incidence of cardiovascular disease in patients suffering from chronic kidney disease (CKD) [158, 159]. It was shown to be a predictive marker of subsequent cardiovascular morbidity and mortality and even if the mechanism of its pathogenesis is not fully understood, a contribution of lost mineral homeostasis, oxidative stress and activation of an innate immune response was described [158, 160-163]. Additionally, a role of calciprotein particles (CPPs) has been described, which are formed in circulation in presence of serum proteins preventing the formation of hydroxyapatite precipitates from calcium and phosphate [164, 165]. These initially small spherical complexes called primary CPPs can transform into larger spindle-shaped structures, the secondary CPPs [164-167]. A role of CPPs in VC is supported by studies detecting secondary CPPs in CKD patients whereas they were absent in healthy control subjects [168]. Furthermore, circulating CPP concentration in these patients was associated with VC [169, 170]. Increased circulating markers of innate immunity associated with CPP concentrations as well as co-localization of macrophages with calcium deposits in plaques led to the hypothesis, that the chronic inflammation observed in CKD patients is mediated via macrophage activation [171-173]. Furthermore, studies showed that activation of the macrophage cell line RAW264.7 by secondary CPPs caused secretion of pro-inflammatory cytokines [174]. In this process, the transcription factor nuclear factor erythroid 2-related factor 2 (*NRF2*), a master regulator of antioxidant response, was shown to suppress macrophage cytokine release in a mouse model of atherosclerosis, whereas a suppression of oxidative stress in macrophages caused a decrease in severity [175-179]. Since the *Nrf2* system was found to be compromised in peripheral blood mononuclear cells (PBMCs) isolated from CKD patients, their activation by secondary CPPs could be an important mechanism of chronic inflammation in CKD [180].

As macrophages are the key element in the mechanism under investigation and a mouse model of *Nrf2* KO is available, BMDMs were used to investigate the role of CPPs and NRF2 in macrophages in the pathology of VC. Additionally, they can be isolated in a rather quiescent state, which is vital when studying activation and cytokine release elicited by particles. Since *in vitro* systems of primary cells allow for efficient activation or inhibition of specific targets, the process under investigation can be manipulated using the *Nrf2* inducer bardoxolone

methyl (CDDO-Me) to reproduce and modulate the *in vivo* situation and to perform mechanistic studies. The following paper illustrates the implementation of BMDMs in mechanistic investigations of VC and inflammation as well as the role of NRF2 therein.

4.1.5 Submitted Manuscript: Absence of Nrf2 Exacerbates Secondary Calciprotein Particle Induced Pro-Inflammatory Cytokine Transcription and Secretion by Primary Macrophages

Thomas G. Hammond[1,2,#], Adam Lister[1,2,#], Philippe Marbet[1,2,#], Ian M. Copple[3], Michael H.L. Wong[3,4], Prakash G. Chandak[2,5], Parisa Aghagolzadeh[2,5], Paul M. O'Neill[3,4], Andreas Pasch[2,5], Christopher E. Goldring[3], Alex Odermatt[1,2]

[1]Division of Molecular and Systems Toxicology, University of Basel, Basel, Switzerland
[2]Swiss National Centre of Competence in Research (NCCR) Kidney Control of Homeostasis
[3]MRC Centre for Drug Safety Science, Department of Molecular and Clinical Pharmacology, University of Liverpool, Liverpool, United Kingdom
[4]Department of Chemistry, University of Liverpool, Liverpool, United Kingdom
[5]Department for Biomedical Research, University Hospital Bern, Inselspital, Bern, Switzerland
[#]These authors contributed equally to this manuscript

Contribution:

- Planned and carried out experiments in RAW264.7
- Isolated bone marrow-derived macrophages and performed primary cell experiments
- Analysed data

W

W

W

W

W

W

W

W

W

W

W

W

W

W

W

W

W

W

W

W

W

W

W

W

W

W

W

W

W

W

W

W

W

W

W

W

W

W

W

W

W

W

W

W

W

W

W

W

W

W

W

W

W

W

W

W

W

W

W

W

W

W

W

W

W

W

W

W

W

W

W

W

W

W

W

W

W

W

W

W

W

W

W

W

W

W

W

W

W

W

W

W

W

W

W

W

W

W

W

W

W

W

W

W

W

W

W

W

W

W

W

W

W

W

W

W

W

W

W

W

W

W

W

W

W

W

W

W

W

W

W

W

W

W

W

W

W

W

W

W

W

W

W

W

W

W

W

W

W

W

W

W

W

W

W

W

W

W

W

W

W

W

W

W

W

W

W

W

W

W

W

W

W

W

W

W

W

W

W

W

W

W

W

W

W

W

W

W

W

W

W

W

W

W

W

W

W

W

W

W

W

W

W

W

W

W

W

W

W

W

W

W

W

W

W

W

W

W

W

W

W

W

W

W

W

W

W

W

W

W

W

W

W

W

W

W

W

W

W

W

W

W

W

W

W

W

W

W

W

W

W

W

W

W

W

W

W

W

W

W

W

W

W

W

W

W

W

W

W

W

W

W

W

W

W

W

W

W

W

W

W

W

W

W

W

W

W

W

W

W

W

W

W

W

W

W

W

W

W

W

W

W

W

W

W

W

W

W

W

W

W

W

W

W

W

W

W

W

W

W

W

W

W

W

W

W

W

W

W

W

W

W

W

W

W

W

W

W

W

W

W

W

W

W

W

W

W

W

W

W

W

W

W

W

W

W

W

W

W

W

W

W

W

W

W

W

W

W

W

W

W

W

W

W

W

W

W

W

W

W

W

W

W

W

W

W

W

W

W

W

W

W

W

W

W

W

W

W

W

W

W

W

W

W

W

W

W

W

W

W

W

W

W

W

W

W

W

W

W

W

W

W

W

W

W

W

W

W

W

W

W

W

W

W

W

W

W

W

W

W

W

W

W

W

W

W

W

W

W

W

W

W

W

W

W

W

W

W

W

W

W

W

W

W

W

W

W

W

W

W

W

W

W

W

W

W

W

W

W

W

W

W

W

W

W

W

W

W

W

W

W

W

W

W

W

W

W

W

W

W

W

W

W

W

W

W

W

W

W

W

W

W

W

W

W

W

W

W

W

W

W

W

W

W

W

W

W

W

W

W

W

W

W

W

W

W

W

W

W

W

W

W

W

W

W

W

W

W

W

W

W

W

W

W

W

W

W

W

W

W

W

W

W

W

W

W

W

W

W

W

W

W

W

W

W

W

W

W

W

W

W

W

W

W

W

W

W

W

W

W

W

W

W

W

W

W

W

W

W

W

W

W

W

W

W

W

W

W

W

W

W

W

W

W

W

W

W

W

W

W

W

W

W

W

W

W

W

W

W

W

W

W

W W

W

W

W

W

W

W

W

W

W

W

W

W

W

W

W

W

W

W

W

W

W

W

W

W

W

W

W

W

W

W

W

W

W

W

W

W

W

W

W

W

W

W

W

W

W

W

W

W

W

W

W

W

W

W

W

W

W

W

W

W

W

W

W

W

W

W

4.1.6 Discussion

The study aims to elucidate the induction of macrophages by CPPs, which could play a role in VC, a common contributor to cardiovascular disease in CKD patients [158, 160]. Since the release of pro-inflammatory cytokines, which consists a hallmark of macrophage activation is conserved in the mouse macrophage cell line RAW264.7, they offer a suitable tool to investigate the potential of CPPs to elicit an immune response [174, 181]. However, since the study intents to show macrophage stimulation by CPP concentrations found in CKD patients, the more sensitive BMDMs are a better model to draw conclusions about the *in vivo* situation. Primary macrophages are not only suitable to study TLR4 mediated response to CPPs, but also to other colloidal particles like hydroxyapatite or graphene oxide, which have been reported to activate the same receptor [182, 183]. Like in the case of CPPs, BMDMs show a higher sensitivity to graphene oxide compared to cell lines like the RAW264.7 [183]. Furthermore, as they are derived directly from the animal, primary macrophages from *Nrf2* KO and WT animals allow studying the role of the gene without siRNA knockdown, which is incomplete and possibly interferes with the measured release of pro-inflammatory cytokines.

A major limitation is of course the use of mouse cells while aiming to produce evidence for a mechanism of CPPs in human. To increase translational relevance, mechanistic studies should be performed in a human model like human PBMCs. They can be isolated from donor blood using a density gradient and a selection by CD14+ labeled magnetic beads and subsequent differentiation of the selected fraction by human M-CSF. Using this method, reasonable numbers of relatively pure and quiescent macrophages can be obtained, but compared to a defined mice strain the cells from human blood will most likely show greater donor-donor variability. Mechanistic studies done in RAW264.7 cells could then be repeated using the same TLR4 inhibitors or NRF2 inducers already applied in mouse, as they are not species specific. Additionally, to further corroborate the involvement of the suggested JNK/AP-1 pathway, the phosphorylation of cJun, which is an essential step therein, could be inhibited and should prevent elicitation of a macrophage response.

Overall, the use of both the RAW264.7 cell line as well as BMDMs is justified in this project. Whereas the cell line is suitable for mechanistic studies, the more sensitive primary cells are to be preferred to investigate effects of human relevant CPP concentrations. Finally, PBMCs isolated from human blood would corroborate the findings and further increase the relevance for the human situation.

4.2 Implementation of 3D Rat Brain Culture

4.2.1 Use of 3D Rat Brain Culture to Investigate Mechanisms of Neurodegeneration

The metabolic syndrome characterized by peripheral hyperglycemia and hyperinsulinaemia is a risk factor for neurodegenerative diseases [184]. Type II diabetes, often observed in metabolic syndrome, leads to a decreased insulin transport into the brain, which was shown to cause cognitive impairment [185-187]. Additionally, patients with metabolic syndrome often present elevated circulating cortisol levels suggested to impair hippocampus-dependent memory formation [188, 189]. Another risk factor for neurodegenerative disease are environmental pollutants like the organotin compound trimethyltin (TMT) used as plastic stabilizers and biocides shown to accumulate in the food chain and to cause neurotoxicity [190-195]. All of these three risk factors, low brain insulin, high GC and TMT exposure, contribute to neuroinflammation, which involves microglia cells and astrocytes [87, 88, 186, 188, 195]. Similar to other macrophages, microglia cells can assume an alternative phenotype favoring tissue repair, or a classical phenotype promoting neurodegeneration [85, 86]. Overall, microglia play a central role in neuroinflammation, which in turn is considered a major contributing mechanism to neurodegeneration [196, 197]. GCs play a key role in the regulation of microglial inflammation by binding to the mineralocorticoid receptor (MR) and the GC receptor (GR) [198-201]. In this process, the balance of GC is important, as high concentrations activate the GR and suppress the inflammatory response, whereas low doses of endogenous GC activate the MR thereby stimulating inflammation [126, 202, 203]. This balance between GR and MR activity can be influenced by the action of 11β-HSD1, which locally activates GC [202].

We aimed to investigate the risk of the above-described factors and their combination to cause neurodegeneration. Neuroinflammation is a key contributing element therein and not exclusively mediated by microglia but also through their interplay with other cell types in the brain. Therefore, we not only used BV-2 microglial cells in an isolated setting, but also 3D rat brain cultures containing all cell types present in the brain along with *in vivo* experiments. The *in vitro* systems allow for tight control of contributing factors like GC or insulin content as well as TMT exposure and also to assess the contribution of microglia to neurodegeneration. The BV-2 cell line mimics microglia and is able to activate astrocytes via cytokine release, as it would occur *in vivo* [91, 204]. 3D cultures established from rat brain form aggregates creating a tissue-specific environment that allows for physiological interactions between the different cell types as well as exchange of soluble messengers, ideal to simulate the interaction between microglia and astrocytes leading to neuroinflammation [90]. The following paper is an example of the implementation of primary cell cultures and cell lines to assess complex processes like neurodegeneration.

4.2.2 Submitted Manuscript: Insulin and Glucocorticoids Modulate Heavy Metal-Induced Neuroinflammation and Neurodegeneration

[§1,5]Jenny Sandström, [§2,5]Denise V. Kratschmar, [1] Alexandra Broyer, A, [3] Olivier Poirot O, [2]Philippe Marbet, [2]Boonrat Chantong, [1,5] Fanny Zufferey, [1] Tania Dos Santos, [3,4] Roman Chrast R, [§2,5]Alex Odermatt, *[§1,5]Florianne Monnet-Tschudi

[1] Department of Physiology, University of Lausanne, Lausanne, Switzerland

[2] Division of Molecular and Systems Toxicology, Department of Pharmaceutical Sciences, University of Basel, Basel, Switzerland

[3] Department of Medical Genetics, University of Lausanne, Switzerland

[4] Department of Neuroscience and Department of Clinical Neuroscience, Karolinska Institute, Stockholm, Sweden

[5] Swiss Centre for Applied Human Toxicology

[§] These authors contributed equally to the work

Contribution:

- Performed gene expression analysis (RT-PCR) of 3D rat brain culture samples

W

W

W

W

W

W

W

W

W

W

W

W

W

W

W

W

W

W

W

W

W

W

W

W

W

W

W

W

W

W

W

W

W

W

W

W

W

W

W

W

W

W

W

W

W

W

W

W

W

W

W

W

W

W

W

W

W

W

W

W

W

W

W

W

W

W

W

W

W

W

W

W

W

W

W

W

W

W

W

W

W

W

W

W

W

W

W

W

W

W

W

W

W

W

W

W

W

W

W

W

W

W

W

W

W

W

W

W

W

W

W

W

W

W

W

W

W

W

W

W

W

W

W

W

W

W

W

W

W

W

W

W

W

W

W

W

W

W

W

W

W

W

W

W

W

W

W

W

W

W

W

W

W

W

W

W

W

W

W

W

W

W

W

W

W

W

W

W

W

W

W

W

W

W

W

W

W

W

W

W

W

W

W

W

W

W

W

W

W

W

W

W

W

W

W

W

W

W

W

W

W

W

W

W

W

W

W

W

W

W

W

W

W

W

W

W

W

W

W

W

W

W

W

W

W

W

W

W

W

W

W

W

W

W

W

W

W

W

W

W

W

W

W

W

W

W

W

W

W

W

W

W

W

W

W

W

W

W

W

W

W

W

W

W

W

W

W

W

W

W

W

W

W

W

W

W

W

W

W

W

W

W

W

W

W

W

W

W

W

W

W

W

W

W

W

W

W

W

W

W

W

W

W

W

W

W

W

W

W

W

W

W

W

W

W

W

W

W

W

W

W

W

W

W

W

W

W

W

W

W

W

W

W

W

W

W

W

W

W

W

W

W

W

W

W

W

W

W

W

W

W

W

W

W

W

W

W

W

W

W

W

W

W

W

W

W

W

W

W

W

W

W

W

W

W

W

W

W

W

W

W

W

W

W

W

W

W

W

W

W

W

W

W

W

W

W

W

W

W

W

W

W

W

W

W

W

W

W

W

W

W

W

W

W

W

W

W

W

W

W

W

W

W

W

W

W

W

W

W

W

W

W

W

W

W

W

W

W

W

W

W

W

W

W

W

W

W

W

W

W

W

W

W

W

W

W

W

W

W

W

W

W

W

W

W

W

W

W

W

W

W

W

W

W

W

W

W

W

W

W

W

W

W

W

W

W

W

W

W

W

W

W

W

W

W

W

W

W

W

W

W

W

W

W

W

W

W

W

W

W

W

W

W

W

W

W

W

W

W

W

W

W

W

W

W

W

W

W

W

W

W

W

W

W

W

W

W

W

W

W

W

W

W

W

W

W

W

W

W

W

W

W

W

W

W

W

W

W

W

W

W

W

W

W

W

W

W

W

W

W

W

W

W

W

W

W

W

W

W

W

W

W

W

W

W

W

W

W

W

W

W

W

W

W

W

W

W

W

W

W

W

W

W

W

W

W

W

W

W

W

W

W

W

W

W

W

W

W

W

W

W

W

W

W

W

W

W

W

W

W

W

W

W

W

W

W

W

W

W

W

W

W

W

W

W

W

W

W

W

W

W

W

W

W

W

W

W

W

W

W

W

W

W

W

W

W

W

W

W

W

W

W

W

W

W

W

W

W

W

W

W

W

W

W

W

W

W

W

W

W

W

W

W

W

W

W

W

W

W

W

W

W

W

W

W

W

W

W

W

W

W

W

W

W

W

W

W

W

W

W

W

W

W

W

W

W

W

W

W

W

W

W

W

W

W

W

W

W

W

W

W

W

W

W

W

W

W

W

W

W

W

W

W

W

W

W

W

W

W

W

W

W

W

W

W

W

W

W

W

W

W

W

W

W

W

W

W

W

W

W

W

W

W

W

W

W

W

W

W

W

W

W

W

W

W

W

W

W

W

W

W

W

W

W

W

W

W

W

W

W

W

W

W

W

W

W

W

W

W

W

W

W

W

W

W

W

W

W

W

W

W

W

W

W

W

W

W

W

W

W

W

W

W

W

W

W

W

W

W

W

W

W

W

W

W

W

W

W

W

W

W

W

W

W

W

W

W

W

W

W

W

W

W

W

W

W

W

W

W

W

W

W

W

W

W

W

W

W

W

W

W

W

W

W

W

W

W

W

W

W

W

W

W

W

W

W

W

W

W

W

W

W

W

W

W

W

W

W

W

W

W

W

W

W

W

W

W

W

W

W

W

W

W

W

W

W

W

W

W

W

W

W

W

W

W

W

W

W

W

W

W

W

W

W

W

W

W

W

W

W

W

W

W

W

W

W

W

W

W

W

W

W

W

W

W

W

W

W

W

W

W

W

W

W

W

W

W

W

W

W

W

W

W

W

W

W

W

W

W

W

W

W

W

W

W

W

W

W

W

W

W

W

W

W

W

W

W

W

W

W

W

W

W

W

W

W

W

W

W

W

W W

W

W

W

W

W

W

W

W

W

W

W

W

W

W

W

W

W

W

W

W

W

W

W

W

W

W

W

W

W

W

W

W

W

W

W

W

W

W

W

W

W

W

W

W

W

W

W

W

W

W

W

W

W

W

W

W

W

W

W

4.2.3 Discussion

This study is a good example for the combined implementation of primary cells, cell lines and an *in vivo* animal model to investigate highly complex and multifactorial pathologies like neurodegenerative diseases. By knowing the strengths and limitations of each model, they can be applied at the appropriate stage of the study course. At the beginning, 3D rat brain cultures were used to examine the contribution of low brain insulin and high GC to TMT-induced neurotoxicity and neuroinflammation. This 3D *in vitro* system offers the complexity of containing all cells types found *in vivo* in a tissue-specific environment while still allowing for easy manipulation of single or multiple external factors to simulate different combinations of known contributors to neurodegeneration. The resulting correlation between microglial reactivity and TMT treatment, which was enhanced by conditions simulating metabolic syndrome, was further investigated in murine BV-2 cells. Cell lines are often used in mechanistic studies as they are available in high numbers and greatly reduce animal to animal variations which would occur in primary cells or during *in vivo* experiments. Additionally, BV-2 cells are a suitable model to study activation of microglia by TMT as they were already shown to closely mimic primary microglia in this aspect [91, 205, 206]. In turn, the interaction with other cells like neurons or astrocytes is lost when using pure microglia cultures which is important as astrocytes were reported to dampen microglial activation in response to TMT treatment in astrocyte-microglia co-cultures [207]. Upon mechanistic investigation of microglial activation by TMT and the modulatory effects of insulin and the MR therein, a mouse model of diabetes was used to investigate the consequences *in vivo*. This approach helps to establish a translational relevance which can barely be achieved by *in vitro* experiments. Indeed, it showed that the activation of BV-2 microglia cells by TMT clearly observed *in vitro* only translates into a minor contribution of neurotoxicity to neurodegeneration *in vivo*. As *in vitro* experiments lack many factors like other contributing cell types or adaptive response mechanisms that *in vivo* could amplify or compensate effects, they should be tested in an *in vivo* model whenever possible.

Especially when investigating neurodegenerative diseases where GC play a role, the difference in the primary GC between rodent and human should be considered. Whereas corticosterone is predominant in rodents, in human periphery it is found to circulate at 10-20 fold lower concentrations than cortisol [208-210]. Also, there is a difference between the cerebrospinal fluid and the peripheral GC levels as endothelial cells of the blood brain barrier highly express a p-glycoprotein membrane pump, which reduces the access of cortisol but not corticosterone to the brain in both rodent and human [211-213]. This leads to a corticosterone concentration of 40 % of all GC in human brain suggesting a role therein, supported by the fact that corticosterone has a higher affinity for human MR than cortisol and the microglial activation in mouse was suggested to be MR mediated [201, 211, 214-216].

To further improve the relevance to human, many 3D models using human stem cells are developed using human pluripotent stem cells (PSCs) or induced pluripotent stem cells (iPSCs) [217]. Unfortunately, when investigating inflammatory components of neurodegenerative diseases, 3D systems established from PSCs used to be of questionable relevance, as they do not contain microglia cells, since those are of embryonic origin [217-219]. However, recently the efficient generation of microglia from human PSCs has been reported and a 3D neural construct including microglia and a vascular network was established, showing ongoing efforts in improving human 3D brain models [220-222]. As human PSCs raise ethical questions, many newly developed models make use of iPSCs, which can be generated from adult cells and even allow a differentiation into microglia like cells [223, 224]. Currently, 3D brain models derived from such cells are being developed offering a valuable tool to investigate complex brain disorders [217, 225].

Overall, the study shows the combined implementation of the microglia cell line BV-2 and more complex 3D rat brain cultures as well as mouse models of diabetes to investigate the combination of multiple factors mediating neurotoxicity. As the final aim is to describe a process in human brain, 3D models of human iPSCs should be taken into account for future studies.

4.3 Implementation of Primary Proximal Tubular Cells

4.3.1 Application of Primary Proximal Tubular Cells to Investigate the Role of the Oxidative Stress Response Pathway in Metabolic Acidosis

Through excretion and reabsorption of amino acids as well as synthesis of bicarbonate (HCO_3^-), the kidney plays an important role in maintaining body pH homeostasis [101]. The *de novo* synthesis of HCO_3^- mainly occurs in the proximal tubule by ammoniagenesis, a multistep process using glutamine to produce ammonium and HCO_3^- [226]. The excreted ammonia acts as a urinary buffer in the filtrate allowing for additional proton excretion whereas the HCO_3^- replaces the fraction already consumed by acids [101, 227]. During metabolic acidosis the extraction rate of glutamine from the plasma is increased, which is most likely mediated to a great extent by basolateral glutamine influx transporters of the proximal tubular cells [226]. SNAT3 is one of those transporters and was found to be upregulated under chronic metabolic acidosis whereas in a *Snat3* KO mouse the excretion of urinary NH_4^+ was reduced [228-231]. Recently, *Snat3* was found to be the most significantly down-regulated transcript in a microarray study comparing WT and *Nrf2* KO mice [232]. *Nrf2* regulates basal and inducible expression of various genes involved in cell defense facilitating a response mechanism against chemical and oxidative stress [233, 234]. This raised the question whether in absence of NRF2 the glutamine efflux transporter SNAT3 can still be induced in kidney in response to metabolic acidosis.

Although a *Nrf2* KO mice is available in which metabolic acidosis can be induced by dietary acid loading, prior to performing *in vivo* experiments, first insights can be gained using a much more controlled *in vitro* setup. As the process under investigation occurs in the proximal tubule *in vivo*, primary PTCs are the model of choice. They allow for siRNA knockdown and can be cultured in acidified medium simulating metabolic acidosis. Additionally, based on own observations, mRNA of *Snat3*, *Nrf2* as well as the NRF2 target gene NAD(P)H-dependent quinone oxidoreductase 1 (*Nqo1*) is detectable in mouse primary PTCs, even though expression of *Snat3* is rather low. Also, the SNAT3 transporter is primarily expressed in the S3 segment of the proximal tubule but can be induced in the S2 segment in response to metabolic acidosis [230, 235, 236]. Therefore, contaminations by cells of other segments possibly introduced by incomplete dissection or faulty separation of the fragments by sieving are negligible since they will most likely not contribute to the process under investigation. Overall, the study tests the usefulness of primary PTCs as a model for NRF2 mediated oxidative response and SNAT3 induction in response to metabolic acidosis.

4.3.2 Submitted Manuscript: NRF2 Regulates the Glutamine Transporter Slc38a3 (SNAT3) in Kidney in Response to Metabolic Acidosis

Adam Lister[1,3+], Soline Bourgeois[2,3+], Pedro H. Imenez Silva[2,3+], Isabel Rubio-Aliaga[2,3], Philippe Marbet[1,3], Joanne Walsh[4], Luke M. Shelton[4], Bettina Keller[2], Francois Verrey[2,3], Olivier Devuyst[2], Pieter Giesbertz[5], Hannelore Daniel[5], Christopher E. Goldring[4], Ian M. Copple[4], Carsten A. Wagner[2,3*], Alex Odermatt[1,3*]

[1] Division of Molecular and Systems Toxicology, Department of Pharmaceutical Sciences, University of Basel, Klingelbergstrasse 50, 4056, Basel, Switzerland; [2] Institute of Physiology, Zürich Centre for Integrative Human Physiology, University of Zürich. Winterthurerstrasse 190, 8057 Zürich, Switzerland; [3]National Center for Competence in Research Kidney.CH, Switzerland, [4] MRC Centre for Drug Safety Science, Department of Molecular and Clinical Pharmacology, University of Liverpool, L69 3GE, UK; [5]ZIEL Research Center of Nutrition and Food Sciences, Department of Biochemistry, Technische Universität München, Freising, Germany

+ contributed equally and share first authorship

Contribution:

- Isolated primary proximal tubular cells and performed experiments

W

W

W

W

W

W

W

W

W

W

W

W

W

W

W

W

W

W

W

W

W

W

W

W

W

W

W

W

W

W

W

W

W

W

W

W

W

W

W

W

W

W

W

W

W

W

W

W

W

W

W

W

W

W

W

W

W

W

W

W

W

W

W

W

W

W

W

W

W

W

W

W

W

W

W

W

W

W

W

W

W

W

W

W

W

W

W

W

W

W

W

W

W

W

W

W

W

W

W

W

W

W

W

W

W

W

W

W

W

W

W

W

W

W

W

W

W

W

W

W

W

W

W

W

W

W

W

W

W

W

W

W

W

W

W

W

W

W

W

W

W

W

W

W

W

W

W

W

W

W

W

W

W

W

W

W

W

W

W

W

W

W

W

W

W

W

W

W

W

W

W

W

W

W

W

W

W

W

W

W

W

W

W

W

W

W

W

W

W

W

W

W

W

W

W

W

W

W

W

W

W

W

W

W

W

W

W

W

W

W

W

W

W

W

W

W

W

W

W

W

W

W

W

W

W

W

W

W

W

W

W

W

W

W

W

W

W

W

W

W

W

W

W

W

W

W

W

W

W

W

W

W

W

W

W

W

W

W

W

W

W

W

W

W

W

W

W

W

W

W

W

W

W

W

W

W

W

W

W

W

W

W

W

W

W

W

W

W

W

W

W

W

W

W

W

W

W

W

W

W

W

W

W

W

W

W

W

W

W

W

W

W

W

W

W

W

W

W

W

W

W

W

W

W

W

W

W

W

W

W

W

W

W

W

W

W

W

W

W

W

W

W

W

W

W

W

W

W

W

W

W

W

W

W

W

W

W

W

W

W

W

W

W

W

W

W

W

W

W

W

W

W

W

W

W

W

W

W

W

W

W

W

W

W

W

W

W

W

W

W

W

W

W

W

W

W

W

W

W

W

W

W

W

W

W

W

W

W

W

W

W

W

W

W

W

W

W

W

W

W

W

W

W

W

W

W

W

W

W

W

W

W

W

W

W

W

W

W

W

W

W

W

W

W

W

W

W

W

W

W

W

W

W

W

W

W

W

W

W

W

W

W

W

W

W

W

W

W

W

W

W

W

W

W

W

W

W

W

W

W

W

W

W

W

W

W

W

W

W

W

W

W

W

W

W

W

W

W

W

W

W

W

W

W

W

W

W

W

W

W

W

W

W

W

W

W

W

W

W

W

W

W

W

W

W

W

W

W

W

W

W

W

W

W

W

W

W

W

W

W

W

W

W

W

W

W

W

W

W

W

W

W

W

W

W

W

W

W

W

W

W

W

W

W

W

W

W

W

W

W

W

W

W

W

W

W

W

W

W

W

W

W

W

W

W

W

W

W

W

W

W

W

W

W

W

W

W

W

W

W

W

W

W

W

W

W

W

W

W

W

W

W

W

W

W

W

W

W

W

W

W

W

W

W

W

W

W

W

W

W

W

W

W

W

W

W

W

W

W

W

W

W

W

W

W

W

W

W

W

W

W

W

W

W

W

W

W

W

W

W

W

W

W

W

W

W

W

W

W

W

W

W

W

W

W

W

W

W

W

W

W

W

W

W

W

W

W

W

W

W

W

W

W

W

W

W

W

W

W

W

W

W

W

W

W

W

W

W

W

W

W

W

W

W

W

W

W

W

W

W

W

W

W

W

W

W

W

W

W

W

W

W

W

W

W

W

W

W

W

W

W

W

W

W

W

W

W

W

W

W

W

W

W

W

W

W

W

W

W

W

W

W

W

W

W

W

W

W

W

W

4.3.3 Discussion

The implementation of mouse primary PTCs revealed many abilities of the system, but also some clear limitations as a model to study oxidative stress response in metabolic acidosis. PTCs were well suited for siRNA depletion of *Nrf2* and tolerated subsequent treatment with acidified medium. Furthermore, *Snat3* mRNA expression was induced in response to decreased pH in scrambled siRNA control cells whereas this did no longer occur in *Nrf2* knockdown cells, indicating an *Nrf2*-dependent regulation of *Snat3*. Finally, the knockdown of *Nrf2* caused a significant downregulation of various NRF2 target genes like *Nqo1*, glutathione S-transferase M1 (*Gstm1*) or glutamate-cystein ligase catalytic subunit (*Gclc*) which is in agreement with observations in *Nrf2* KO animals. Overall, the model is suited to show the regulation of *Snat3* transcription by *Nrf2* in response to medium simulating metabolic acidosis.

However, the study also exposed clear limitations of the primary cell system, limiting its implementation in further mechanistic studies of SNAT3 regulation. The most detrimental limitation is the lack of SNAT3 protein detection under any conditions. This is not surprising, as despite being induced in response to acidified medium the *Snat3* mRNA was detected at rather low levels as revealed by RT-PCR gene expression analysis. The reason for this could simply be de-differentiation, as it often occurs in primary cells since they are taken from their original tissue surrounding providing complex tissue architecture and cultured on 2D culture plates. Another explanation could be the isolation method, which theoretically yields a mixture of fragments of all S1, S2 and S3 segments of the proximal tubule as well as some “impurities” from other segments. While under physiological conditions the SNAT3 transporter was only found to be expressed in the S3 segment its expression is induced in the S2 segment during metabolic acidosis [230, 235, 236]. This raises the possibility, that the applied method of isolation predominantly yields fragments of the S1 segment or that the culture conditions somehow favor the outgrowth of this specific segment. This could be tested by staining the cultures with segment specific markers such as the S3-specific glucose transporter 5 or the solute carrier family 36 member 1 characteristic for the S1 segment [237, 238]. Alternatively, there are established isolation and separation protocols that allow for segment specific preparations using a Percoll density gradient followed by an antibody-based selection [239]. Finally, *in vivo* studies using an *Nrf2* KO mouse model revealed no impairment in the adaption of acid-excretion during metabolic acidosis, most likely due to compensatory changes of other transporters of the kidney or metabolic redirection of glutamine. Since transport effects cannot be detected in a 2D *in vitro* model of primary PTCs due to the lack of access to the basolateral side as it is attached to the culture plate, they do not replace *in vivo* experiments in this aspect.

Overall, *in vitro* experiments with primary PTCs allow for gene knockdown studies and the simulation of oxidative stress responses mediated by *Nrf2* under metabolic acidosis on the

mRNA level. As they do not express SNAT3 protein and since transport functions and compensatory mechanisms cannot be assessed in the current 2D setting they are not applicable for more detailed mechanistic studies of the SNAT3 transporter.

5. General Conclusion and Outlook

The four projects contained in this thesis highlight many abilities but also expose some disabilities of the *in vitro* systems applied therein. Investigating the role of H6PD displayed the versatile implementations of BMDMs in gene expression analysis, cytokine measurements and many macrophage specific functional assays as well as their use in examining phenotypic differentiation processes. Additionally, when looking at the activation of macrophages by CPP concentrations found in CKD patients, the often-reported increased sensitivity of primary cells compared to a respective cell line, in this case the RAW264.7, could be exploited. However, in order to draw conclusions for the situation in human, data generated in mouse models like the BMDMs should be further corroborated with a human model like the human PBMCs to increase translational relevance. Apart from the primary macrophages, the implementation of primary PTCs as a model of metabolic acidosis was evaluated. Whilst they were suitable in a proof-of-concept experiment displaying *Nrf2*-dependent upregulation of the glutamine transporter SNAT3 in response to acidified medium, they could not be applied for further mechanistic investigations due to a lack of SNAT3 protein expression. Overall, certainly the strongest argument for the use of primary cells was the possibility of deriving them from WT and *H6pd* KO or *Nrf2* KO mice, as this circumvents the use of incomplete gene knockdown procedures which could influence normal cell behavior.

Currently, many efforts are being undertaken into the direction of models more relevant to human, but gaining human primary cells or tissue is rather difficult for many reasons. Whereas monocytes can be derived from easily accessible PBMCs, gaining other cell types often relies on control samples taken during biopsies of a diseased organ or even require a body donation which mostly represents the aged population. Cells derived from control biopsies might unknowingly be affected by the neighboring diseased sections and therefore not always represent the situation in health. This could result in higher donor variability making it necessary to use higher numbers of donors to get significant results, further limiting the use of such sources. Probably the most promising approach to circumvent those problems are human iPSCs gained from mature somatic cells by treatment with specific factors [223]. The iPSC technology has the potential to generate improved *in vitro* models in all areas discussed in this thesis such as the investigation of neurodegenerative processes, macrophage research, and modelling of kidney pathologies. Brain research could profit from the recent development in 3D brain models generated from human iPSC of patients, which allows for example to generate organoids mimicking Alzheimer's disease *in vitro* [217]. Furthermore, in the field of macrophage research the iPSC technology enables high throughput generation of disease specific macrophages from patient derived human iPSCs, which is a powerful tool to study macrophage function and differentiation in health and various disorders [240, 241]. Finally, the modelling of kidney diseases and nephrotoxicity screening could vastly be improved by human

iPSC-derived kidney organoids reported to contain complete nephrons with all relevant segments [242].

Even though the human iPSC-technology will continue to improve *in vitro* models in most research fields, primary cell models like BMDMs or primary PTCs will probably remain viable tools. Especially in basic research or proof-of-concept experiments, they are an appropriate method when balancing ease of use and relevance.

6. Acknowledgements

I would like to thank Prof. Alex Odermatt for his constant support, valuable guidance and for giving me the opportunity to conduct this thesis in his laboratory. In addition, I thank Prof. Jörg Huwyler for co-refereeing my PhD thesis. Further, I would like to thank Dr. Petra Klusonova and Dr. Julia Birk for handling the animal colonies and Dr. Denise Kratschmar for the helpful project inputs. Also, I thank all the people I could collaborate with on the different projects. Finally, my sincere thanks goes to all members from the group of Molecular and Systems Toxicology for the project discussions, their support and the good time we had together and to my family for their continuous support throughout my thesis.

7. Appendix

7.1 Supplementary of Chapter 4.1.2

Table 1: Primer Sequences

	Forward	Reverse
Ppia	CAAATGCTGGACCAAACACAAACG	GTTCATGCCTTCTTTCACCTTCCC
Gr	TGCTATGCTTTGCTCCTGATCTG	TGTCAGTTGATAAAACCGCTGCC
11β-hsd1	TGGTGCTCTTCCTGGCCTACT	CCCAGTGACAATCACTTTCTTT
H6pd	CTTGAAGGAGACCATAGATGCG	TGATGTTGAGAGGCAGTTCC
inos	ATGAGGTACTCAGCGTGCTCCA	CCACAATAGTACAATACTACTT
Mcp-1	TTAAAAACCTGGATCGGAACCAA	GCATTAGCTTCAGATTTACGGGT
Il-1β	CAACCAACAAGTGATATTCTCCATG	GATCCACACTCTCCAGCTGCA
Tnfα	CTTCTGTCTACTGAACTTCGGG	TGTCTTTGAGATCCATGCCG
Il-6	TCCAGTTGCCTTCTTGGGAC	AGTCTCCTCTCCGGACTTGT
Cd206	CTCTGTTCAGCTATTGGACGC	TGGCACTCCCAAACATAATTTGA
Ym1	GATGCAGAACAATGAGATCACC	ATGGTAGTGAAAGGAGCAGTTC
Fizz1	AAGCCTACACTGTGTTTCCTTTT	GCTTCCTTGATCCTTTGATCCAC

7.2 Supplementary of Chapter 4.1.5

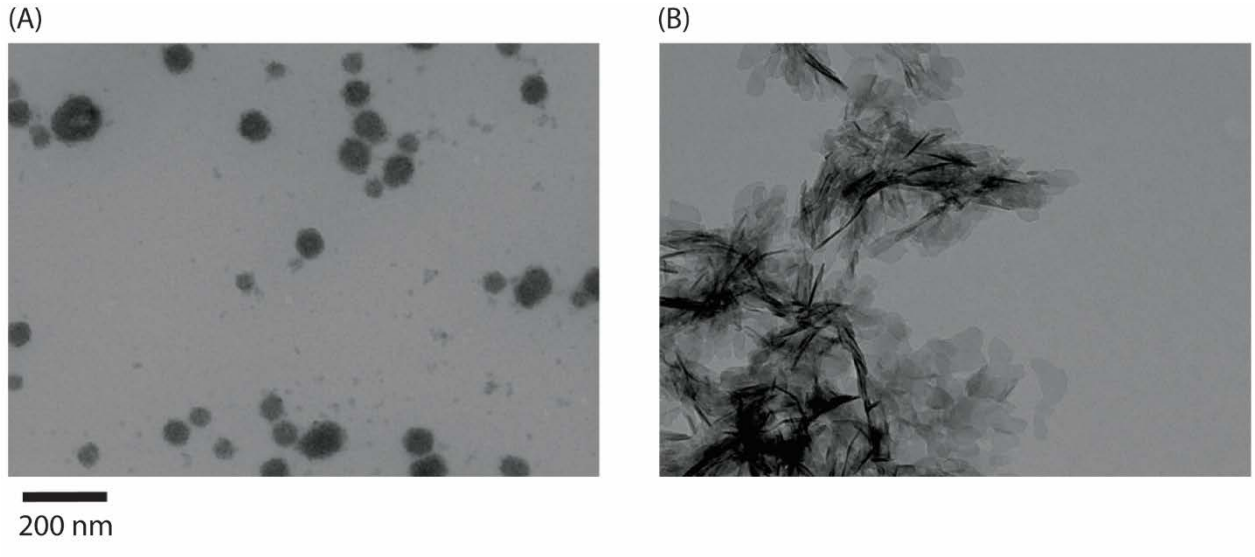

Supplemental Figure I. Validation of Artificial 1ºCPP and 2ºCPP Size and Architecture by Transmission Electron Microscopy

Artificial 1ºCPP (A) and 2ºCPP (B) were generated as described in the Materials and Methods section. The resulting CPP were subsequently imaged using transmission electron microscopy.

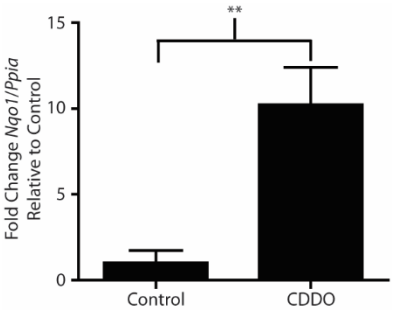

Supplemental Figure II. CDDO-Me Increased the Transcription of the Nrf2 Target Gene *Nqo1* in Primary Murine Bone Marrow-Derived Macrophages

Primary bone marrow-derived macrophages isolated from C57BL6 mice were exposed to CDDO-Me at a concentration of 30 nM or a vehicle control for a period of 12 h. Resulting transcription of the Nrf2 target gene *Nqo1* was measured by real-time PCR and normalized to the house-keeping gene *Ppia*. Statistical analyses were performed using a Mann-Whitney test, and represented as follows: ($p \leq 0.05$ = *), ($p \leq 0.01$ = **) and ($p \leq 0.005$ = ***)

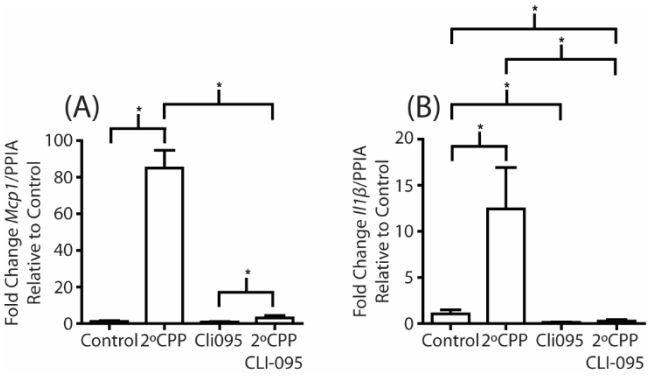

Supplemental Figure III. 2°CPP-Induced Transcription of *Mcp1* and *Il-1β* by Raw 264.7 Macrophages was Attenuated Upon Pre-Treatment with the TLR4 Suppressing Chemical CLI-095

Raw 264.7 cells were exposed to 2°CPP at a concentration of 100 µg/ml calcium content, 3 µM Cli-095 or a combination of both. Cli-095 was exposed to macrophages 1 h prior to 2°CPP administration. Following 2°CPP administration cells were incubated for 12 h. Following this gene transcription of *Mcp1* (A) and *Il-1β* (B) was measured by real-time PCR and normalized to the house-keeping gene *Ppia*. Statistical analyses were performed using a Mann-Whitney test, and represented as follows: ($p \leq 0.05$ = *), ($p \leq 0.01$ = **) and ($p \leq 0.005$ = ***)

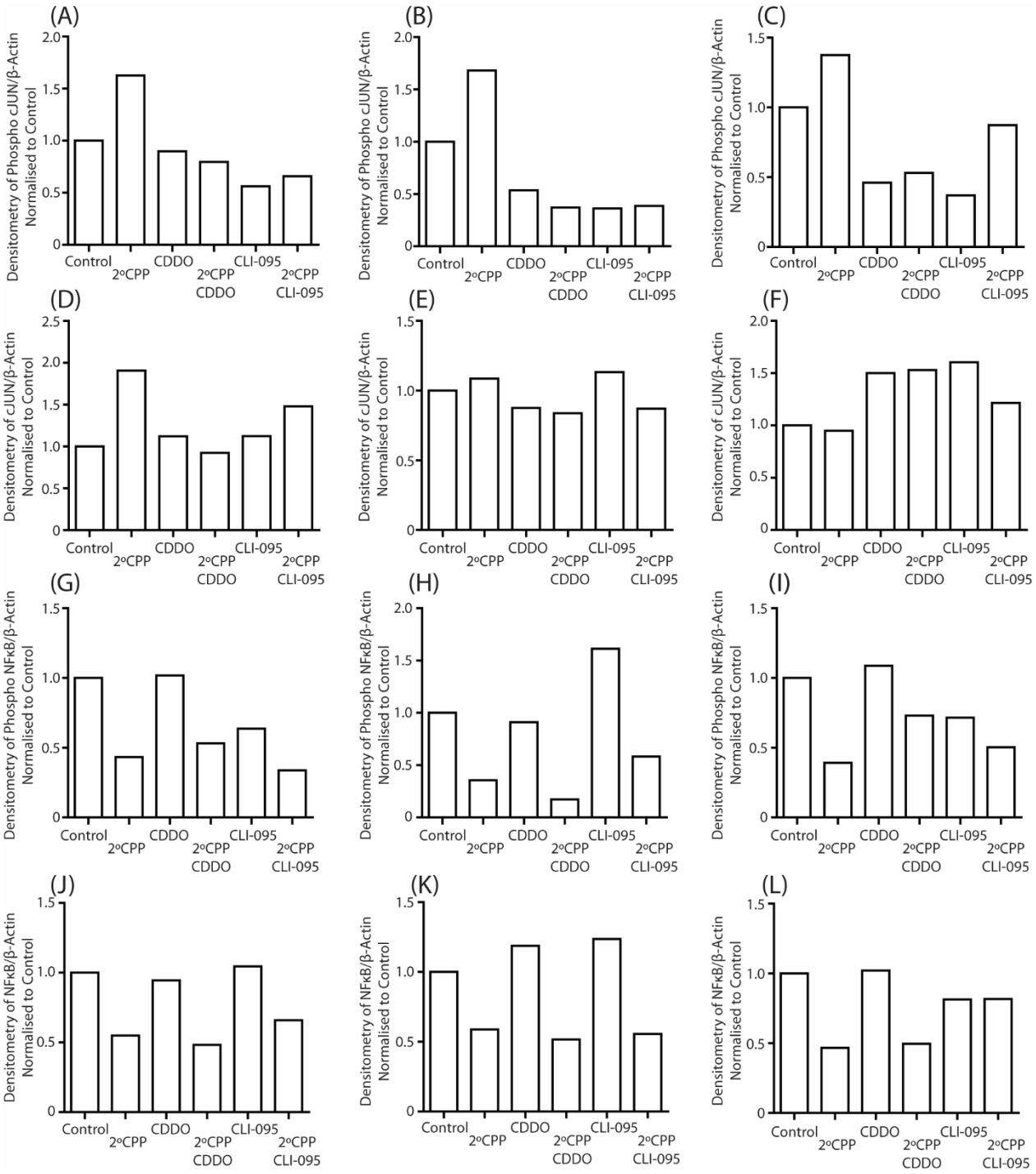

Supplemental Figure IV. 2ºCPP Activate JNK/AP-1 Signaling Through TLR4 and Reduce Phosphorylated and Total NFκB p65 Levels Through a TLR4- and Nrf2-Independent Mechanism

RAW 264.7 cells were exposed to 2°CPP at a concentration of 100 µg/ml calcium content, 30 nM CDDO-Me or a combination of both for 12 h. In the same experiment, RAW 264.7 cells were also exposed to 3 µM CLI-095 for 13 h, or pre-exposed to 3 µM CLI-095 for 1 h before administration of 2ºCPP at a concentration of 100 µg/ml calcium content and incubation for another 12 h. Cell lysates were assessed for protein content of phosphorylated cJUN (A-C), cJUN (D-F), phosphorylated NF-κB p65 (G-I), NF-κB p65 (J-L) and the house-keeping protein β-ACTIN by Western blot. Densitometry was performed on all Western blots with the resulting densitometry data for each blot presented.

Supplemental Table I: Oligonucleotide primers used for RT-PCR

Gene	Primer	Sequence
Mouse Ccl2 (***Mcp1***)	Sense	GCATTAGCTTCAGATTTACGGGT
	Antisense	GGGCCTCTTCTGCGATTTC
Mouse ***Il-1β***	Sense	CAACCAACAAGTGATATTCTCCATG
	Antisense	GATCCACACTCTCCAGCTGCA
Mouse ***Tnf-α***	Sense	CTTCTGTCTACTGAACTTCGGG
	Antisense	TGTCTTTGAGATCCATGCCG
Mouse ***Nqo1***	Sense	TTTAGGGTCGTCTTGGCAAC
	Antisense	GTCTTCTCTGAATGGGCCAG
Mouse ***Ppia***	Sense	CAAATGCTGGACCAAACACAAACG
	Antisense	GTTCATGCCTTCTTTCACCTTCCC

7.3 Supplementary of Chapter 4.2.2

Supplemental figure 1

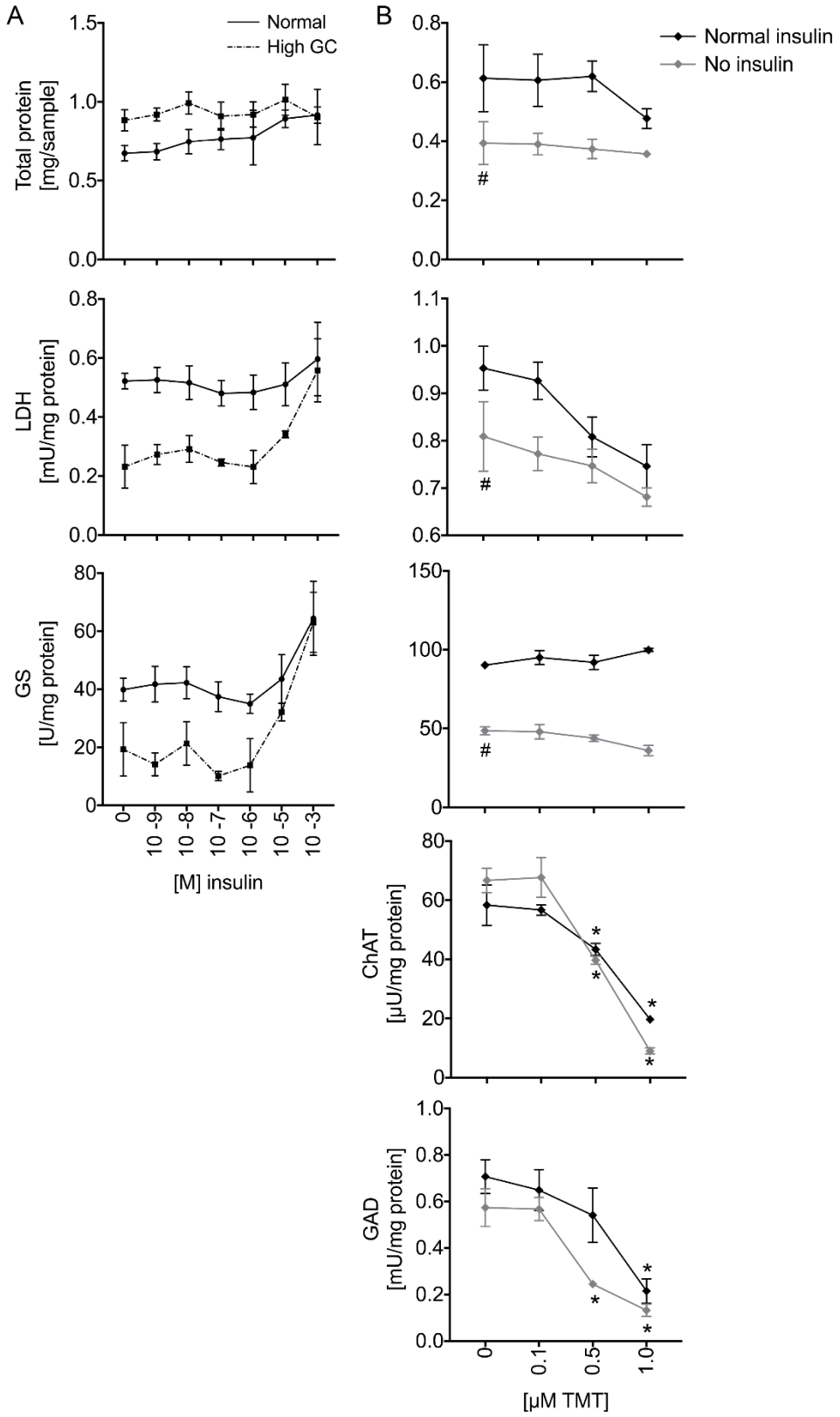

Supplementary Figure 1

Effects of insulin and GC on 3D rat brain cell cultures. (**A**) **Dose response of 0 up to 1 mM insulin in normal versus high GC medium of 3D cell cultures**. Effects were assessed at DIV31, after 10 day treatment. Effects on cell death were assessed, by total protein content and intracellular LDH, and effects on astrocytes, by GS activity measurement. (**B**) **Effect of normal insulin versus no insulin in combination with TMT-treatment**. Aggregates were treated with 0.1, 0.5, and 1 µM of TMT, and effects were assessed on cell death, by total protein content and intracellular LDH, on astrocytes, by GS activity measurement, and on neurons by activity measurement of ChAT and GAD.

Statistical significance is indicated with * for effect of the TMT treatment as compared to the control (CTR/0), and with # for effects of the medium alone. Two-way ANOVA was performed and significance was determined for p-values below 0.05.

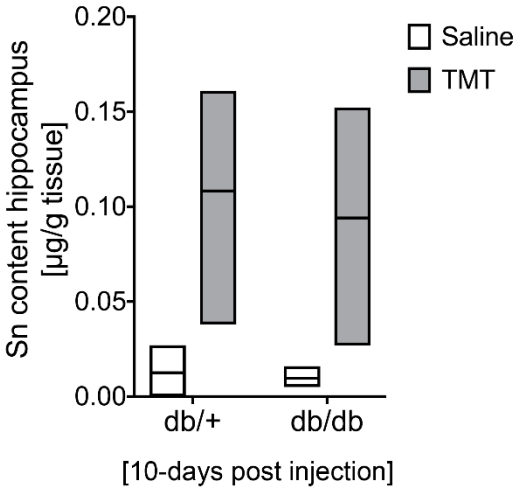

Supplementary Figure 2

TMT level in brain of lean versus obese mice. TMT in the anterior brain was indirectly estimated by measuring the amount of Sn by inductively coupled plasma mass spectrometry (ICP-MS). The Sn concentration (µg/g of brain tissue) was compared between db/+ and db/db and showing overall similar brain Sn concentrations for the two genotypes (grey bars). Graphs show min-max distribution of a minimum of five individuals per groups, line at mean.

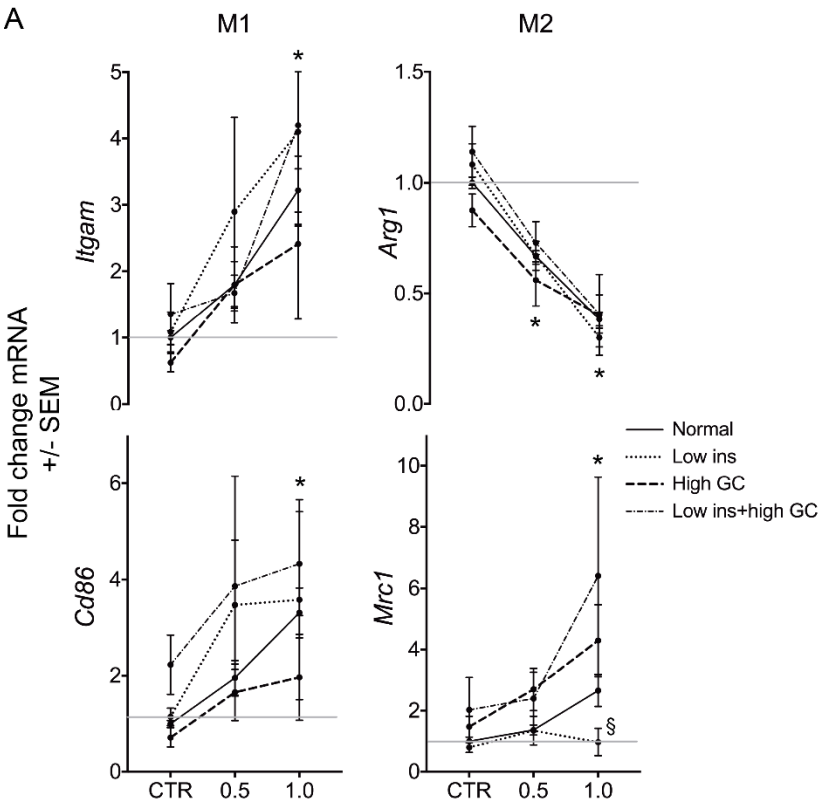
A
M1
M2
Fold change mRNA
+/- SEM
Itgam
Arg1
Cd86
Mrc1
Normal
Low ins
High GC
Low ins+high GC
CTR
0.5
1.0
*
§

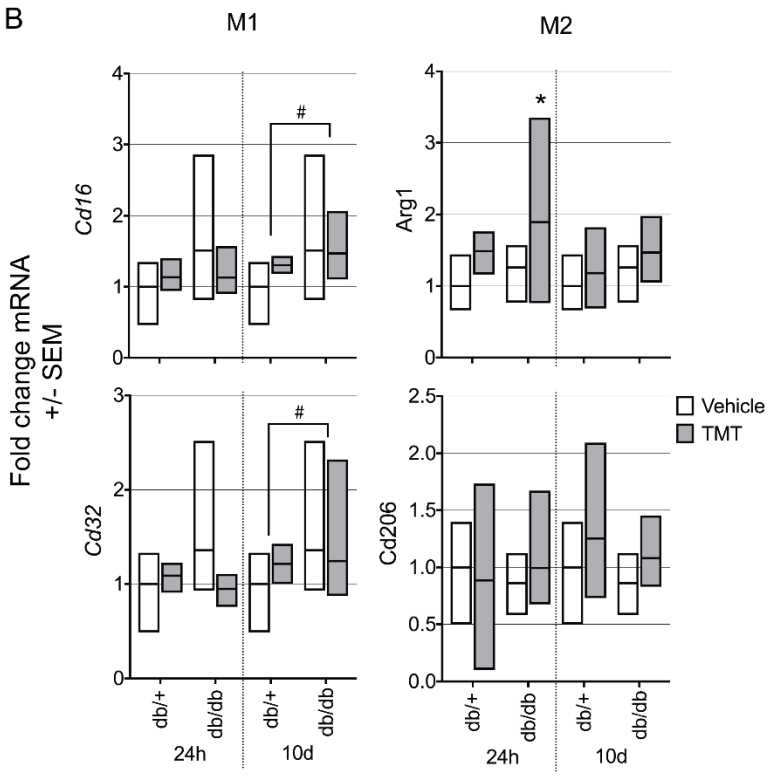
B
M1
M2
Fold change mRNA
+/- SEM
Cd16
Arg1
Cd32
Cd206
Vehicle
TMT
#
*
db/+
db/db
24h
10d

Supplementary Figure 3

Microglial phenotype markers in 3D rat brain cell model (A) and in brain of lean versus obese mice (B). (**A**) 3D rat brain cell cultures maintained in normal, low insulin, high GC and low insulin combined to high GC medium, respectively. Results are expressed as fold change of untreated cultures maintained under normal conditions. mRNA expression of M1 markers *Integrin alpha M* (*Itgam*) and *Cluster of differentiation 86* (*Cd86*), and M2 markers *Arginase 1* (*Arg1*) and *Mannose receptor 1* (*Mrc1*). Data represent the mean of 9 replicates derived from 3 independent experiments. The effect of TMT was found to be significant for all four genes, whereas insulin alone affected *Cd86* expression, and GC alone had a significant effect on *Mrc1*.

Microglial phenotype markers in BKS db mice. (B) M1 microglial markers Cluster of differentiation 16 and 32 (*Cd16, Cd32*), and M2 markers Arginase 1 (*Arg1*) and cluster of differentiation 206 *Cd206* at stages 24 h and 10 days post TMT injection. Graph shows min-max distribution of expression determined in 4 animals of the vehicle group, and 7 animals of the TMT group, horizontal bar at mean. *Cd16* and *Cd32* expression was tendentially higher in saline treated db/db as compared to db/+ (P=0.061 and 0.072 respectively), no such tendencies were present in the TMT-treated groups. In the 10 day post-injection group *Cd16* and *Cd32* was higher in db/db groups as compared to db/+, showing effect for the genotype alone. *Arg1* was significantly upregulated in 24 h TMT-treated db/db animals compared to db/+, this difference was no longer present after 10 days.

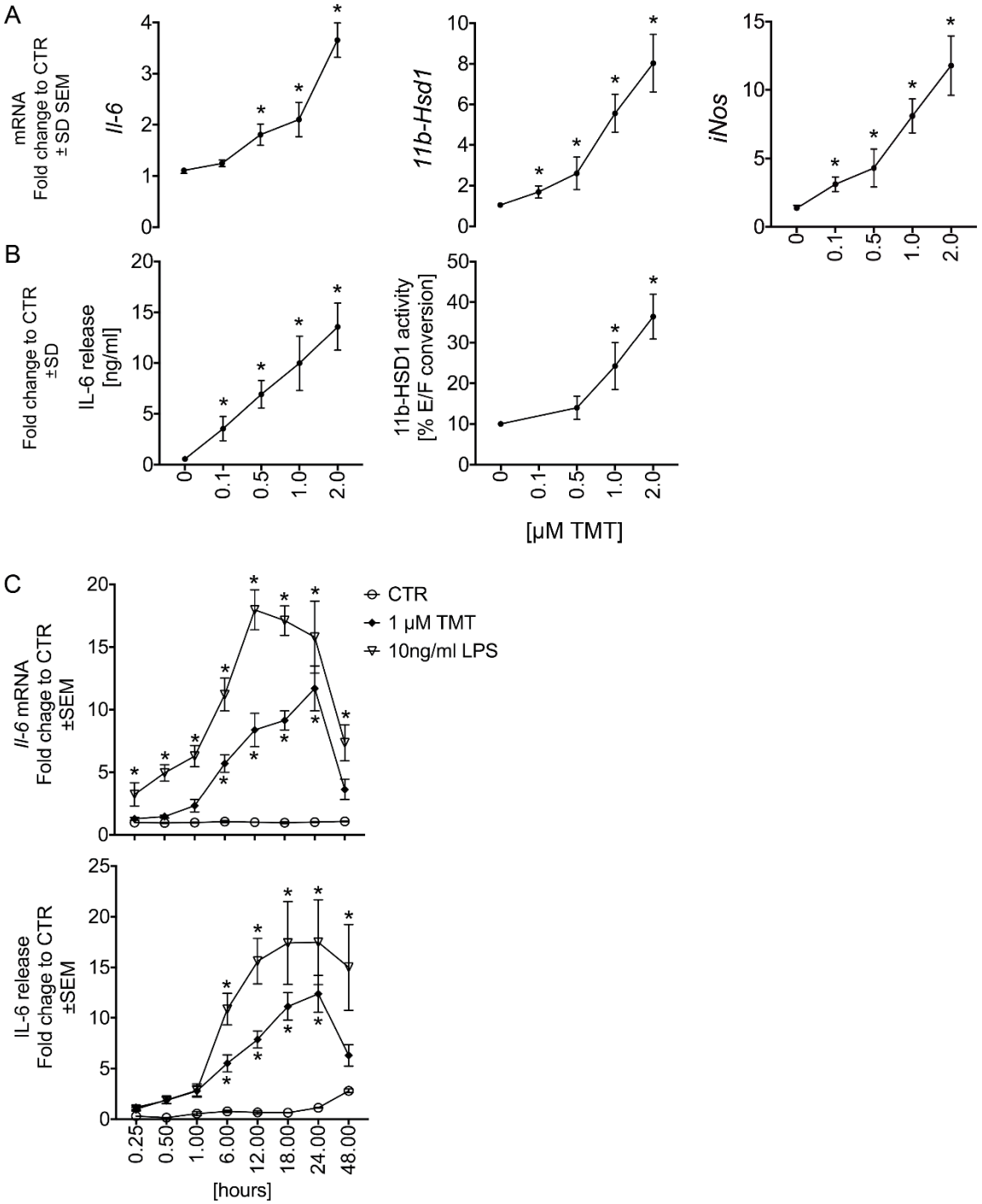

Supplementary Figure 4

Concentration- and time-dependent effects of TMT in BV-2 microglial cells.

(**A-B**) Cells were treated with TMT at concentrations ranging from 0.1 to 2 µM for 24 h. **(A)** Expression of *Il-6, 11β-Hsd1* and *iNos* mRNA upregulated in a TMT concentration-dependent manner. (**B**) TMT concentration-dependent increased release of IL-6 in the culture medium as measured by ELISA, and increased 11β-HSD1 activity as assessed by the conversion of cortisone to cortisol (% E/F conversion). **(C)** BV-2 cells were treated either with TMT (1 µM) or

LPS (10 ng/ml) for 0.25, 0.5, 1, 6, 12, 24 and 48 h. Expression and release of IL-6 was measured as above, revealing the peak at 18-24 h of exposure. Results represent mean ± SEM of three independent experiments. Significance was determined by one-way ANOVA followed by Tukey's posttest, *$p < 0.05$.

7.4 Supplementary of Chapter 4.3.2

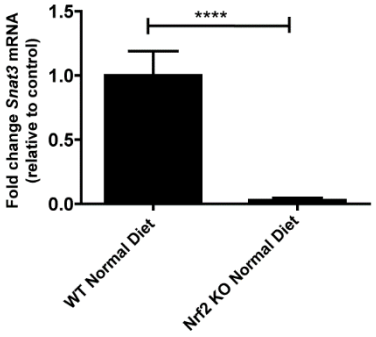

Supplemental Figure S1 Confirmation of *Snat3 depletion in Nrf2* KO kidney. WT and *Nrf2* KO mice were fed a normal diet and *Snat3* mRNA expression in the kidney was determined by qPCR analysis. Statistical analysis for qPCR was performed with a student's paired t-test ****P≤0.0001.

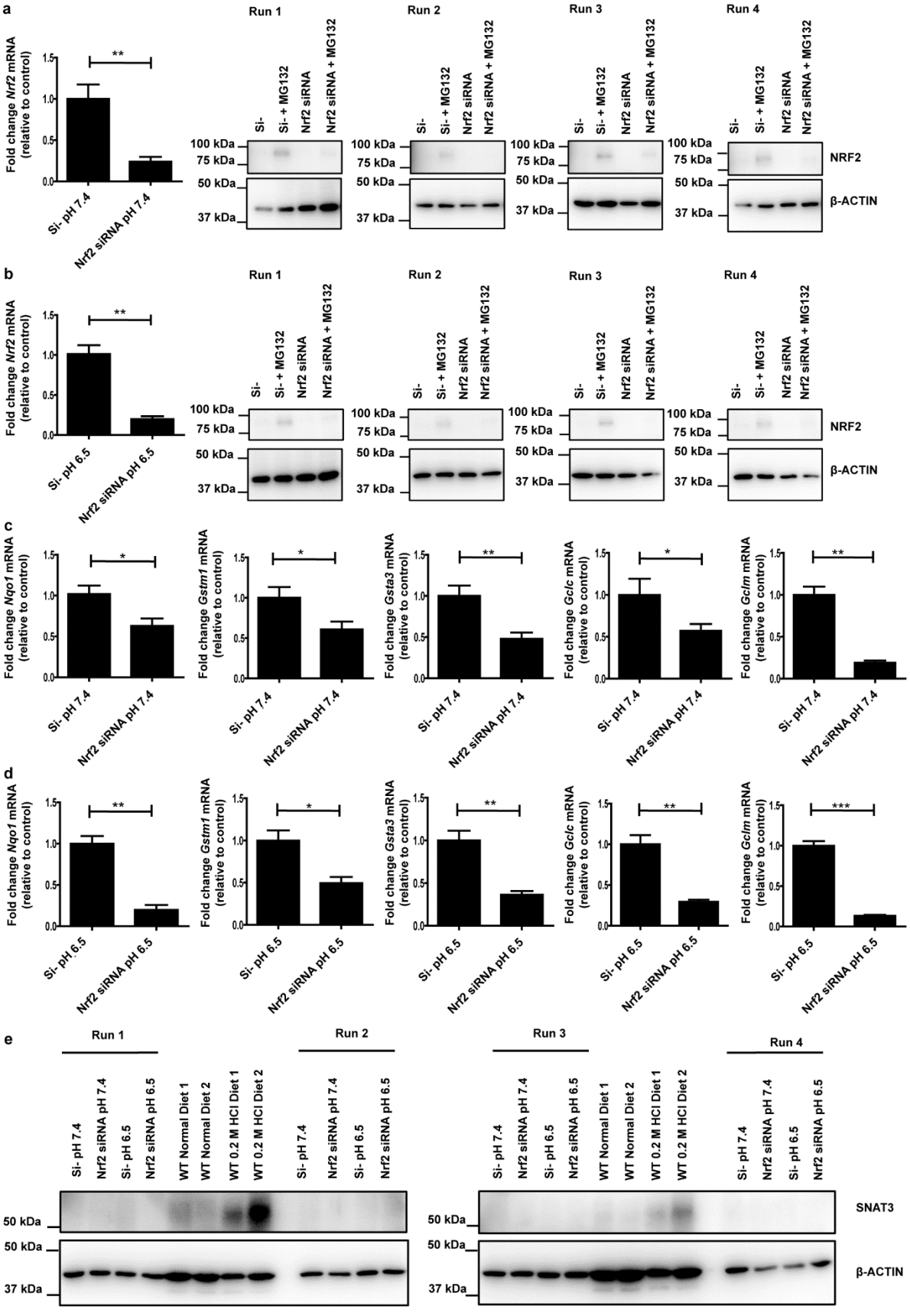

Supplemental Figure S2 Characterization of primary proximal convoluted tubular cells (PCT) as a model to investigate the biological mechanisms of action of the SNAT3 transporter. Confluent isolated

PCT were either transfected with 20 nM siRNA targeting *Nrf2* or the non-targeting scrambled control, si-. Following incubation for 24 h, cells were exposed to media adjusted to pH 7.4 or 6.5 for a further 24 h. Due to its short half-life, in order to visualize the NRF2 protein, cells were exposed to the proteasome inhibitor MG132 at 10 µM for 2 h prior to lysis. QPCR and immunoblotting confirmed the depletion of *Nrf2* mRNA and protein following *Nrf2* siRNA in PCT cells cultured in medium adjusted to **a,** pH 7.4 and **b,** 6.5. QPCR confirmation of the depletion of the NRF2 target genes *Nqo1*, *Gstm1*, *Gsta3, Gclc* and *Gclm* following *Nrf2* siRNA in primary PCT cultured in medium adjusted to **c,** pH 7.4 and **d,** 6.5. **e,** SNAT3 protein levels following *Nrf2* siRNA in primary PCT cultured in medium adjusted to pH 7.4 and 6.5. Whole kidney lysates from WT normal diet and WT HCl diet animals were used as a positive control. 25 µg of sample and control protein were loaded for all immunoblots. The mRNA levels were normalized to *Ppia*. β-ACTIN was used as a house-keeping protein control. Data represent mean ± S.D. of n=4 independent PCT preparations. Statistical analysis for qPCR was performed with a student's paired t-test *P≤0.05; **P≤0.01.

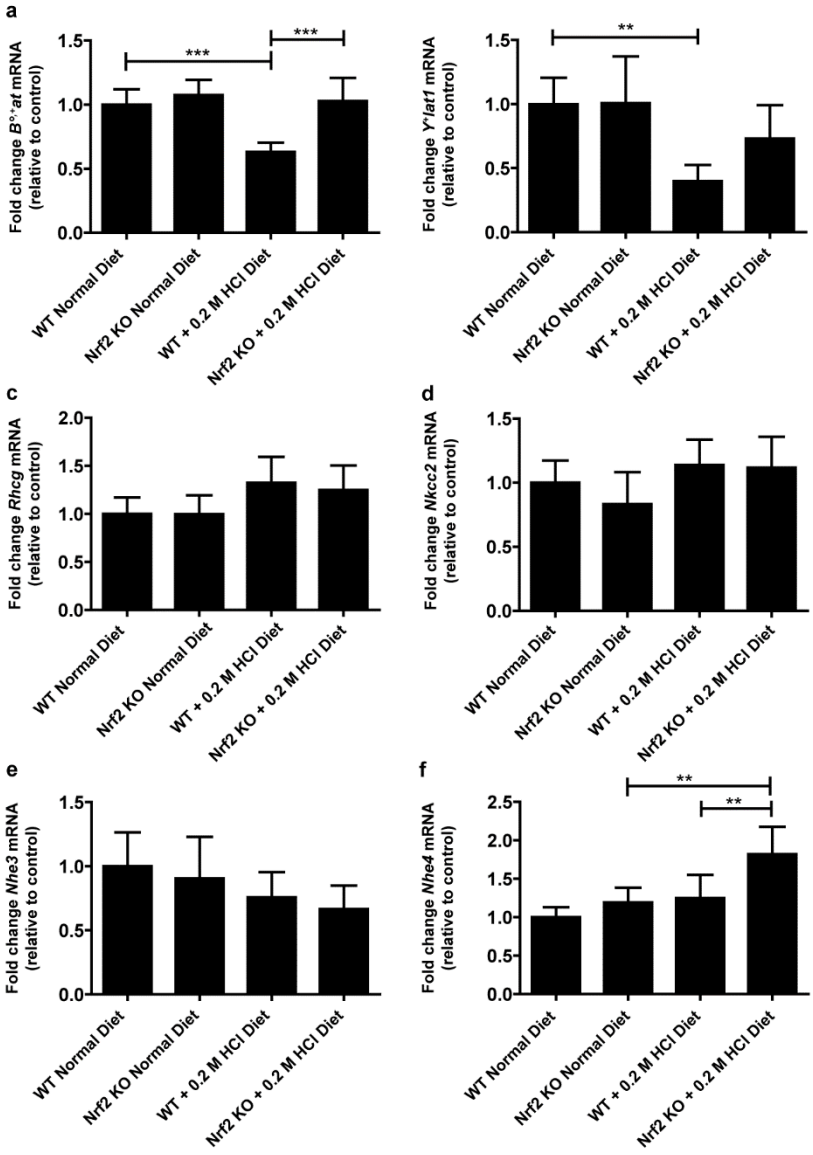

Supplementary Figure S3 The proton handling transporter *Nhe4* may help to compensate for the loss of *Snat3* in *Nrf2* KO kidney upon metabolic acidosis**.** WT and *Nrf2* KO mice were fed a normal diet or a 0.2 M HCl containing diet for 7 days. qPCR analysis of the kidney transporters for; amino acids, **a-b**, *B°,⁺at* and *y⁺Lat1*, **c** -**d** for ammonium *Rhgc* and *Nkcc2*, and **e-f** the sodium/proton exchangers *Nhe3* and *Nhe4*. mRNA values were normalized to *Ppia*. Data represent mean ± S.D. of n=6 animals per group. Statistical analysis was performed with a one-way analysis of variance (with Tukey's post test); *P≤0.05; **P≤0.01; ***P≤0.001.

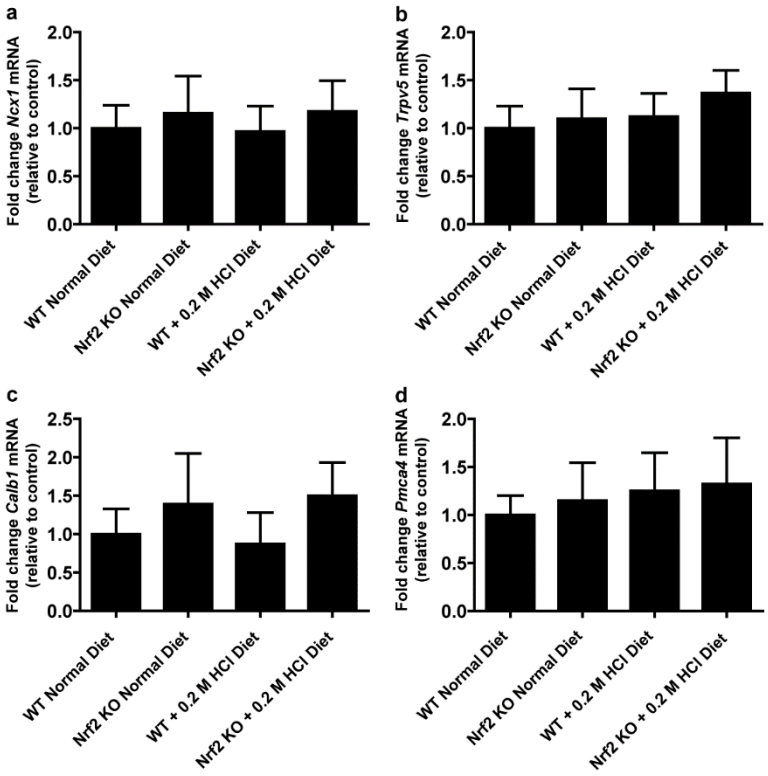

Supplementary Figure S4 Metabolic acidosis caused no changes in the mRNA expression of proteins involved in renal calcium handling in *Nrf2* KO kidney. WT and *Nrf2* KO mice were fed a normal diet or a 0.2 M HCl containing diet for 7 days. qPCR analysis for **a**, *Ncx1*, **b**, *Trpv5*, **c**, *Calb1* and **d**, *Pmca4a*. mRNA values were normalized to *Ppia*. Data represent mean ± S.D. of n=6 animals per group.

a

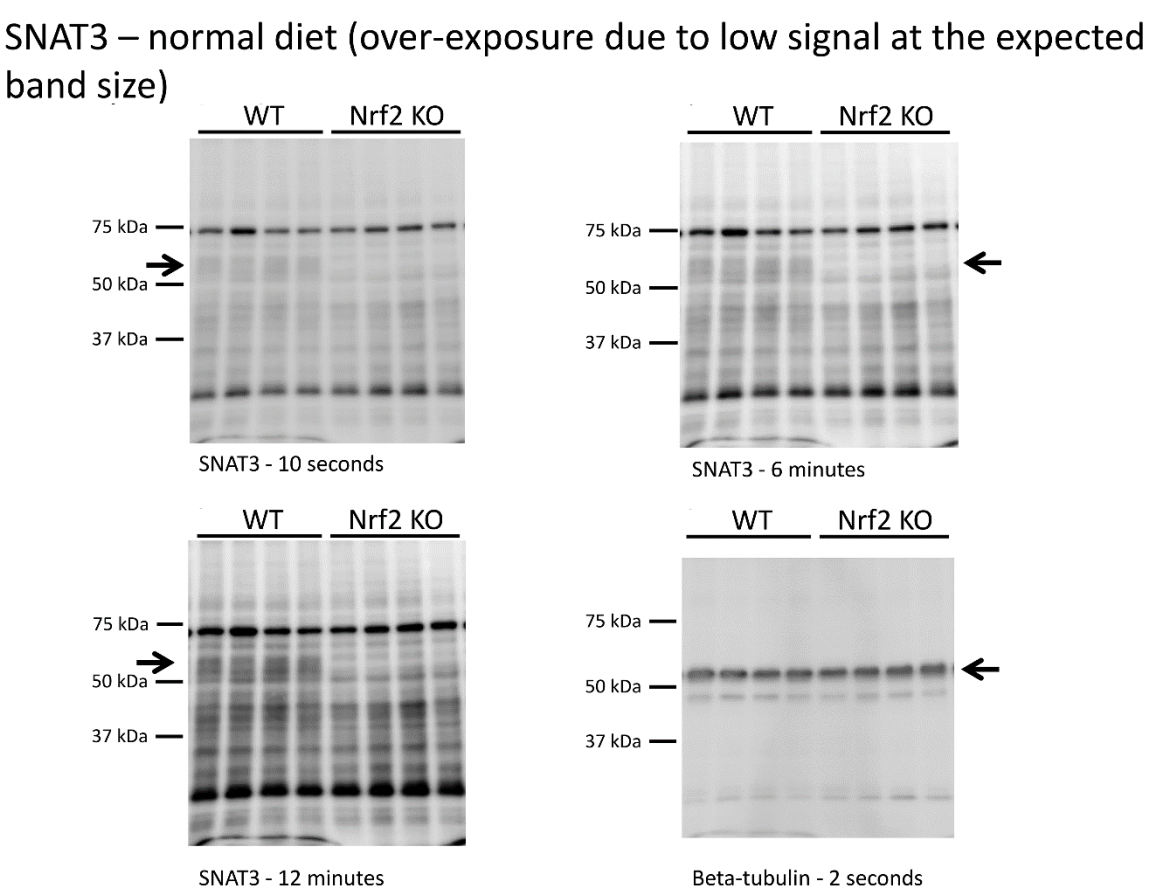

b

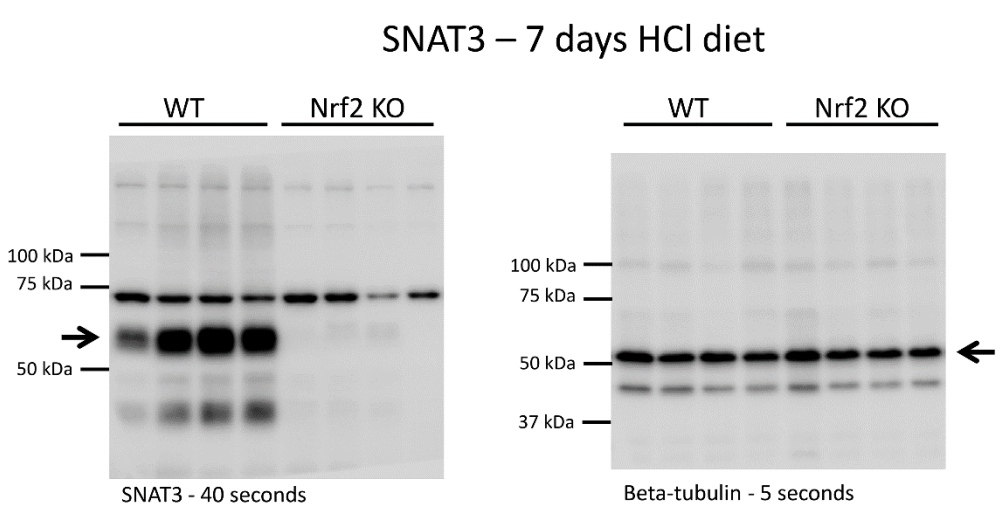

Supplementary Figure S5 Original full-length images used to create the cropped blots shown in Figure 1. **a**, SNAT3 expression under normal diet, **b**, SNAT3 expression upon 7 days HCl diet. Arrows indicate the band quantified by densitometry. Exposure time is shown below each western blotting image.

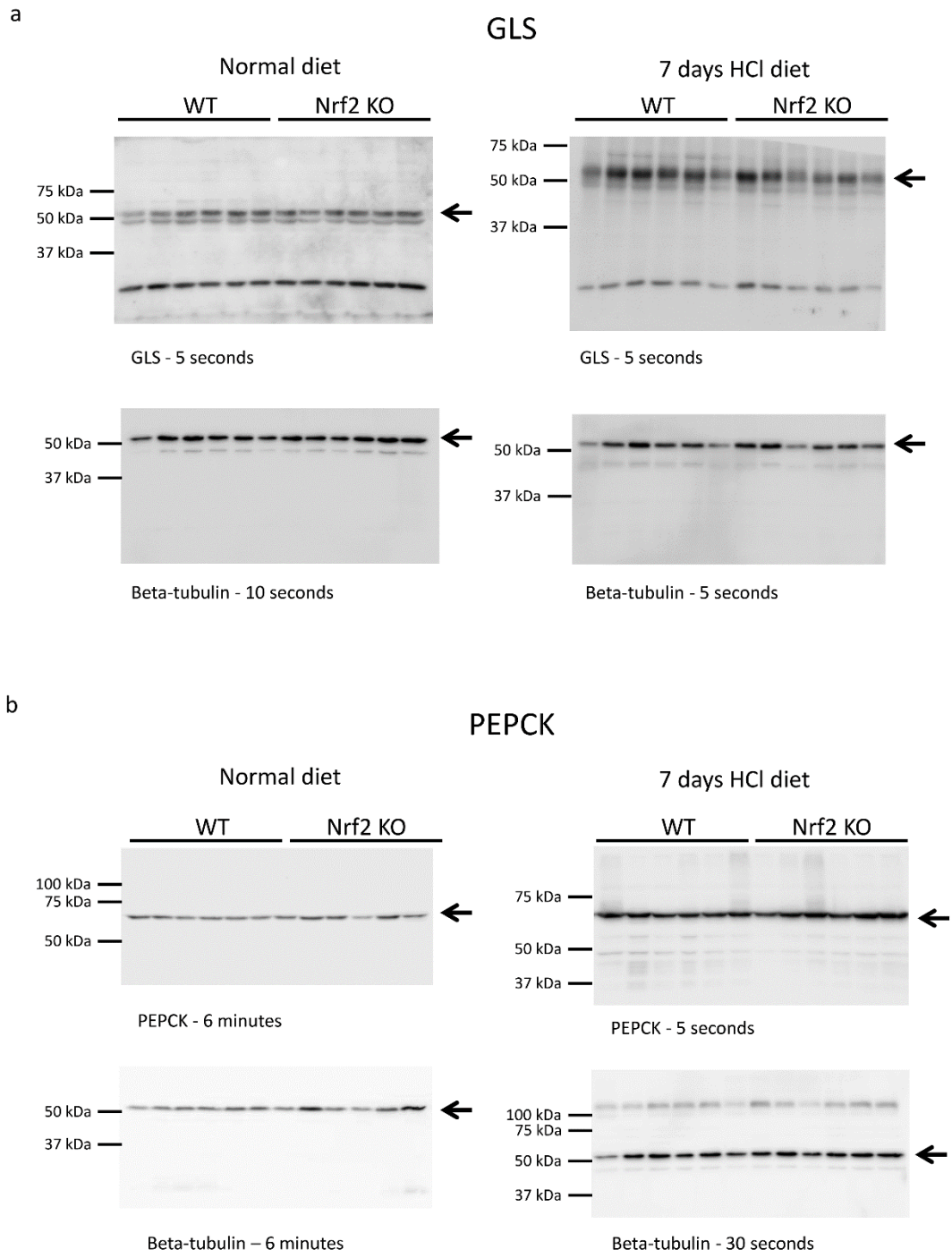

Supplementary Figure S6 Original full-length images used to create the cropped blots shown in Figure 2. **a**, GLS expression, **b**, PEPCK expression. Arrows indicate the band quantified by densitometry. Exposure time is shown below each western blotting image.

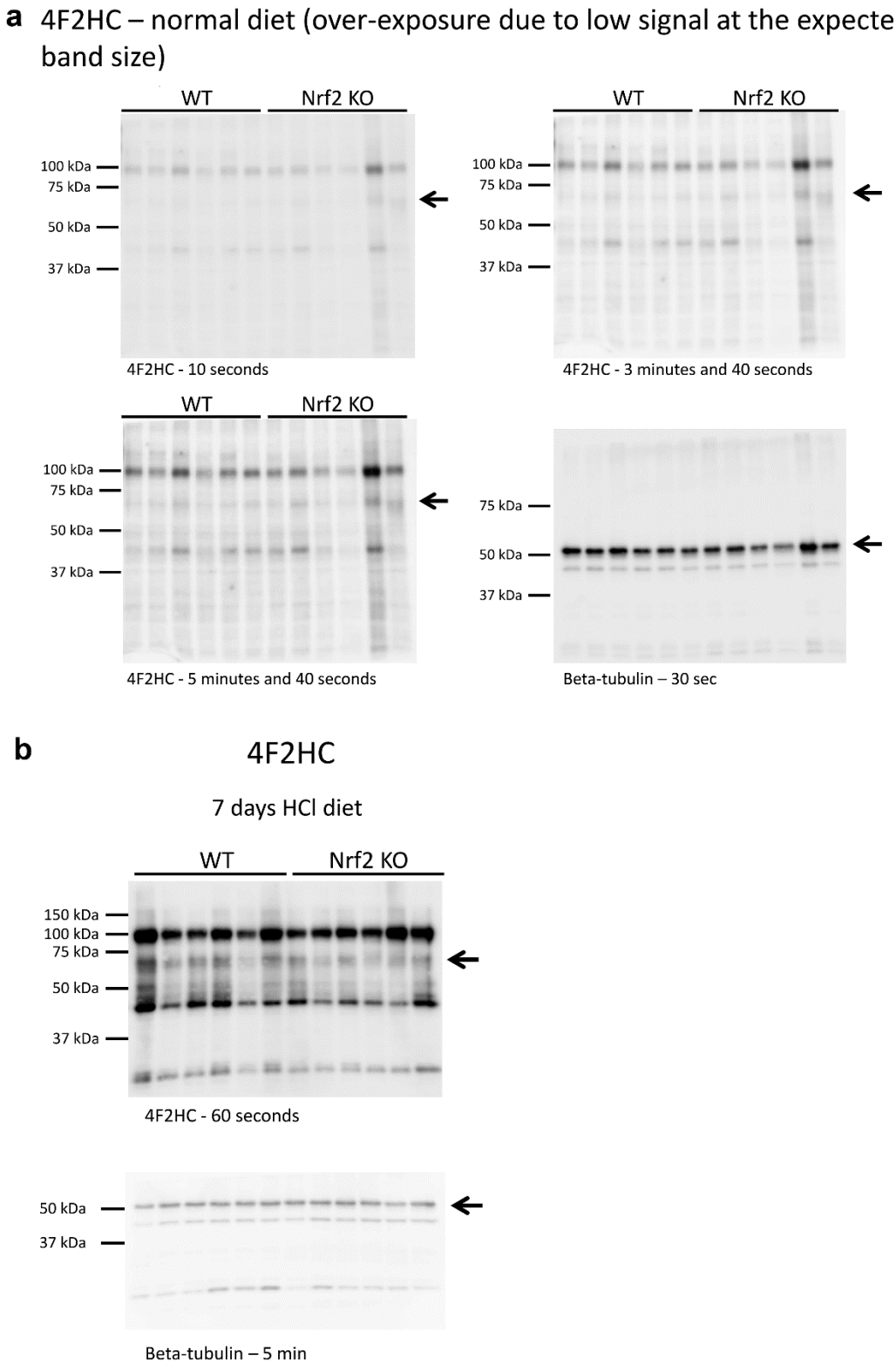

Supplementary Figure S7 Original full-length images used to create the cropped blots shown in Figure 4a-b. **a**, 4F2HC expression under normal diet, **b**, and upon 7 days HCl diet. Arrows indicate the band quantified by densitometry. Exposure time is shown below each western blotting image.

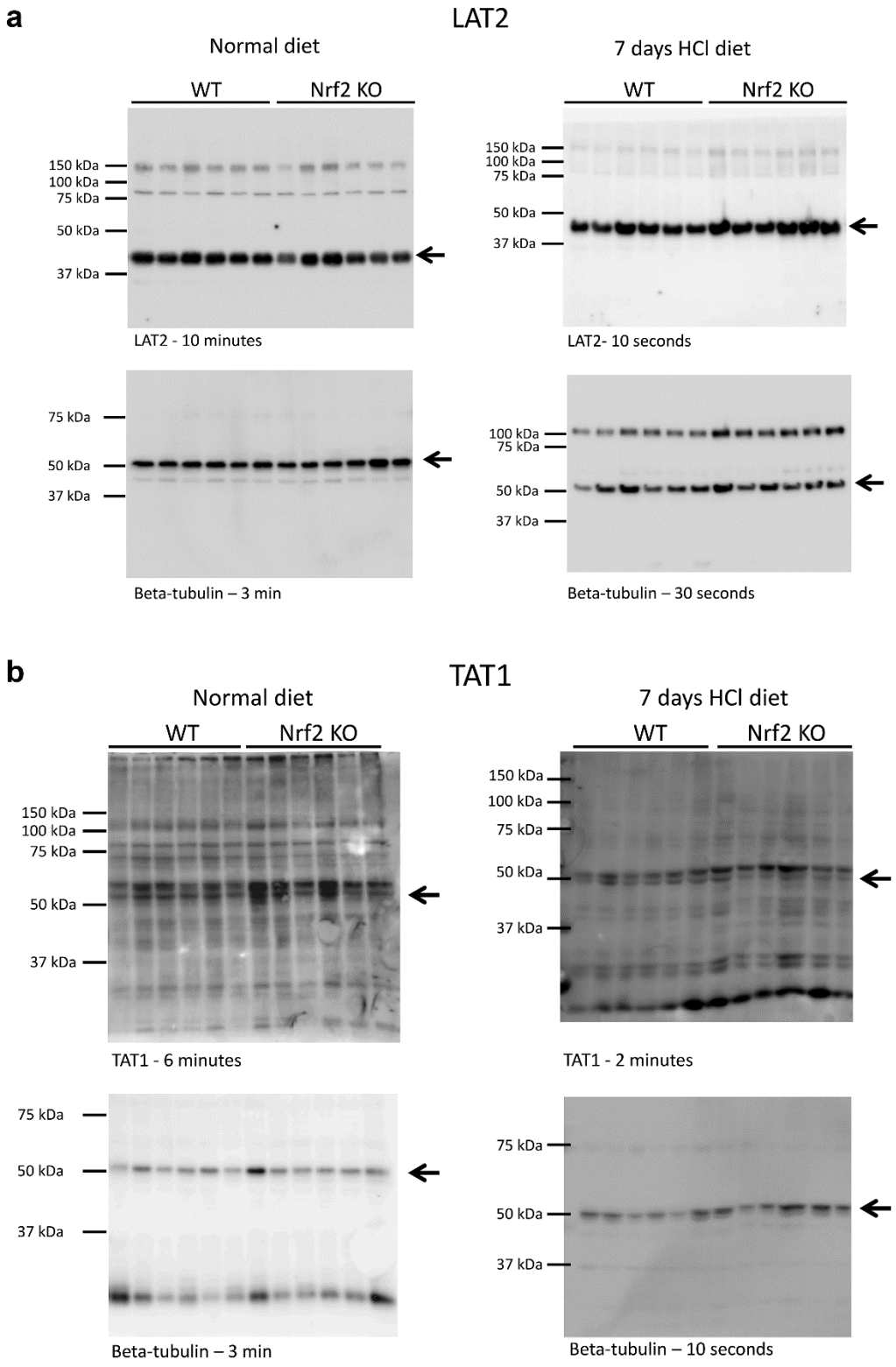

Supplementary Figure S8 Original full-length images used to create the cropped blots shown in Figure 4c-f. **a**, LAT2, **b**, TAT1 expression. Arrows indicate the band quantified by densitometry. Exposure time is shown below each western blotting image.

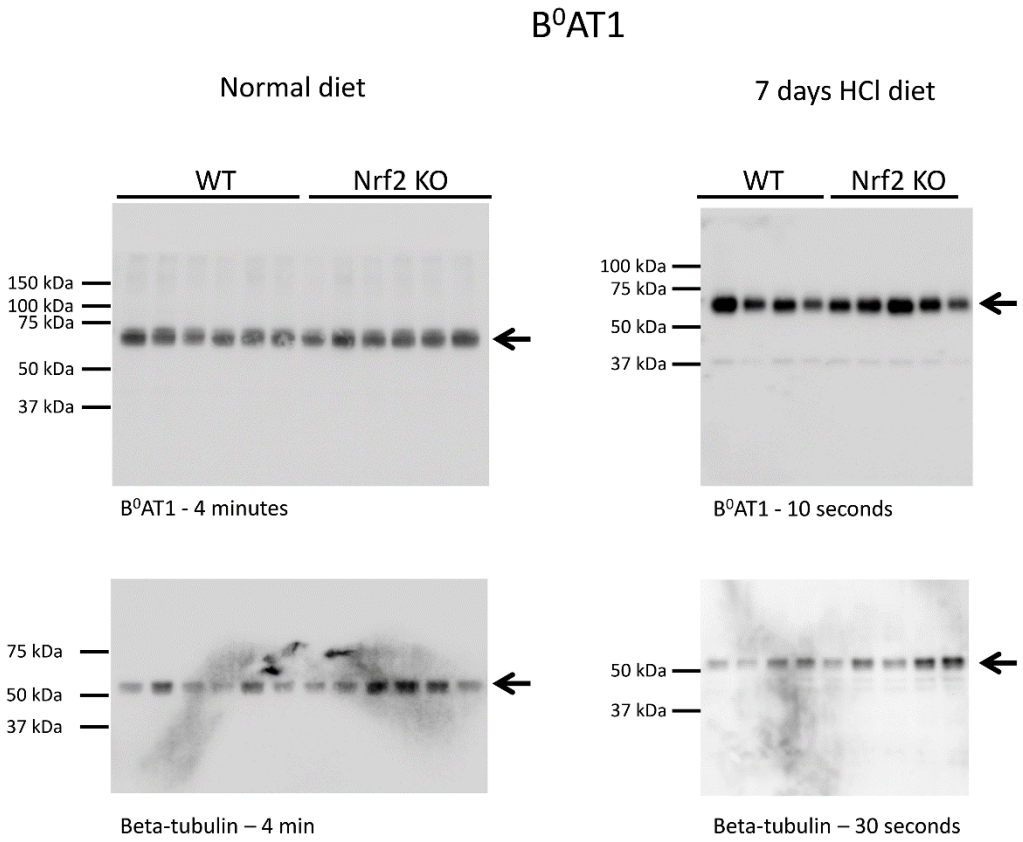

Supplementary Figure S9 Original full-length images used to create the cropped blots shown in Figure 4g-h. B^0AT1 expression. Arrows indicate the band quantified by densitometry. Exposure time is shown below each western blotting image.

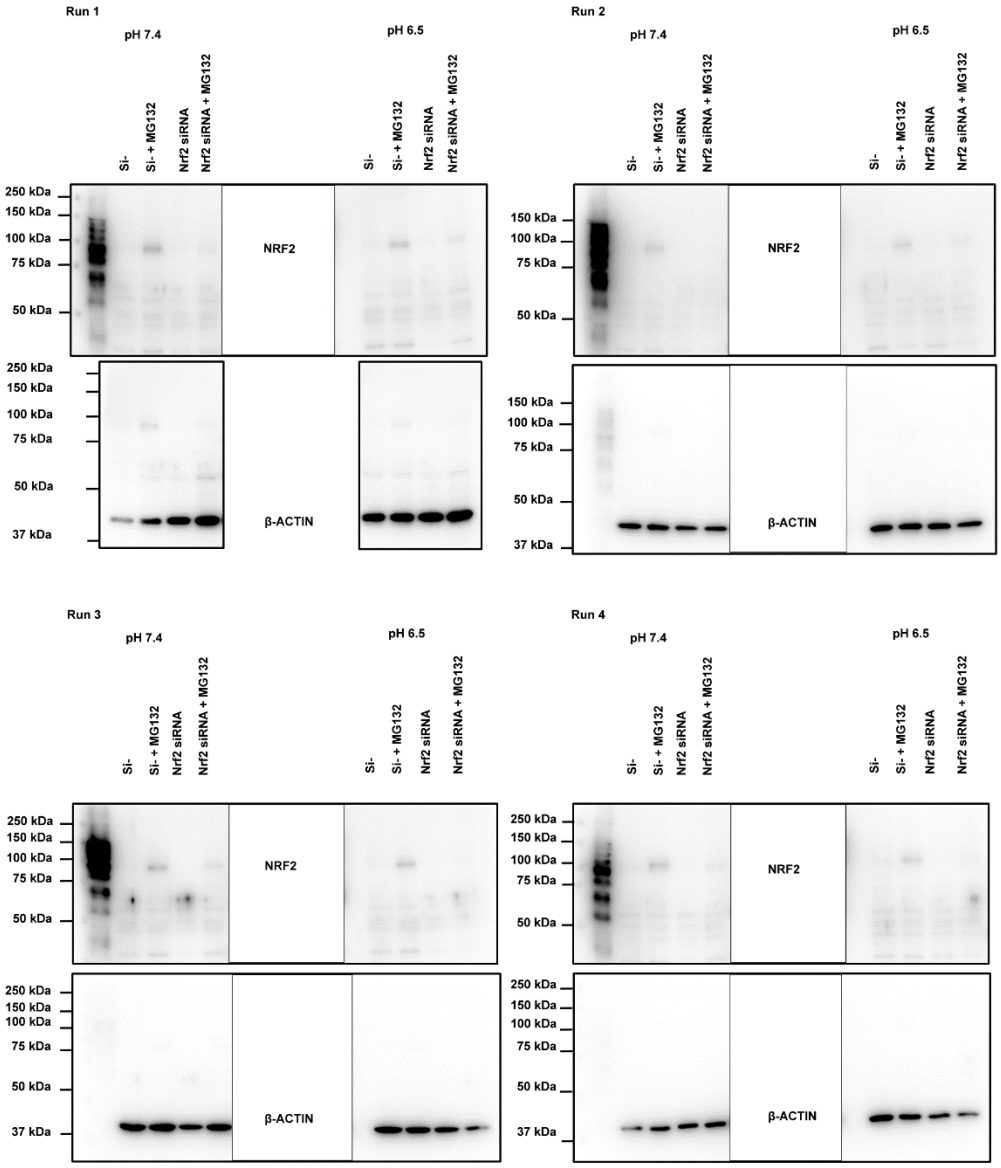

Supplemental Figure S10 Full length immunoblots from images presented in supplemental Figure S2a and b. Images confirm the depletion of NRF2 protein following *Nrf2* siRNA in PCT cells cultured in medium adjusted to pH 7.4 and pH 6.5. An amount of 25 µg of sample and control protein were loaded for all immunoblots. β-ACTIN was used as a house-keeping protein control. Images were acquired with the Imagequant LAS-4000 (Fujifilm) following exposure for 1 min (NRF2) and 10 sec (β-ACTIN).

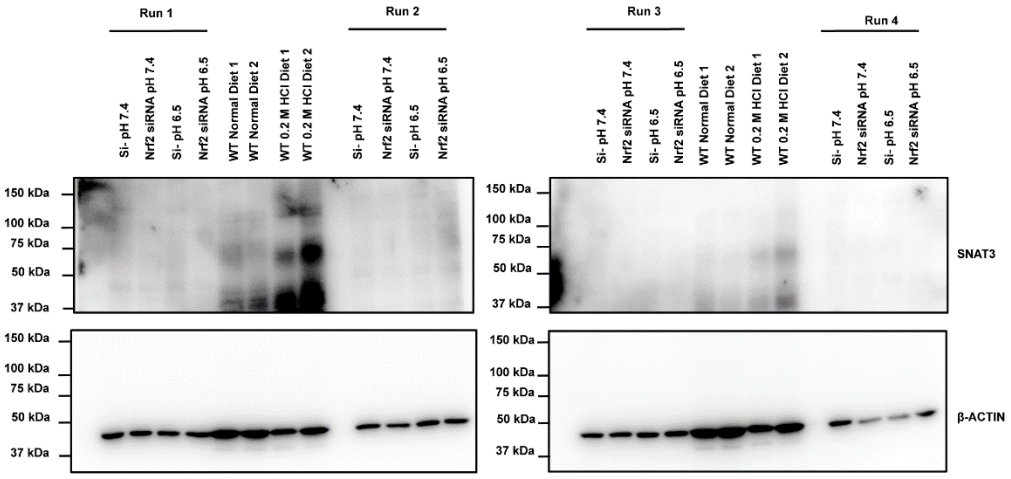

Supplemental Figure S11 Full length immunoblots from images presented in supplemental Figure S2e. Images show SNAT3 protein levels following *Nrf2* siRNA in primary PCT cultured in medium adjusted to pH 7.4 and pH 6.5. Whole kidney lysates from WT normal diet and WT HCl diet animals were used as a positive control. An amount of 25 µg of sample and control protein were loaded for all immunoblots. β-ACTIN was used as a house-keeping protein control. Images were acquired with the Imagequant LAS-4000 (Fujifilm) following exposure for 10 min (SNAT3) and 10 sec (β-ACTIN).

Supplementary Table 1. Amino acids in plasma in wild-type and *Nrf2* KO mice after a 7 days HCl load.

Amino acid (μM)	**WT**	***Nrf2* KO**	**P-value**
Alanine	424.17 ± 185.51	484.5 ± 97.4	n.s.
Arginine	48 ± 11.64	59.05 ± 8.27	n.s.
Asparagine	40.68 ± 13.26	49.32 ± 15.44	n.s.
Aspartate	7.9 ± 3.51	9.38 ± 1.1	n.s.
Glutamine	509 ± 36.17	653.67 ± 79.55	0.002
Glutamate	34.57 ± 4.28	44.05 ± 4.7	0.009
Glycine	353.33 ± 115.87	669.17 ± 698.89	n.s.
Histidine	69.83 ± 8.06	88.72 ± 12.04	0.026
Isoleucine	86.67 ± 21.42	92.18 ± 31.57	n.s.
Leucine	139.33 ± 16.72	143.33 ± 24.73	n.s.
Lysine	206.67 ± 43.07	256 ± 39.58	n.s.
Methionine	58.82 ± 20.41	64.9 ± 10.38	n.s.
Phenylalanine	73.13 ± 11.18	95.43 ± 17.74	0.026
Proline	104.78 ± 49.3	123.77 ± 33.62	n.s.
Serine	166.5 ± 63.7	169.33 ± 34.03	n.s.
Threonine	258.17 ± 79.58	226.33 ± 68.95	n.s.
Tryptophan	66.22 ± 14.14	83.1 ± 23.72	n.s.
Tyrosine	65.77 ± 17.93	78.17 ± 24.4	n.s.
Valine	215 ± 34.89	234.67 ± 40.12	n.s.
α-aminoadipic acid	15.25 ± 4.86	13.67 ± 2.81	n.s.
γ-aminobutyric acid	8.17 ± 1.3	9.85 ± 2.3	n.s.
Anserine	1.07 ± 1.2	0.88 ± 0.79	n.s.
β-Alanine	1.24 ± 0.54	1.26 ± 0.28	n.s.
Citrulline	52.15 ± 11.81	59.55 ± 11.17	n.s.
Cystine	9.18 ± 4.63	4.46 ± 2.69	n.s.
GABA	0.2 ± 0.07	0.44 ± 0.17	0.015
1-M-histidine	4.2 ± 0.86	4.66 ± 0.78	n.s.
3-M-histidine	3.64 ± 0.88	8.52 ± 0.98	0.002
OH-Proline	31.63 ± 12.17	27.05 ± 8.98	n.s.
Ornithine	36.2 ± 13.78	54.23 ± 16.37	n.s.

Values as mean ± SD, P-value calculated with the Mann-Whitney test
n.s.: not significant differences

Supplementary Table 2. Amino acids in kidney in wild-type and *Nrf2* KO mice after a 7 days HCl load.

Amino acid (μmol/kg kidney)	**WT**	***Nrf2* KO**	**P-value**
Alanine	1187 ± 233.96	1160.5 ± 243.83	n.s.
Arginine	44.6 ± 5.68	38.65 ± 6.35	n.s.
Asparagine	97.9 ± 12.76	116.5 ± 22.66	n.s.
Aspartate	1902 ± 481.24	1831 ± 364.58	n.s.
Glutamine	678 ± 149.25	727.5 ± 210.15	n.s.
Glutamate	3780 ± 431.83	3870 ± 376.62	n.s.
Glycine	6845 ± 675.21	5205 ± 590.86	0.004
Histidine	184.75 ± 35.12	116.2 ± 18.48	0.004
Isoleucine	93.9 ± 21.11	98.35 ± 14.39	n.s.
Leucine	221.95 ± 19.82	225.65 ± 20.94	n.s.
Lysine	65.9 ± 11.84	63.05 ± 9.14	n.s.
Methionine	61.66 ± 37.59	66.45 ± 15.11	n.s.
Phenylalanine	75.2 ± 8.95	108.7 ± 22.05	0.004
Proline	102.85 ± 20.03	131.1 ± 30.93	n.s.
Serine	564 ± 118.08	566 ± 67.93	n.s.
Threonine	367 ± 85.04	293.75 ± 55.6	n.s.
Tryptophan	13.13 ± 6.08	20.77 ± 8.29	n.s.
Tyrosine	93.05 ± 10.72	107.35 ± 37.47	n.s.
Valine	220.85 ± 21.89	263.9 ± 25.23	0.026
α-aminoadipic acid	126 ± 16.22	98.55 ± 25.39	n.s.
γ-aminobutyric acid	16.52 ± 4.68	15.65 ± 3.11	n.s.
Anserine	12.52 ± 0.98	15.37 ± 1.7	0.041
β-aminoisobutyric acid	11.05 ± 7.02	23.84 ± 7.93	n.s.
β-Alanine	2.7 ± 0.31	2.35 ± 0.22	0.009
Carnosine	2.91 ± 0.38	4.25 ± 1.21	0.015
Citrulline	19.95 ± 3.87	25.36 ± 4.87	n.s.
Cystine	325.6 ± 95.42	235.75 ± 55.86	n.s.
GABA	26.57 ± 8.91	44.85 ± 9.31	n.s.
1-M-histidine	15.66 ± 3.53	15.55 ± 1.87	n.s.
3-M-histidine	79.65 ± 25.13	48.32 ± 17.62	0.009
Homocystine	0.03 ± 0.03	0.02 ± 0.01	n.s.
OH-Proline	56.05 ± 17.24	41 ± 8.59	n.s.
Ornithine	15.55 ± 10.64	17.01 ± 9.52	n.s.

Values as mean ± SD, P-value calculated with the Mann-Whitney test
n.s.: not significant differences

Supplementary Table 3. Primers used for qPCR analysis of mouse kidney tissue.

Gene	Primer	Sequence
mouse *Snat1* (*Slc38a1*)	sense	TCCTTCAGCCATAAAATCCCTC
	anti-sense	CCACTCGTGTAGCCAAGATAC
mouse *Snat2* (*Slc38a2*)	sense	CCGTCTGCCTTCTACATCAAG
	anti-sense	CCCAATCCAGCACAATCAAG
mouse *Snat3* (*Slc38a3*)	sense	TCGGCTACCTGGGTTACTC
	anti-sense	GGGAACAGAACAATCGGAACTG
mouse *Snat4* (*Slc38a4*)	sense	CCTCGTGCCTACCATCAAATAC
	anti-sense	AGACCAAAGCCCCAATCTTC
mouse *Snat7* (*Slc38a7*)	sense	GTAGTGTACCCGTCTTCAACAG
	anti-sense	AAGGTTAGGAAGCCACAGATG
mouse *Pepck* (*Pck1*)	sense	CTGCATAACGGTCTGGACTTC
	anti-sense	CAGCAACTGCCCGTACTCC
mouse *Gls* (*glutaminase*)	sense	GTGGTTTCTGCCCAATTACTG
	anti-sense	CCCAGCAACTCCAGATTTTG
mouse *Tat1* (*Slc16a10*)	sense	CCCCATCGTGAGTGTCTTC
	anti-sense	TCCATAGGTGAGGTACAGAGG
mouse *4f2hc* (*Slc3a2*)	sense	ACCTCACTCCCAACTACCAG
	anti-sense	ATCAGCTTTCCCACATCCC
mouse *Lat1* (*Slc7a5*)	sense	TCACTACCCTCTCTACCAACC
	anti-sense	TGAACAGAGACCCATTGACAG

mouse *Lat2* (*Slc7a8*)	sense	AAAGAGATCGGATTGGTCAGC
	anti-sense	ATCCAGACAATGAGAGCAAGG
mouse y+lat1 (Slc7a7)	sense	CTTTATCTACGCTGGAAGGACC
	anti-sense	GATGAGGGAGTTGATGGTGTC
mouse *Bo,+at* (*Slc7a9*)	sense	GCTCTTGCAGTCCCAGGCT
	anti-sense	GGGACTACCCAAGATGCTGGA
mouse *B(o)at1* (*Slc6a19*)	sense	CTCATCCTTCTGGTGTTCGAG
	anti-sense	ATGAAGGACACGAACATGGAG
mouse *Nrf2(Nfe2l2)*	sense	CAGCATGTTACGTGATGAGG
	anti-sense	GCTCAGAAAAGGCTCCATCC
mouse *Nqo1*	sense	TTTAGGGTCGTCTTGGCAAC
	anti-sense	GTCTTCTCTGAATGGGCCAG
mouse *Gclc*	sense	GGGGTGACGAGGTGGAGTA
	anti-sense	GTTGGGGTTTGTCCTCTCCC
mouse *Gclm*	sense	AATCAGCCCCGATTTAGTCAG
	anti-sense	CGATCCTACAATGAACAGTTTTGC
mouse *Car3*	sense	TGGACGGAGTAAAATACGCTG
	anti-sense	AATCTGGAACTCGCCTTTCTC
mouse *Nhe3* (*Slc9a3*)	sense	CACACCCCGCCCATCTACT
	anti-sense	CCAGGCATACAGCACTGACATT
mouse *Nhe4* (*Slc9a4*)	sense	GAGGATACAGGGAATCAAGCG
	anti-sense	CTTGCTTCTCACTTGTTTGGG

mouse *Rhcg*	sense	AGTGACCTGGATCCTCTACC
	anti-sense	GAACTGGCTGAATTGAAACTGG
mouse *Nkcc2* (*Slc12a1*)	sense	TGCTAATGGAGATGGGATGC
	anti-sense	CAGGAGAGGCGAATGAAGAG
mouse *Ncx1* (*Slc8a1*)	sense	TCCATCCAGTAGACTTCGTGAT
	anti-sense	CCAAGCAATTCCTTACAGAGTGA
mouse *Trpv5*	sense	TGCTGCTATAATGCTGATGGAG
	anti-sense	GCACGGACTAGGTTCACATTCT
mouse *Calb1* (*Calbindin d28k*)	sense	AGAACTTGATCCAGGAGCTTC
	anti-sense	CTTCTGTGGGTAAGACGTGAG
mouse *Pmca4* (*Atp2b4*)	sense	GGATTGGAGAACTTTTGTGGG
	anti-sense	ATCTCGGCAAGGTCAATCTC
mouse *Cyp2a5*	sense	GGACAAAGAGTTCCTGTCACTGCTTC
	anti-sense	GTGTTCCACTTTCTTGGTTATGAAGTCC
mouse *Gsta3*	sense	GGTTCCTGGTTTGTTCCTTG
	anti-sense	CTATGGGAAGGACATGAAGGAG
mouse *Gstm1*	sense	ATACTGGGATACTGGAACGTCC
	anti-sense	AGTCAGGGTTGTAACAGAGCAT
mouse *Dpys*	sense	TGTGACTATAGCCTGCATGTG
	anti-sense	CGGGCAAGGGTTTTCATTTC
mouse *Kim1* (*Havcr1*)	sense	ACTAAGGGCTTCTATGTTGGC
	anti-sense	AGCTTCAATCTTAGAGACACGG

8. References

1. Maienschein, J. (2010) Ross Granville Harrison (1870-1959) and perspectives on regeneration, *J Exp Zool B Mol Dev Evol.* **314**, 607-15.
2. Harrison, R. (1907) Observations on the living developing nerve fiber, *Anat Rec.* **1**, 116-118.
3. Kaur, G. & Dufour, J. M. (2012) Cell lines: Valuable tools or useless artifacts, *Spermatogenesis.* **2**, 1-5.
4. Hughes, P., Marshall, D., Reid, Y., Parkes, H. & Gelber, C. (2007) The costs of using unauthenticated, over-passaged cell lines: how much more data do we need?, *Biotechniques.* **43**, 575, 577-8, 581-2 passim.
5. Masramon, L., Vendrell, E., Tarafa, G., Capella, G., Miro, R., Ribas, M. & Peinado, M. A. (2006) Genetic instability and divergence of clonal populations in colon cancer cells in vitro, *J Cell Sci.* **119**, 1477-82.
6. Lu, S., Gough, A. W., Bobrowski, W. F. & Stewart, B. H. (1996) Transport properties are not altered across Caco-2 cells with heightened TEER despite underlying physiological and ultrastructural changes, *J Pharm Sci.* **85**, 270-3.
7. Nakamura, T., Sakaeda, T., Ohmoto, N., Tamura, T., Aoyama, N., Shirakawa, T., Kamigaki, T., Nakamura, T., Kim, K. I., Kim, S. R., Kuroda, Y., Matsuo, M., Kasuga, M. & Okumura, K. (2002) Real-time quantitative polymerase chain reaction for MDR1, MRP1, MRP2, and CYP3A-mRNA levels in Caco-2 cell lines, human duodenal enterocytes, normal colorectal tissues, and colorectal adenocarcinomas, *Drug Metab Dispos.* **30**, 4-6.
8. Kato, S., Espinoza, N., Lange, S., Villalon, M., Cuello, M. & Owen, G. I. (2008) Characterization and phenotypic variation with passage number of cultured human endometrial adenocarcinoma cells, *Tissue Cell.* **40**, 95-102.
9. Nelson-Rees, W. A., Daniels, D. W. & Flandermeyer, R. R. (1981) Cross-contamination of cells in culture, *Science.* **212**, 446-52.
10. Capes-Davis, A., Theodosopoulos, G., Atkin, I., Drexler, H. G., Kohara, A., MacLeod, R. A., Masters, J. R., Nakamura, Y., Reid, Y. A., Reddel, R. R. & Freshney, R. I. (2010) Check your cultures! A list of cross-contaminated or misidentified cell lines, *Int J Cancer.* **127**, 1-8.
11. Jiang, L., Zeng, X., Wang, Z. & Chen, Q. (2009) Cell line cross-contamination: KB is not an oral squamous cell carcinoma cell line, *Eur J Oral Sci.* **117**, 90-1.
12. Fleckenstein, E., Uphoff, C. C. & Drexler, H. G. (1994) Effective treatment of mycoplasma contamination in cell lines with enrofloxacin (Baytril), *Leukemia.* **8**, 1424-34.
13. Jans, F., Vandenabeele, F., Helbert, M., Lambrichts, I., Ameloot, M. & Steels, P. (2000) A simple method for obtaining functionally and morphologically intact primary cultures of the medullary thick ascending limb of Henle's loop (MTAL) from rabbit kidneys, *Pflugers Arch.* **440**, 643-51.
14. Liu, S. C. & Karasek, M. (1978) Isolation and growth of adult human epidermal keratinocytes in cell culture, *J Invest Dermatol.* **71**, 157-62.
15. Clover, J. & Gowen, M. (1994) Are MG-63 and HOS TE85 human osteosarcoma cell lines representative models of the osteoblastic phenotype?, *Bone.* **15**, 585-91.
16. Godfrey, R. W. (1997) Human airway epithelial tight junctions, *Microsc Res Tech.* **38**, 488-99.
17. Alge, C. S., Hauck, S. M., Priglinger, S. G., Kampik, A. & Ueffing, M. (2006) Differential protein profiling of primary versus immortalized human RPE cells identifies expression patterns associated with cytoskeletal remodeling and cell survival, *J Proteome Res.* **5**, 862-78.
18. Fang, C. Y., Wu, C. C., Fang, C. L., Chen, W. Y. & Chen, C. L. (2017) Long-term growth comparison studies of FBS and FBS alternatives in six head and neck cell lines, *PLoS One.* **12**, e0178960.
19. Cavaillon, J. M. (2011) The historical milestones in the understanding of leukocyte biology initiated by Elie Metchnikoff, *J Leukoc Biol.* **90**, 413-24.
20. Wynn, T. A., Chawla, A. & Pollard, J. W. (2013) Macrophage biology in development, homeostasis and disease, *Nature.* **496**, 445-55.
21. Wake, K., Decker, K., Kirn, A., Knook, D. L., McCuskey, R. S., Bouwens, L. & Wisse, E. (1989) Cell biology and kinetics of Kupffer cells in the liver, *Int Rev Cytol.* **118**, 173-229.

22. Kahn, A. J. & Simmons, D. J. (1975) Investigation of cell lineage in bone using a chimaera of chick and quial embryonic tissue, *Nature.* **258**, 325-7.
23. Chan, W. Y., Kohsaka, S. & Rezaie, P. (2007) The origin and cell lineage of microglia: new concepts, *Brain Res Rev.* **53**, 344-54.
24. van Furth, R. & Cohn, Z. A. (1968) The origin and kinetics of mononuclear phagocytes, *J Exp Med.* **128**, 415-35.
25. van Furth, R., Cohn, Z. A., Hirsch, J. G., Humphrey, J. H., Spector, W. G. & Langevoort, H. L. (1972) The mononuclear phagocyte system: a new classification of macrophages, monocytes, and their precursor cells, *Bull World Health Organ.* **46**, 845-52.
26. Leibovich, S. J. & Ross, R. (1975) The role of the macrophage in wound repair. A study with hydrocortisone and antimacrophage serum, *Am J Pathol.* **78**, 71-100.
27. Odegaard, J. I. & Chawla, A. (2013) Pleiotropic actions of insulin resistance and inflammation in metabolic homeostasis, *Science.* **339**, 172-7.
28. Parihar, A., Eubank, T. D. & Doseff, A. I. (2010) Monocytes and macrophages regulate immunity through dynamic networks of survival and cell death, *J Innate Immun.* **2**, 204-15.
29. Ginhoux, F. & Jung, S. (2014) Monocytes and macrophages: developmental pathways and tissue homeostasis, *Nat Rev Immunol.* **14**, 392-404.
30. Hashimoto, D., Chow, A., Noizat, C., Teo, P., Beasley, M. B., Leboeuf, M., Becker, C. D., See, P., Price, J., Lucas, D., Greter, M., Mortha, A., Boyer, S. W., Forsberg, E. C., Tanaka, M., van Rooijen, N., Garcia-Sastre, A., Stanley, E. R., Ginhoux, F., Frenette, P. S. & Merad, M. (2013) Tissue-resident macrophages self-maintain locally throughout adult life with minimal contribution from circulating monocytes, *Immunity.* **38**, 792-804.
31. Enzan, H. (1986) Electron microscopic studies of macrophages in early human yolk sacs, *Acta Pathol Jpn.* **36**, 49-64.
32. Migliaccio, G., Migliaccio, A. R., Petti, S., Mavilio, F., Russo, G., Lazzaro, D., Testa, U., Marinucci, M. & Peschle, C. (1986) Human embryonic hemopoiesis. Kinetics of progenitors and precursors underlying the yolk sac----liver transition, *J Clin Invest.* **78**, 51-60.
33. Weisberg, S. P., McCann, D., Desai, M., Rosenbaum, M., Leibel, R. L. & Ferrante, A. W., Jr. (2003) Obesity is associated with macrophage accumulation in adipose tissue, *J Clin Invest.* **112**, 1796-808.
34. Medzhitov, R. (2008) Origin and physiological roles of inflammation, *Nature.* **454**, 428-35.
35. Dai, X. M., Ryan, G. R., Hapel, A. J., Dominguez, M. G., Russell, R. G., Kapp, S., Sylvestre, V. & Stanley, E. R. (2002) Targeted disruption of the mouse colony-stimulating factor 1 receptor gene results in osteopetrosis, mononuclear phagocyte deficiency, increased primitive progenitor cell frequencies, and reproductive defects, *Blood.* **99**, 111-20.
36. Cecchini, M. G., Dominguez, M. G., Mocci, S., Wetterwald, A., Felix, R., Fleisch, H., Chisholm, O., Hofstetter, W., Pollard, J. W. & Stanley, E. R. (1994) Role of colony stimulating factor-1 in the establishment and regulation of tissue macrophages during postnatal development of the mouse, *Development.* **120**, 1357-72.
37. Tushinski, R. J., Oliver, I. T., Guilbert, L. J., Tynan, P. W., Warner, J. R. & Stanley, E. R. (1982) Survival of mononuclear phagocytes depends on a lineage-specific growth factor that the differentiated cells selectively destroy, *Cell.* **28**, 71-81.
38. Ajuebor, M. N., Flower, R. J., Hannon, R., Christie, M., Bowers, K., Verity, A. & Perretti, M. (1998) Endogenous monocyte chemoattractant protein-1 recruits monocytes in the zymosan peritonitis model, *J Leukoc Biol.* **63**, 108-16.
39. Boring, L., Gosling, J., Chensue, S. W., Kunkel, S. L., Farese, R. V., Jr., Broxmeyer, H. E. & Charo, I. F. (1997) Impaired monocyte migration and reduced type 1 (Th1) cytokine responses in C-C chemokine receptor 2 knockout mice, *J Clin Invest.* **100**, 2552-61.
40. Auffray, C., Fogg, D., Garfa, M., Elain, G., Join-Lambert, O., Kayal, S., Sarnacki, S., Cumano, A., Lauvau, G. & Geissmann, F. (2007) Monitoring of blood vessels and tissues by a population of monocytes with patrolling behavior, *Science.* **317**, 666-70.
41. Menendez-Benito, V. & Neefjes, J. (2007) Autophagy in MHC class II presentation: sampling from within, *Immunity.* **26**, 1-3.

42. Celada, A., Klemsz, M. J. & Maki, R. A. (1989) Interferon-gamma activates multiple pathways to regulate the expression of the genes for major histocompatibility class II I-A beta, tumor necrosis factor and complement component C3 in mouse macrophages, *Eur J Immunol.* **19**, 1103-9.
43. Sica, A. & Mantovani, A. (2012) Macrophage plasticity and polarization: in vivo veritas, *J Clin Invest.* **122**, 787-95.
44. Schnare, M., Holt, A. C., Takeda, K., Akira, S. & Medzhitov, R. (2000) Recognition of CpG DNA is mediated by signaling pathways dependent on the adaptor protein MyD88, *Curr Biol.* **10**, 1139-42.
45. Gordon, S. & Taylor, P. R. (2005) Monocyte and macrophage heterogeneity, *Nat Rev Immunol.* **5**, 953-64.
46. Gordon, S. (2003) Alternative activation of macrophages, *Nat Rev Immunol.* **3**, 23-35.
47. El-Behi, M., Ciric, B., Dai, H., Yan, Y., Cullimore, M., Safavi, F., Zhang, G. X., Dittel, B. N. & Rostami, A. (2011) The encephalitogenicity of T(H)17 cells is dependent on IL-1- and IL-23-induced production of the cytokine GM-CSF, *Nat Immunol.* **12**, 568-75.
48. Goerdt, S., Politz, O., Schledzewski, K., Birk, R., Gratchev, A., Guillot, P., Hakiy, N., Klemke, C. D., Dippel, E., Kodelja, V. & Orfanos, C. E. (1999) Alternative versus classical activation of macrophages, *Pathobiology.* **67**, 222-6.
49. Stein, M., Keshav, S., Harris, N. & Gordon, S. (1992) Interleukin 4 potently enhances murine macrophage mannose receptor activity: a marker of alternative immunologic macrophage activation, *J Exp Med.* **176**, 287-92.
50. Erwig, L. P., Kluth, D. C., Walsh, G. M. & Rees, A. J. (1998) Initial cytokine exposure determines function of macrophages and renders them unresponsive to other cytokines, *J Immunol.* **161**, 1983-8.
51. Fadok, V. A., Bratton, D. L., Konowal, A., Freed, P. W., Westcott, J. Y. & Henson, P. M. (1998) Macrophages that have ingested apoptotic cells in vitro inhibit proinflammatory cytokine production through autocrine/paracrine mechanisms involving TGF-beta, PGE2, and PAF, *J Clin Invest.* **101**, 890-8.
52. Ilhan, F. & Kalkanli, S. T. (2015) Atherosclerosis and the role of immune cells, *World J Clin Cases.* **3**, 345-52.
53. Feng, X. & Teitelbaum, S. L. (2013) Osteoclasts: New Insights, *Bone Res.* **1**, 11-26.
54. Heideveld, E. & van den Akker, E. (2017) Digesting the role of bone marrow macrophages on hematopoiesis, *Immunobiology.* **222**, 814-822.
55. Al-Matary, Y. S., Botezatu, L., Opalka, B., Hones, J. M., Lams, R. F., Thivakaran, A., Schutte, J., Koster, R., Lennartz, K., Schroeder, T., Haas, R., Duhrsen, U. & Khandanpour, C. (2016) Acute myeloid leukemia cells polarize macrophages towards a leukemia supporting state in a Growth factor independence 1 dependent manner, *Haematologica.* **101**, 1216-1227.
56. Bhargava, P. & Lee, C. H. (2012) Role and function of macrophages in the metabolic syndrome, *Biochem J.* **442**, 253-62.
57. Ma, Y. & Pope, R. M. (2005) The role of macrophages in rheumatoid arthritis, *Curr Pharm Des.* **11**, 569-80.
58. Raschke, W. C., Baird, S., Ralph, P. & Nakoinz, I. (1978) Functional macrophage cell lines transformed by Abelson leukemia virus, *Cell.* **15**, 261-7.
59. Ralph, P., Prichard, J. & Cohn, M. (1975) Reticulum cell sarcoma: an effector cell in antibody-dependent cell-mediated immunity, *J Immunol.* **114**, 898-905.
60. Mocarelli, P., Palmer, J. & Defendi, V. (1973) A permanent line of macrophages with normal activity in a primary antibody response in vitro, *Immunol Commun.* **2**, 441-7.
61. Blasi, E., Barluzzi, R., Bocchini, V., Mazzolla, R. & Bistoni, F. (1990) Immortalization of murine microglial cells by a v-raf/v-myc carrying retrovirus, *J Neuroimmunol.* **27**, 229-37.
62. Tsuchiya, S., Yamabe, M., Yamaguchi, Y., Kobayashi, Y., Konno, T. & Tada, K. (1980) Establishment and characterization of a human acute monocytic leukemia cell line (THP-1), *Int J Cancer.* **26**, 171-6.
63. Sundstrom, C. & Nilsson, K. (1976) Establishment and characterization of a human histiocytic lymphoma cell line (U-937), *Int J Cancer.* **17**, 565-77.
64. Guo, M., Hartlova, A., Dill, B. D., Prescott, A. R., Gierlinski, M. & Trost, M. (2015) High-resolution quantitative proteome analysis reveals substantial differences between phagosomes of RAW 264.7 and bone marrow derived macrophages, *Proteomics.* **15**, 3169-74.

65. Pelegrin, P., Barroso-Gutierrez, C. & Surprenant, A. (2008) P2X7 receptor differentially couples to distinct release pathways for IL-1beta in mouse macrophage, *J Immunol.* **180**, 7147-57.
66. Andreu, N., Phelan, J., de Sessions, P. F., Cliff, J. M., Clark, T. G. & Hibberd, M. L. (2017) Primary macrophages and J774 cells respond differently to infection with Mycobacterium tuberculosis, *Sci Rep.* **7**, 42225.
67. Schildberger, A., Rossmanith, E., Eichhorn, T., Strassl, K. & Weber, V. (2013) Monocytes, peripheral blood mononuclear cells, and THP-1 cells exhibit different cytokine expression patterns following stimulation with lipopolysaccharide, *Mediators Inflamm.* **2013**, 697972.
68. Bosshart, H. & Heinzelmann, M. (2004) Lipopolysaccharide-mediated cell activation without rapid mobilization of cytosolic free calcium, *Mol Immunol.* **41**, 1023-8.
69. Zhang, X., Goncalves, R. & Mosser, D. M. (2008) The isolation and characterization of murine macrophages, *Curr Protoc Immunol.* **Chapter 14**, Unit 14 1.
70. Warren, M. K. & Vogel, S. N. (1985) Bone marrow-derived macrophages: development and regulation of differentiation markers by colony-stimulating factor and interferons, *J Immunol.* **134**, 982-9.
71. Maus, U., Herold, S., Muth, H., Maus, R., Ermert, L., Ermert, M., Weissmann, N., Rosseau, S., Seeger, W., Grimminger, F. & Lohmeyer, J. (2001) Monocytes recruited into the alveolar air space of mice show a monocytic phenotype but upregulate CD14, *Am J Physiol Lung Cell Mol Physiol.* **280**, L58-68.
72. Morimoto, K., Amano, H., Sonoda, F., Baba, M., Senba, M., Yoshimine, H., Yamamoto, H., Ii, T., Oishi, K. & Nagatake, T. (2001) Alveolar macrophages that phagocytose apoptotic neutrophils produce hepatocyte growth factor during bacterial pneumonia in mice, *Am J Respir Cell Mol Biol.* **24**, 608-15.
73. Yoshikawa, K., Suzuki, Y., Kawai, M., Fukada, M. & Yokochi, T. (1991) Novel cell surface antigens expressed on mouse alveolar macrophages, *Microbiol Immunol.* **35**, 803-7.
74. Austin, P. E., McCulloch, E. A. & Till, J. E. (1971) Characterization of the factor in L-cell conditioned medium capable of stimulating colony formation by mouse marrow cells in culture, *J Cell Physiol.* **77**, 121-34.
75. Stanley, E. R. (1985) The macrophage colony-stimulating factor, CSF-1, *Methods Enzymol.* **116**, 564-87.
76. Jessen, K. R. (2004) Glial cells, *Int J Biochem Cell Biol.* **36**, 1861-7.
77. Herculano-Houzel, S. (2009) The human brain in numbers: a linearly scaled-up primate brain, *Front Hum Neurosci.* **3**, 31.
78. Jakel, S. & Dimou, L. (2017) Glial Cells and Their Function in the Adult Brain: A Journey through the History of Their Ablation, *Front Cell Neurosci.* **11**, 24.
79. Ballabh, P., Braun, A. & Nedergaard, M. (2004) The blood-brain barrier: an overview: structure, regulation, and clinical implications, *Neurobiol Dis.* **16**, 1-13.
80. Kimelberg, H. K. (2010) Functions of mature mammalian astrocytes: a current view, *Neuroscientist.* **16**, 79-106.
81. Kimelberg, H. K. & Nedergaard, M. (2010) Functions of astrocytes and their potential as therapeutic targets, *Neurotherapeutics.* **7**, 338-53.
82. Nave, K. A. (2010) Myelination and support of axonal integrity by glia, *Nature.* **468**, 244-52.
83. Kim, S. U. & de Vellis, J. (2005) Microglia in health and disease, *J Neurosci Res.* **81**, 302-13.
84. Kettenmann, H., Hanisch, U. K., Noda, M. & Verkhratsky, A. (2011) Physiology of microglia, *Physiol Rev.* **91**, 461-553.
85. Kigerl, K. A., Gensel, J. C., Ankeny, D. P., Alexander, J. K., Donnelly, D. J. & Popovich, P. G. (2009) Identification of two distinct macrophage subsets with divergent effects causing either neurotoxicity or regeneration in the injured mouse spinal cord, *J Neurosci.* **29**, 13435-44.
86. Perego, C., Fumagalli, S. & De Simoni, M. G. (2011) Temporal pattern of expression and colocalization of microglia/macrophage phenotype markers following brain ischemic injury in mice, *J Neuroinflammation.* **8**, 174.
87. Aschner, M. (1998) Astrocytes as mediators of immune and inflammatory responses in the CNS, *Neurotoxicology.* **19**, 269-81.

88. Streit, W. J., Conde, J. R., Fendrick, S. E., Flanary, B. E. & Mariani, C. L. (2005) Role of microglia in the central nervous system's immune response, *Neurol Res.* **27**, 685-91.
89. Humpel, C. (2015) Organotypic brain slice cultures: A review, *Neuroscience.* **305**, 86-98.
90. Honegger, P., Defaux, A., Monnet-Tschudi, F. & Zurich, M. G. (2011) Preparation, maintenance, and use of serum-free aggregating brain cell cultures, *Methods Mol Biol.* **758**, 81-97.
91. Henn, A., Lund, S., Hedtjarn, M., Schrattenholz, A., Porzgen, P. & Leist, M. (2009) The suitability of BV2 cells as alternative model system for primary microglia cultures or for animal experiments examining brain inflammation, *ALTEX.* **26**, 83-94.
92. Dong, H. W. & Buonomano, D. V. (2005) A technique for repeated recordings in cortical organotypic slices, *J Neurosci Methods.* **146**, 69-75.
93. Ullrich, C. & Humpel, C. (2011) Mini-ruby is rapidly taken up by neurons and astrocytes in organotypic brain slices, *Neurochem Res.* **36**, 1817-23.
94. Gogolla, N., Galimberti, I., DePaola, V. & Caroni, P. (2006) Long-term live imaging of neuronal circuits in organotypic hippocampal slice cultures, *Nat Protoc.* **1**, 1223-6.
95. Ni, M. & Aschner, M. (2010) Neonatal rat primary microglia: isolation, culturing, and selected applications, *Curr Protoc Toxicol.* **Chapter 12**, Unit 12 17.
96. Kirkley, K. S., Popichak, K. A., Afzali, M. F., Legare, M. E. & Tjalkens, R. B. (2017) Microglia amplify inflammatory activation of astrocytes in manganese neurotoxicity, *J Neuroinflammation.* **14**, 99.
97. Ray, B., Chopra, N., Long, J. M. & Lahiri, D. K. (2014) Human primary mixed brain cultures: preparation, differentiation, characterization and application to neuroscience research, *Mol Brain.* **7**, 63.
98. Zurich, M. G. & Monnet-Tschudi, F. (2009) Contribution of in vitro neurotoxicology studies to the elucidation of neurodegenerative processes, *Brain Res Bull.* **80**, 211-6.
99. Honegger, P., Lenoir, D. & Favrod, P. (1979) Growth and differentiation of aggregating fetal brain cells in a serum-free defined medium, *Nature.* **282**, 305-8.
100. Hall, J. E., Brands, M. W. & Shek, E. W. (1996) Central role of the kidney and abnormal fluid volume control in hypertension, *J Hum Hypertens.* **10**, 633-9.
101. Hamm, L. L., Nakhoul, N. & Hering-Smith, K. S. (2015) Acid-Base Homeostasis, *Clin J Am Soc Nephrol.* **10**, 2232-42.
102. Greger, R. (2000) Physiology of renal sodium transport, *Am J Med Sci.* **319**, 51-62.
103. Zhuo, J. L. & Li, X. C. (2013) Proximal nephron, *Compr Physiol.* **3**, 1079-123.
104. McDonough, A. A. (2010) Mechanisms of proximal tubule sodium transport regulation that link extracellular fluid volume and blood pressure, *Am J Physiol Regul Integr Comp Physiol.* **298**, R851-61.
105. Rector, F. C., Jr. (1983) Sodium, bicarbonate, and chloride absorption by the proximal tubule, *Am J Physiol.* **244**, F461-71.
106. Skelton, L. A., Boron, W. F. & Zhou, Y. (2010) Acid-base transport by the renal proximal tubule, *J Nephrol.* **23 Suppl 16**, S4-18.
107. Abuladze, N., Lee, I., Newman, D., Hwang, J., Pushkin, A. & Kurtz, I. (1998) Axial heterogeneity of sodium-bicarbonate cotransporter expression in the rabbit proximal tubule, *Am J Physiol.* **274**, F628-33.
108. Vallon, V., Platt, K. A., Cunard, R., Schroth, J., Whaley, J., Thomson, S. C., Koepsell, H. & Rieg, T. (2011) SGLT2 mediates glucose reabsorption in the early proximal tubule, *J Am Soc Nephrol.* **22**, 104-12.
109. Ferguson, M. A., Vaidya, V. S. & Bonventre, J. V. (2008) Biomarkers of nephrotoxic acute kidney injury, *Toxicology.* **245**, 182-93.
110. Tiong, H. Y., Huang, P., Xiong, S., Li, Y., Vathsala, A. & Zink, D. (2014) Drug-induced nephrotoxicity: clinical impact and preclinical in vitro models, *Mol Pharm.* **11**, 1933-48.
111. Homan, K. A., Kolesky, D. B., Skylar-Scott, M. A., Herrmann, J., Obuobi, H., Moisan, A. & Lewis, J. A. (2016) Bioprinting of 3D Convoluted Renal Proximal Tubules on Perfusable Chips, *Sci Rep.* **6**, 34845.
112. Ryan, M. J., Johnson, G., Kirk, J., Fuerstenberg, S. M., Zager, R. A. & Torok-Storb, B. (1994) HK-2: an immortalized proximal tubule epithelial cell line from normal adult human kidney, *Kidney Int.* **45**, 48-57.

113. Koyama, H., Goodpasture, C., Miller, M. M., Teplitz, R. L. & Riggs, A. D. (1978) Establishment and characterization of a cell line from the American opossum (Didelphys virginiana), *In Vitro.* **14**, 239-46.
114. Madin, S. H., Andriese, P. C. & Darby, N. B. (1957) The in vitro cultivation of tissues of domestic and laboratory animals, *Am J Vet Res.* **18**, 932-41.
115. Hull, R. N., Cherry, W. R. & Weaver, G. W. (1976) The origin and characteristics of a pig kidney cell strain, LLC-PK, *In Vitro.* **12**, 670-7.
116. Jenkinson, S. E., Chung, G. W., van Loon, E., Bakar, N. S., Dalzell, A. M. & Brown, C. D. (2012) The limitations of renal epithelial cell line HK-2 as a model of drug transporter expression and function in the proximal tubule, *Pflugers Arch.* **464**, 601-11.
117. Curthoys, N. P. & Gstraunthaler, G. (2014) pH-responsive, gluconeogenic renal epithelial LLC-PK1-FBPase+cells: a versatile in vitro model to study renal proximal tubule metabolism and function, *Am J Physiol Renal Physiol.* **307**, F1-F11.
118. Gstraunthaler, G., Landauer, F. & Pfaller, W. (1992) Ammoniagenesis in LLC-PK1 cultures: role of transamination, *Am J Physiol.* **263**, C47-54.
119. Gstraunthaler, G., Pfaller, W. & Kotanko, P. (1985) Biochemical characterization of renal epithelial cell cultures (LLC-PK1 and MDCK), *Am J Physiol.* **248**, F536-44.
120. Racusen, L. C., Monteil, C., Sgrignoli, A., Lucskay, M., Marouillat, S., Rhim, J. G. & Morin, J. P. (1997) Cell lines with extended in vitro growth potential from human renal proximal tubule: characterization, response to inducers, and comparison with established cell lines, *J Lab Clin Med.* **129**, 318-29.
121. Terryn, S., Jouret, F., Vandenabeele, F., Smolders, I., Moreels, M., Devuyst, O., Steels, P. & Van Kerkhove, E. (2007) A primary culture of mouse proximal tubular cells, established on collagen-coated membranes, *Am J Physiol Renal Physiol.* **293**, F476-85.
122. O'Brien, L. L., Guo, Q., Lee, Y., Tran, T., Benazet, J. D., Whitney, P. H., Valouev, A. & McMahon, A. P. (2016) Differential regulation of mouse and human nephron progenitors by the Six family of transcriptional regulators, *Development.* **143**, 595-608.
123. Bell, C. L., Tenenhouse, H. S. & Scriver, C. R. (1988) Initiation and characterization of primary mouse kidney epithelial cultures, *In Vitro Cell Dev Biol.* **24**, 683-95.
124. Beutler, E. & Morrison, M. (1967) Localization and characteristics of hexose 6-phosphate dehydrogenase (glucose dehydrogenase), *J Biol Chem.* **242**, 5289-93.
125. Banhegyi, G., Benedetti, A., Fulceri, R. & Senesi, S. (2004) Cooperativity between 11beta-hydroxysteroid dehydrogenase type 1 and hexose-6-phosphate dehydrogenase in the lumen of the endoplasmic reticulum, *J Biol Chem.* **279**, 27017-21.
126. Odermatt, A. & Kratschmar, D. V. (2012) Tissue-specific modulation of mineralocorticoid receptor function by 11beta-hydroxysteroid dehydrogenases: An overview, *Mol Cell Endocrinol.* **350**, 168-86.
127. Atanasov, A. G., Nashev, L. G., Schweizer, R. A., Frick, C. & Odermatt, A. (2004) Hexose-6-phosphate dehydrogenase determines the reaction direction of 11beta-hydroxysteroid dehydrogenase type 1 as an oxoreductase, *FEBS Lett.* **571**, 129-33.
128. Ozols, J. (1995) Lumenal orientation and post-translational modifications of the liver microsomal 11 beta-hydroxysteroid dehydrogenase, *J Biol Chem.* **270**, 10360.
129. Tuckermann, J. P., Kleiman, A., McPherson, K. G. & Reichardt, H. M. (2005) Molecular mechanisms of glucocorticoids in the control of inflammation and lymphocyte apoptosis, *Crit Rev Clin Lab Sci.* **42**, 71-104.
130. Coutinho, A. E. & Chapman, K. E. (2011) The anti-inflammatory and immunosuppressive effects of glucocorticoids, recent developments and mechanistic insights, *Mol Cell Endocrinol.* **335**, 2-13.
131. Amano, Y., Lee, S. W. & Allison, A. C. (1993) Inhibition by glucocorticoids of the formation of interleukin-1 alpha, interleukin-1 beta, and interleukin-6: mediation by decreased mRNA stability, *Mol Pharmacol.* **43**, 176-82.
132. Hino, Y. & Minakami, S. (1982) Hexose-6-phosphate and 6-phosphogluconate dehydrogenases of rat liver microsomes. Involvement in NADPH and carbon dioxide generation in the luminal space of microsomal vesicles, *J Biochem.* **92**, 547-57.

133. Clarke, J. L. & Mason, P. J. (2003) Murine hexose-6-phosphate dehydrogenase: a bifunctional enzyme with broad substrate specificity and 6-phosphogluconolactonase activity, *Arch Biochem Biophys.* **415**, 229-34.
134. Krawczyk, C. M., Holowka, T., Sun, J., Blagih, J., Amiel, E., DeBerardinis, R. J., Cross, J. R., Jung, E., Thompson, C. B., Jones, R. G. & Pearce, E. J. (2010) Toll-like receptor-induced changes in glycolytic metabolism regulate dendritic cell activation, *Blood.* **115**, 4742-9.
135. Gilmour, J. S., Coutinho, A. E., Cailhier, J. F., Man, T. Y., Clay, M., Thomas, G., Harris, H. J., Mullins, J. J., Seckl, J. R., Savill, J. S. & Chapman, K. E. (2006) Local amplification of glucocorticoids by 11 beta-hydroxysteroid dehydrogenase type 1 promotes macrophage phagocytosis of apoptotic leukocytes, *J Immunol.* **176**, 7605-11.
136. Yang, C., Nixon, M., Kenyon, C. J., Livingstone, D. E., Duffin, R., Rossi, A. G., Walker, B. R. & Andrew, R. (2011) 5alpha-reduced glucocorticoids exhibit dissociated anti-inflammatory and metabolic effects, *Br J Pharmacol.* **164**, 1661-71.
137. Khallou-Laschet, J., Varthaman, A., Fornasa, G., Compain, C., Gaston, A. T., Clement, M., Dussiot, M., Levillain, O., Graff-Dubois, S., Nicoletti, A. & Caligiuri, G. (2010) Macrophage plasticity in experimental atherosclerosis, *PLoS One.* **5**, e8852.
138. Ying, W., Cheruku, P. S., Bazer, F. W., Safe, S. H. & Zhou, B. (2013) Investigation of macrophage polarization using bone marrow derived macrophages, *J Vis Exp*.
139. Aznar, C., Fitting, C. & Cavaillon, J. M. (1990) Lipopolysaccharide-induced production of cytokines by bone marrow-derived macrophages: dissociation between intracellular interleukin 1 production and interleukin 1 release, *Cytokine.* **2**, 259-65.
140. Hauschildt, S., Bassenge, E., Bessler, W., Busse, R. & Mulsch, A. (1990) L-arginine-dependent nitric oxide formation and nitrite release in bone marrow-derived macrophages stimulated with bacterial lipopeptide and lipopolysaccharide, *Immunology.* **70**, 332-7.
141. Spartano, N. L., Lamon-Fava, S., Matthan, N. R., Obin, M. S., Greenberg, A. S. & Lichtenstein, A. H. (2014) Linoleic acid suppresses cholesterol efflux and ATP-binding cassette transporters in murine bone marrow-derived macrophages, *Lipids.* **49**, 415-22.
142. Van den Bossche, J., Baardman, J. & de Winther, M. P. (2015) Metabolic Characterization of Polarized M1 and M2 Bone Marrow-derived Macrophages Using Real-time Extracellular Flux Analysis, *J Vis Exp*.
143. Murray, P. J., Allen, J. E., Biswas, S. K., Fisher, E. A., Gilroy, D. W., Goerdt, S., Gordon, S., Hamilton, J. A., Ivashkiv, L. B., Lawrence, T., Locati, M., Mantovani, A., Martinez, F. O., Mege, J. L., Mosser, D. M., Natoli, G., Saeij, J. P., Schultze, J. L., Shirey, K. A., Sica, A., Suttles, J., Udalova, I., van Ginderachter, J. A., Vogel, S. N. & Wynn, T. A. (2014) Macrophage activation and polarization: nomenclature and experimental guidelines, *Immunity.* **41**, 14-20.
144. Abrahams, L., Semjonous, N. M., Guest, P., Zielinska, A., Hughes, B., Lavery, G. G. & Stewart, P. M. (2012) Biomarkers of hypothalamic-pituitary-adrenal axis activity in mice lacking 11beta-HSD1 and H6PDH, *J Endocrinol.* **214**, 367-72.
145. Zielinska, A. E., Walker, E. A., Stewart, P. M. & Lavery, G. G. (2011) Biochemistry and physiology of hexose-6-phosphate knockout mice, *Mol Cell Endocrinol.* **336**, 213-8.
146. Harris, H. J., Kotelevtsev, Y., Mullins, J. J., Seckl, J. R. & Holmes, M. C. (2001) Intracellular regeneration of glucocorticoids by 11beta-hydroxysteroid dehydrogenase (11beta-HSD)-1 plays a key role in regulation of the hypothalamic-pituitary-adrenal axis: analysis of 11beta-HSD-1-deficient mice, *Endocrinology.* **142**, 114-20.
147. Zhang, T. Y. & Daynes, R. A. (2007) Macrophages from 11beta-hydroxysteroid dehydrogenase type 1-deficient mice exhibit an increased sensitivity to lipopolysaccharide stimulation due to TGF-beta-mediated up-regulation of SHIP1 expression, *J Immunol.* **179**, 6325-35.
148. Chinetti-Gbaguidi, G., Bouhlel, M. A., Copin, C., Duhem, C., Derudas, B., Neve, B., Noel, B., Eeckhoute, J., Lefebvre, P., Seckl, J. R. & Staels, B. (2012) Peroxisome proliferator-activated receptor-gamma activation induces 11beta-hydroxysteroid dehydrogenase type 1 activity in human alternative macrophages, *Arterioscler Thromb Vasc Biol.* **32**, 677-85.
149. Margittai, E. & Banhegyi, G. (2008) Isocitrate dehydrogenase: A NADPH-generating enzyme in the lumen of the endoplasmic reticulum, *Arch Biochem Biophys.* **471**, 184-90.

150. Wang, X., Mick, G. J., Maser, E. & McCormick, K. (2011) Manifold effects of palmitoylcarnitine on endoplasmic reticulum metabolism: 11beta-hydroxysteroid dehydrogenase 1, flux through hexose-6-phosphate dehydrogenase and NADPH concentration, *Biochem J.* **437**, 109-15.
151. Bujaslka, I. R., JP & Stewart, PM & Walker, Elizabeth (2010) 6-Phosphogluconate Dehydrogenase – An NADPH-Generating Enzyme in the Lumen of the Endoplasmic Reticulum, *endo-meetings.* **Part3**, P1.P3-28.
152. Roux, K. J., Kim, D. I., Raida, M. & Burke, B. (2012) A promiscuous biotin ligase fusion protein identifies proximal and interacting proteins in mammalian cells, *J Cell Biol.* **196**, 801-10.
153. Pearce, E. L. & Pearce, E. J. (2013) Metabolic pathways in immune cell activation and quiescence, *Immunity.* **38**, 633-43.
154. Freemerman, A. J., Johnson, A. R., Sacks, G. N., Milner, J. J., Kirk, E. L., Troester, M. A., Macintyre, A. N., Goraksha-Hicks, P., Rathmell, J. C. & Makowski, L. (2014) Metabolic reprogramming of macrophages: glucose transporter 1 (GLUT1)-mediated glucose metabolism drives a proinflammatory phenotype, *J Biol Chem.* **289**, 7884-96.
155. Tavakoli, S., Zamora, D., Ullevig, S. & Asmis, R. (2013) Bioenergetic profiles diverge during macrophage polarization: implications for the interpretation of 18F-FDG PET imaging of atherosclerosis, *J Nucl Med.* **54**, 1661-7.
156. Vats, D., Mukundan, L., Odegaard, J. I., Zhang, L., Smith, K. L., Morel, C. R., Wagner, R. A., Greaves, D. R., Murray, P. J. & Chawla, A. (2006) Oxidative metabolism and PGC-1beta attenuate macrophage-mediated inflammation, *Cell Metab.* **4**, 13-24.
157. Huang, S. C., Everts, B., Ivanova, Y., O'Sullivan, D., Nascimento, M., Smith, A. M., Beatty, W., Love-Gregory, L., Lam, W. Y., O'Neill, C. M., Yan, C., Du, H., Abumrad, N. A., Urban, J. F., Jr., Artyomov, M. N., Pearce, E. L. & Pearce, E. J. (2014) Cell-intrinsic lysosomal lipolysis is essential for alternative activation of macrophages, *Nat Immunol.* **15**, 846-55.
158. Blacher, J., Safar, M. E., Guerin, A. P., Pannier, B., Marchais, S. J. & London, G. M. (2003) Aortic pulse wave velocity index and mortality in end-stage renal disease, *Kidney Int.* **63**, 1852-60.
159. Blacher, J., Guerin, A. P., Pannier, B., Marchais, S. J. & London, G. M. (2001) Arterial calcifications, arterial stiffness, and cardiovascular risk in end-stage renal disease, *Hypertension.* **38**, 938-42.
160. Kramer, H., Toto, R., Peshock, R., Cooper, R. & Victor, R. (2005) Association between chronic kidney disease and coronary artery calcification: the Dallas Heart Study, *J Am Soc Nephrol.* **16**, 507-13.
161. Massy, Z. A., Maziere, C., Kamel, S., Brazier, M., Choukroun, G., Tribouilloy, C., Slama, M., Andrejak, M. & Maziere, J. C. (2005) Impact of inflammation and oxidative stress on vascular calcifications in chronic kidney disease, *Pediatr Nephrol.* **20**, 380-2.
162. Goodman, W. G., London, G., Amann, K., Block, G. A., Giachelli, C., Hruska, K. A., Ketteler, M., Levin, A., Massy, Z., McCarron, D. A., Raggi, P., Shanahan, C. M., Yorioka, N. & Vascular Calcification Work, G. (2004) Vascular calcification in chronic kidney disease, *Am J Kidney Dis.* **43**, 572-9.
163. London, G. M., Guerin, A. P., Marchais, S. J., Metivier, F., Pannier, B. & Adda, H. (2003) Arterial media calcification in end-stage renal disease: impact on all-cause and cardiovascular mortality, *Nephrol Dial Transplant.* **18**, 1731-40.
164. Kuro-o, M. (2014) Calciprotein particle (CPP): a true culprit of phosphorus woes?, *Nefrologia.* **34**, 1-4.
165. Kuro-o, M. (2013) Klotho, phosphate and FGF-23 in ageing and disturbed mineral metabolism, *Nat Rev Nephrol.* **9**, 650-60.
166. Heiss, A., DuChesne, A., Denecke, B., Grotzinger, J., Yamamoto, K., Renne, T. & Jahnen-Dechent, W. (2003) Structural basis of calcification inhibition by alpha 2-HS glycoprotein/fetuin-A. Formation of colloidal calciprotein particles, *J Biol Chem.* **278**, 13333-41.
167. Heiss, A., Jahnen-Dechent, W., Endo, H. & Schwahn, D. (2007) Structural dynamics of a colloidal protein-mineral complex bestowing on calcium phosphate a high solubility in biological fluids, *Biointerphases.* **2**, 16-20.

168. Smith, E. R., Hewitson, T. D., Cai, M. M. X., Aghagolzadeh, P., Bachtler, M., Pasch, A. & Holt, S. G. (2017) A novel fluorescent probe-based flow cytometric assay for mineral-containing nanoparticles in serum, *Sci Rep.* **7**, 5686.
169. Hamano, T., Matsui, I., Mikami, S., Tomida, K., Fujii, N., Imai, E., Rakugi, H. & Isaka, Y. (2010) Fetuin-mineral complex reflects extraosseous calcification stress in CKD, *J Am Soc Nephrol.* **21**, 1998-2007.
170. Smith, E. R., Ford, M. L., Tomlinson, L. A., Rajkumar, C., McMahon, L. P. & Holt, S. G. (2012) Phosphorylated fetuin-A-containing calciprotein particles are associated with aortic stiffness and a procalcific milieu in patients with pre-dialysis CKD, *Nephrol Dial Transplant.* **27**, 1957-66.
171. Peyster, E., Chen, J., Feldman, H. I., Go, A. S., Gupta, J., Mitra, N., Pan, Q., Porter, A., Rahman, M., Raj, D., Reilly, M., Wing, M. R., Yang, W., Townsend, R. R. & Investigators, C. S. (2017) Inflammation and Arterial Stiffness in Chronic Kidney Disease: Findings From the CRIC Study, *Am J Hypertens.* **30**, 400-408.
172. Smith, E. R., Ford, M. L., Tomlinson, L. A., Bodenham, E., McMahon, L. P., Farese, S., Rajkumar, C., Holt, S. G. & Pasch, A. (2014) Serum calcification propensity predicts all-cause mortality in predialysis CKD, *J Am Soc Nephrol.* **25**, 339-48.
173. Jeziorska, M., McCollum, C. & Woolley, D. E. (1998) Calcification in atherosclerotic plaque of human carotid arteries: associations with mast cells and macrophages, *J Pathol.* **185**, 10-7.
174. Smith, E. R., Hanssen, E., McMahon, L. P. & Holt, S. G. (2013) Fetuin-A-containing calciprotein particles reduce mineral stress in the macrophage, *PLoS One.* **8**, e60904.
175. Cruz, C. M., Rinna, A., Forman, H. J., Ventura, A. L., Persechini, P. M. & Ojcius, D. M. (2007) ATP activates a reactive oxygen species-dependent oxidative stress response and secretion of proinflammatory cytokines in macrophages, *J Biol Chem.* **282**, 2871-9.
176. Driscoll, K. E. (2000) TNFalpha and MIP-2: role in particle-induced inflammation and regulation by oxidative stress, *Toxicol Lett.* **112-113**, 177-83.
177. Kong, X., Thimmulappa, R., Kombairaju, P. & Biswal, S. (2010) NADPH oxidase-dependent reactive oxygen species mediate amplified TLR4 signaling and sepsis-induced mortality in Nrf2-deficient mice, *J Immunol.* **185**, 569-77.
178. Kobayashi, E. H., Suzuki, T., Funayama, R., Nagashima, T., Hayashi, M., Sekine, H., Tanaka, N., Moriguchi, T., Motohashi, H., Nakayama, K. & Yamamoto, M. (2016) Nrf2 suppresses macrophage inflammatory response by blocking proinflammatory cytokine transcription, *Nat Commun.* **7**, 11624.
179. Wang, Y., Wang, G. Z., Rabinovitch, P. S. & Tabas, I. (2014) Macrophage mitochondrial oxidative stress promotes atherosclerosis and nuclear factor-kappaB-mediated inflammation in macrophages, *Circ Res.* **114**, 421-33.
180. Pedruzzi, L. M., Cardozo, L. F., Daleprane, J. B., Stockler-Pinto, M. B., Monteiro, E. B., Leite, M., Jr., Vaziri, N. D. & Mafra, D. (2015) Systemic inflammation and oxidative stress in hemodialysis patients are associated with down-regulation of Nrf2, *J Nephrol.* **28**, 495-501.
181. Wang, G., Petzke, M. M., Iyer, R., Wu, H. & Schwartz, I. (2008) Pattern of proinflammatory cytokine induction in RAW264.7 mouse macrophages is identical for virulent and attenuated Borrelia burgdorferi, *J Immunol.* **180**, 8306-15.
182. Grandjean-Laquerriere, A., Tabary, O., Jacquot, J., Richard, D., Frayssinet, P., Guenounou, M., Laurent-Maquin, D., Laquerriere, P. & Gangloff, S. (2007) Involvement of toll-like receptor 4 in the inflammatory reaction induced by hydroxyapatite particles, *Biomaterials.* **28**, 400-4.
183. Qu, G., Liu, S., Zhang, S., Wang, L., Wang, X., Sun, B., Yin, N., Gao, X., Xia, T., Chen, J. J. & Jiang, G. B. (2013) Graphene oxide induces toll-like receptor 4 (TLR4)-dependent necrosis in macrophages, *ACS Nano.* **7**, 5732-45.
184. Watson, G. S. & Craft, S. (2006) Insulin resistance, inflammation, and cognition in Alzheimer's Disease: lessons for multiple sclerosis, *J Neurol Sci.* **245**, 21-33.
185. Park, C. R. (2001) Cognitive effects of insulin in the central nervous system, *Neurosci Biobehav Rev.* **25**, 311-23.
186. Moreira, T., Cebers, G., Pickering, C., Ostenson, C. G., Efendic, S. & Liljequist, S. (2007) Diabetic Goto-Kakizaki rats display pronounced hyperglycemia and longer-lasting cognitive impairments following ischemia induced by cortical compression, *Neuroscience.* **144**, 1169-85.

187. Biessels, G. J., Staekenborg, S., Brunner, E., Brayne, C. & Scheltens, P. (2006) Risk of dementia in diabetes mellitus: a systematic review, *Lancet Neurol.* **5**, 64-74.
188. Fietta, P., Fietta, P. & Delsante, G. (2009) Central nervous system effects of natural and synthetic glucocorticoids, *Psychiatry Clin Neurosci.* **63**, 613-22.
189. McIntyre, R. S., Soczynska, J. K., Konarski, J. Z., Woldeyohannes, H. O., Law, C. W., Miranda, A., Fulgosi, D. & Kennedy, S. H. (2007) Should Depressive Syndromes Be Reclassified as "Metabolic Syndrome Type II"?, *Ann Clin Psychiatry.* **19**, 257-64.
190. Mutter, J., Naumann, J., Sadaghiani, C., Schneider, R. & Walach, H. (2004) Alzheimer disease: mercury as pathogenetic factor and apolipoprotein E as a moderator, *Neuro Endocrinol Lett.* **25**, 331-9.
191. Monnet-Tschudi, F., Zurich, M. G., Boschat, C., Corbaz, A. & Honegger, P. (2006) Involvement of environmental mercury and lead in the etiology of neurodegenerative diseases, *Rev Environ Health.* **21**, 105-17.
192. Dopp, E., Hartmann, L. M., von Recklinghausen, U., Florea, A. M., Rabieh, S., Shokouhi, B., Hirner, A. V., Obe, G. & Rettenmeier, A. W. (2007) The cyto- and genotoxicity of organotin compounds is dependent on the cellular uptake capability, *Toxicology.* **232**, 226-34.
193. Chang, L. W. (1990) The neurotoxicology and pathology of organomercury, organolead, and organotin, *J Toxicol Sci.* **15 Suppl 4**, 125-51.
194. Monnet-Tschudi, F., Zurich, M. G., Riederer, B. M. & Honegger, P. (1995) Effects of trimethyltin (TMT) on glial and neuronal cells in aggregate cultures: dependence on the developmental stage, *Neurotoxicology.* **16**, 97-104.
195. Shintani, N., Ogita, K., Hashimoto, H. & Baba, A. (2007) Recent studies on the trimethyltin actions in central nervous systems, *Yakugaku Zasshi.* **127**, 451-61.
196. Dheen, S. T., Kaur, C. & Ling, E. A. (2007) Microglial activation and its implications in the brain diseases, *Curr Med Chem.* **14**, 1189-97.
197. Krstic, D., Madhusudan, A., Doehner, J., Vogel, P., Notter, T., Imhof, C., Manalastas, A., Hilfiker, M., Pfister, S., Schwerdel, C., Riether, C., Meyer, U. & Knuesel, I. (2012) Systemic immune challenges trigger and drive Alzheimer-like neuropathology in mice, *J Neuroinflammation.* **9**, 151.
198. Tischner, D. & Reichardt, H. M. (2007) Glucocorticoids in the control of neuroinflammation, *Mol Cell Endocrinol.* **275**, 62-70.
199. Schweingruber, N., Reichardt, S. D., Luhder, F. & Reichardt, H. M. (2012) Mechanisms of glucocorticoids in the control of neuroinflammation, *J Neuroendocrinol.* **24**, 174-82.
200. De Kloet, E. R., Vreugdenhil, E., Oitzl, M. S. & Joels, M. (1998) Brain corticosteroid receptor balance in health and disease, *Endocr Rev.* **19**, 269-301.
201. De Kloet, E. R., Veldhuis, H. D., Wagenaars, J. L. & Bergink, E. W. (1984) Relative binding affinity of steroids for the corticosterone receptor system in rat hippocampus, *J Steroid Biochem.* **21**, 173-8.
202. Chantong, B., Kratschmar, D. V., Nashev, L. G., Balazs, Z. & Odermatt, A. (2012) Mineralocorticoid and glucocorticoid receptors differentially regulate NF-kappaB activity and pro-inflammatory cytokine production in murine BV-2 microglial cells, *J Neuroinflammation.* **9**, 260.
203. Carrillo-de Sauvage, M. A., Maatouk, L., Arnoux, I., Pasco, M., Sanz Diez, A., Delahaye, M., Herrero, M. T., Newman, T. A., Calvo, C. F., Audinat, E., Tronche, F. & Vyas, S. (2013) Potent and multiple regulatory actions of microglial glucocorticoid receptors during CNS inflammation, *Cell Death Differ.* **20**, 1546-57.
204. Falsig, J., van Beek, J., Hermann, C. & Leist, M. (2008) Molecular basis for detection of invading pathogens in the brain, *J Neurosci Res.* **86**, 1434-47.
205. Kim, D. J. & Kim, Y. S. (2015) Trimethyltin-Induced Microglial Activation via NADPH Oxidase and MAPKs Pathway in BV-2 Microglial Cells, *Mediators Inflamm.* **2015**, 729509.
206. Stansley, B., Post, J. & Hensley, K. (2012) A comparative review of cell culture systems for the study of microglial biology in Alzheimer's disease, *J Neuroinflammation.* **9**, 115.
207. Eskes, C., Juillerat-Jeanneret, L., Leuba, G., Honegger, P. & Monnet-Tschudi, F. (2003) Involvement of microglia-neuron interactions in the tumor necrosis factor-alpha release, microglial activation, and neurodegeneration induced by trimethyltin, *J Neurosci Res.* **71**, 583-90.

208. Underwood, R. H. & Williams, G. H. (1972) The simultaneous measurement of aldosterone, cortisol, and corticosterone in human peripheral plasma by displacement analysis, *J Lab Clin Med.* **79**, 848-62.
209. West, C. D., Mahajan, D. K., Chavre, V. J., Nabors, C. J. & Tyler, F. H. (1973) Simultaneous measurement of multiple plasma steroids by radioimmunoassay demonstrating episodic secretion, *J Clin Endocrinol Metab.* **36**, 1230-6.
210. Nishida, S., Matsumura, S., Horino, M., Oyama, H. & Tenku, A. (1977) The variations of plasma corticosterone/cortisol ratios following ACTH stimulation or dexamethasone administration in normal men, *J Clin Endocrinol Metab.* **45**, 585-8.
211. Cordon-Cardo, C., O'Brien, J. P., Casals, D., Rittman-Grauer, L., Biedler, J. L., Melamed, M. R. & Bertino, J. R. (1989) Multidrug-resistance gene (P-glycoprotein) is expressed by endothelial cells at blood-brain barrier sites, *Proc Natl Acad Sci U S A.* **86**, 695-8.
212. Meijer, O. C., de Lange, E. C., Breimer, D. D., de Boer, A. G., Workel, J. O. & de Kloet, E. R. (1998) Penetration of dexamethasone into brain glucocorticoid targets is enhanced in mdr1A P-glycoprotein knockout mice, *Endocrinology.* **139**, 1789-93.
213. Karssen, A. M., Meijer, O. C., van der Sandt, I. C., Lucassen, P. J., de Lange, E. C., de Boer, A. G. & de Kloet, E. R. (2001) Multidrug resistance P-glycoprotein hampers the access of cortisol but not of corticosterone to mouse and human brain, *Endocrinology.* **142**, 2686-94.
214. Brooksbank, B. W., Brammall, M. A. & Shaw, D. M. (1973) Estimation of cortisol, cortisone and corticosterone in cerebral cortex, hypothalamus and other regions of the human brain after natural death and after death by suicide, *Steroids Lipids Res.* **4**, 162-83.
215. Raubenheimer, P. J., Young, E. A., Andrew, R. & Seckl, J. R. (2006) The role of corticosterone in human hypothalamic-pituitary-adrenal axis feedback, *Clin Endocrinol (Oxf).* **65**, 22-6.
216. Arriza, J. L., Weinberger, C., Cerelli, G., Glaser, T. M., Handelin, B. L., Housman, D. E. & Evans, R. M. (1987) Cloning of human mineralocorticoid receptor complementary DNA: structural and functional kinship with the glucocorticoid receptor, *Science.* **237**, 268-75.
217. Lee, C. T., Bendriem, R. M., Wu, W. W. & Shen, R. F. (2017) 3D brain Organoids derived from pluripotent stem cells: promising experimental models for brain development and neurodegenerative disorders, *J Biomed Sci.* **24**, 59.
218. Tay, T. L., Savage, J. C., Hui, C. W., Bisht, K. & Tremblay, M. E. (2017) Microglia across the lifespan: from origin to function in brain development, plasticity and cognition, *J Physiol.* **595**, 1929-1945.
219. Ginhoux, F., Greter, M., Leboeuf, M., Nandi, S., See, P., Gokhan, S., Mehler, M. F., Conway, S. J., Ng, L. G., Stanley, E. R., Samokhvalov, I. M. & Merad, M. (2010) Fate mapping analysis reveals that adult microglia derive from primitive macrophages, *Science.* **330**, 841-5.
220. Muffat, J., Li, Y., Yuan, B., Mitalipova, M., Omer, A., Corcoran, S., Bakiasi, G., Tsai, L. H., Aubourg, P., Ransohoff, R. M. & Jaenisch, R. (2016) Efficient derivation of microglia-like cells from human pluripotent stem cells, *Nat Med.* **22**, 1358-1367.
221. Pandya, H., Shen, M. J., Ichikawa, D. M., Sedlock, A. B., Choi, Y., Johnson, K. R., Kim, G., Brown, M. A., Elkahloun, A. G., Maric, D., Sweeney, C. L., Gossa, S., Malech, H. L., McGavern, D. B. & Park, J. K. (2017) Differentiation of human and murine induced pluripotent stem cells to microglia-like cells, *Nat Neurosci.* **20**, 753-759.
222. Schwartz, M. P., Hou, Z., Propson, N. E., Zhang, J., Engstrom, C. J., Santos Costa, V., Jiang, P., Nguyen, B. K., Bolin, J. M., Daly, W., Wang, Y., Stewart, R., Page, C. D., Murphy, W. L. & Thomson, J. A. (2015) Human pluripotent stem cell-derived neural constructs for predicting neural toxicity, *Proc Natl Acad Sci U S A.* **112**, 12516-21.
223. Takahashi, K. & Yamanaka, S. (2006) Induction of pluripotent stem cells from mouse embryonic and adult fibroblast cultures by defined factors, *Cell.* **126**, 663-76.
224. Abud, E. M., Ramirez, R. N., Martinez, E. S., Healy, L. M., Nguyen, C. H. H., Newman, S. A., Yeromin, A. V., Scarfone, V. M., Marsh, S. E., Fimbres, C., Caraway, C. A., Fote, G. M., Madany, A. M., Agrawal, A., Kayed, R., Gylys, K. H., Cahalan, M. D., Cummings, B. J., Antel, J. P., Mortazavi, A., Carson, M. J., Poon, W. W. & Blurton-Jones, M. (2017) iPSC-Derived Human Microglia-like Cells to Study Neurological Diseases, *Neuron.* **94**, 278-293 e9.

225. Gabriel, E. & Gopalakrishnan, J. (2017) Generation of iPSC-derived Human Brain Organoids to Model Early Neurodevelopmental Disorders, *J Vis Exp*.
226. Curthoys, N. P. & Moe, O. W. (2014) Proximal tubule function and response to acidosis, *Clin J Am Soc Nephrol.* **9**, 1627-38.
227. Weiner, I. D. & Verlander, J. W. (2013) Renal ammonia metabolism and transport, *Compr Physiol.* **3**, 201-20.
228. Busque, S. M. & Wagner, C. A. (2009) Potassium restriction, high protein intake, and metabolic acidosis increase expression of the glutamine transporter SNAT3 (Slc38a3) in mouse kidney, *Am J Physiol Renal Physiol.* **297**, F440-50.
229. Busque, S. M., Stange, G. & Wagner, C. A. (2014) Dysregulation of the glutamine transporter Slc38a3 (SNAT3) and ammoniagenic enzymes in obese, glucose-intolerant mice, *Cell Physiol Biochem.* **34**, 575-89.
230. Solbu, T. T., Boulland, J. L., Zahid, W., Lyamouri Bredahl, M. K., Amiry-Moghaddam, M., Storm-Mathisen, J., Roberg, B. A. & Chaudhry, F. A. (2005) Induction and targeting of the glutamine transporter SN1 to the basolateral membranes of cortical kidney tubule cells during chronic metabolic acidosis suggest a role in pH regulation, *J Am Soc Nephrol.* **16**, 869-77.
231. Chan, K., Busque, S. M., Sailer, M., Stoeger, C., Broer, S., Daniel, H., Rubio-Aliaga, I. & Wagner, C. A. (2016) Loss of function mutation of the Slc38a3 glutamine transporter reveals its critical role for amino acid metabolism in the liver, brain, and kidney, *Pflugers Arch.* **468**, 213-27.
232. Shelton, L. M., Lister, A., Walsh, J., Jenkins, R. E., Wong, M. H., Rowe, C., Ricci, E., Ressel, L., Fang, Y., Demougin, P., Vukojevic, V., O'Neill, P. M., Goldring, C. E., Kitteringham, N. R., Park, B. K., Odermatt, A. & Copple, I. M. (2015) Integrated transcriptomic and proteomic analyses uncover regulatory roles of Nrf2 in the kidney, *Kidney Int.* **88**, 1261-1273.
233. Kobayashi, M. & Yamamoto, M. (2006) Nrf2-Keap1 regulation of cellular defense mechanisms against electrophiles and reactive oxygen species, *Adv Enzyme Regul.* **46**, 113-40.
234. Copple, I. M., Goldring, C. E., Kitteringham, N. R. & Park, B. K. (2010) The keap1-nrf2 cellular defense pathway: mechanisms of regulation and role in protection against drug-induced toxicity, *Handb Exp Pharmacol*, 233-66.
235. Nowik, M., Lecca, M. R., Velic, A., Rehrauer, H., Brandli, A. W. & Wagner, C. A. (2008) Genome-wide gene expression profiling reveals renal genes regulated during metabolic acidosis, *Physiol Genomics.* **32**, 322-34.
236. Moret, C., Dave, M. H., Schulz, N., Jiang, J. X., Verrey, F. & Wagner, C. A. (2007) Regulation of renal amino acid transporters during metabolic acidosis, *Am J Physiol Renal Physiol.* **292**, F555-66.
237. Sugawara-Yokoo, M., Suzuki, T., Matsuzaki, T., Naruse, T. & Takata, K. (1999) Presence of fructose transporter GLUT5 in the S3 proximal tubules in the rat kidney, *Kidney Int.* **56**, 1022-8.
238. Vanslambrouck, J. M., Broer, A., Thavyogarajah, T., Holst, J., Bailey, C. G., Broer, S. & Rasko, J. E. (2010) Renal imino acid and glycine transport system ontogeny and involvement in developmental iminoglycinuria, *Biochem J.* **428**, 397-407.
239. Kamiyama, M., Garner, M. K., Farragut, K. M. & Kobori, H. (2012) The establishment of a primary culture system of proximal tubule segments using specific markers from normal mouse kidneys, *Int J Mol Sci.* **13**, 5098-111.
240. Buchrieser, J., James, W. & Moore, M. D. (2017) Human Induced Pluripotent Stem Cell-Derived Macrophages Share Ontogeny with MYB-Independent Tissue-Resident Macrophages, *Stem Cell Reports.* **8**, 334-345.
241. Zhang, H., Xue, C., Shah, R., Bermingham, K., Hinkle, C. C., Li, W., Rodrigues, A., Tabita-Martinez, J., Millar, J. S., Cuchel, M., Pashos, E. E., Liu, Y., Yan, R., Yang, W., Gosai, S. J., VanDorn, D., Chou, S. T., Gregory, B. D., Morrisey, E. E., Li, M., Rader, D. J. & Reilly, M. P. (2015) Functional analysis and transcriptomic profiling of iPSC-derived macrophages and their application in modeling Mendelian disease, *Circ Res.* **117**, 17-28.
242. Takasato, M., Er, P. X., Chiu, H. S., Maier, B., Baillie, G. J., Ferguson, C., Parton, R. G., Wolvetang, E. J., Roost, M. S., Lopes, S. M. & Little, M. H. (2016) Kidney organoids from human iPS cells contain multiple lineages and model human nephrogenesis, *Nature.* **536**, 238.